

University of Southern Queensland
Faculty of Health, Engineering & Sciences

Optimisation of the Spoked Bicycle Wheel

Submitted by

Jason Keller

In fulfilment of the requirements of the

ENG4112 Research Project

towards the degree of

Bachelor of Engineering (Mechanical, in full)

Submitted: October, 2013

{Page left intentionally blank}

ABSTRACT

Despite the long history of bicycle wheels, there has been very few design changes because the current design is known to work.

This study aimed to develop a method to provide optimised spoking geometries for rear bicycle wheels. MATLAB® was used to optimise the spoke geometries based on the best combination of torsional and lateral stiffness. The developed script can be easily adapted to calculate the optimised geometry for any wheel with tensioned spokes. The load responses of the optimised wheels were then compared with conventional 2X and 3X spoke patterns and three commercially available wheels using ANSYS® FEA software.

When the optimised geometries were simulated in ANSYS® under torsional, radial and lateral loads, their performance was better than the conventionally spoked and commercial wheels that had similar specifications. These results confirmed that wheel design can be improved. The recommended guidelines produced in this study only apply to the wheel geometries contain herein, as certain limits were imposed on the hub flange radius and the spoke diameters. Limitations on the use of existing theoretical models have also been identified.

Keywords: *Bicycle wheel, rear wheel, dished wheel, ANSYS, MATLAB, torsional stiffness, lateral stiffness, design, optimisation.*

University of Southern Queensland
Faculty of Health, Engineering and Sciences

ENG4111 & ENG4112 *Research Project*

Limitations of Use

The Council of the University of Southern Queensland, its Faculty of Health, Engineering & Sciences, and the staff of the University of Southern Queensland, do not accept any responsibility for the truth, accuracy or completeness of material contained within or associated with this dissertation.

Persons using all or any part of this material do so at their own risk, and not at the risk of the Council of the University of Southern Queensland, the Faculty of Health, Engineering & Sciences or the staff of the University of Southern Queensland.

The dissertation reports an educational exercise and has no purpose or validity beyond this exercise. The sole purpose of the course pair entitled “Research Project” is to contribute to the overall education within the student’s chosen degree program. This document, the associated hardware, software, drawings, and other material set out in the associated appendices should not be used for any other purpose: if they are so used, it is entirely at the risk of the user.

Dean

Faculty of Health, Engineering & Sciences

CERTIFICATION

I certify that the ideas, designs and experimental work, results, analyses and conclusions set out in this dissertation are entirely my own effort, except where otherwise indicated and acknowledged.

I further certify that the work is original and has not been previously submitted for assessment in any other course or institution, except where specifically stated.

Jason Peter Keller

Student Number: 0050093222



Signature

02 October 2013

Date

ACKNOWLEDGEMENTS

This research was carried out under the principal supervision of Dr. Ray Malpress. His help and guidance has been welcomed throughout and I would like to thank him for always being available when I needed him.

I would also like to thank all of the USQ library staff for their dedication and success in gaining access to many out of publication texts. Without this help the work contained within this document would not have been possible.

Finally, thanks go to my family, for providing an ear to listen, a shoulder to cry on and providing secretarial relief during the development of my spread sheets. Even though only a small contribution, the time away from the computer screen was much appreciated.

TABLE OF CONTENTS

ABSTRACT	i
CERTIFICATION	iii
ACKNOWLEDGEMENTS	iv
LIST OF FIGURES	viii
LIST OF TABLES	x
NOMENCLATURE	xiii
GLOSSARY OF TERMS	xiv
CHAPTER 1 - BACKGROUND	1
1.1 Outline of the Study	1
1.2 Introduction	2
1.3 The Problem	3
1.4 Spoked Wheel Design Variables	3
1.5 Project Objectives.....	4
1.6 Wheel Buckling.....	6
1.7 Conclusion.....	7
CHAPTER 2 - LITERATURE REVIEW	8
2.1 Introduction	8
2.1.1 A note on A.J.S Pippard and his work on the theory of the spoked wheel	8
2.2 The Spoked Bicycle Wheel	9
2.2.1 History of the Spoked Wheel	10
2.2.2 Theoretical Analysis of the Spoked Wheel	13
2.2.3 Finite Element Analysis of the Spoked Wheel	18
2.2.4 Experimental Studies of the behaviour of a Spoked Bicycle Wheel	22
2.2.5 Identified areas where further study is required.....	29
2.3 Conclusions from literature	31
CHAPTER 3 - METHODOLOGY	32

3.1	Introduction	32
3.2	The Optimisation Method.....	33
3.2.1	How Version 1.0 of the code works.....	34
3.3	The CAD models.....	38
3.4	Simulation of the optimised wheel geometries and commercial wheels.....	40
3.4.1	Simulation Pre-processing	42
3.4.2	Simulation Post-Processing.....	46
3.5	Laboratory Test Procedure	48
CHAPTER 4 - RESULTS AND VALIDATION		51
4.1	The MATLAB® Optimisation Results	51
4.1.1	20 Spoke Wheels Optimisation Results and Discussion.....	52
4.1.2	24 Spoke Wheels Optimisation Results and Discussion.....	53
4.1.3	28 Spoke Wheels Optimisation Results and Discussion.....	53
4.1.4	32 Spoke Wheels Optimisation Results and Discussion.....	55
4.1.5	36 Spoke Wheels Optimisation Results and Discussion.....	55
4.1.6	48 Spoke Wheels Optimisation Results and Discussion.....	56
4.1.7	Conclusions from MATLAB®	57
4.2	The CAD Models of the optimised geometries.....	60
4.3	The Finite Element Analysis Results	63
4.3.1	Validation of the FE Analysis.....	64
4.4	Radial, Lateral and Torsional Stiffness values calculated from the FE Analysis	72
4.4.1	Acceptance of the calculated radial stiffness values.....	74
4.4.2	Acceptance of the calculated lateral stiffness values.....	75
4.4.3	Acceptance of the calculated torsional stiffness values.....	75
4.5	The Effective Modulus of Elasticity.....	78
CHAPTER 5 - DISCUSSION.....		83
5.1	Discussion of the Stiffness values calculated from the FEA results	83

5.2	Discussion of the MATLAB® Optimisation Results.....	88
CHAPTER 6 - SUMMARY AND DESIGN RECOMMENDATIONS		89
6.1	Project Summary	89
6.2	Design Recommendations	90
CHAPTER 7 - CONCLUSIONS AND FURTHER WORK.....		92
7.1	Conclusions	92
7.2	Recommendations for Further Work.....	93
APPENDICES		96
APPENDIX A. PROJECT SPECIFICATION.....		97
APPENDIX B. MATLAB® SCRIPTS.....		99
B.1	Optimised_wheel_stiffness.m - V1.0	100
B.2	Example of Optimisation Results.....	109
B.3	Check_Stiffness_Properties.m.....	112
APPENDIX C. ANSYS® PRE-PROCESSING.....		115
C.1	Mesh Convergence	116
APPENDIX D. THEORETICAL CALCULATIONS		118
D.1	An example of Pippard' s Calculations	119
APPENDIX E. OPTIMISED GEOMETRY RESULTS		131
E.1	Optimised Wheel Geometry for Rear Wheels with a 55 mm hub.....	132
APPENDIX F. REVISED MATLAB® SCRIPT AND RESULTS		134
F.1	Optimised_wheel_stiffness_Ver_2.m	135
LIST OF REFERENCES		141

LIST OF FIGURES

Figure 2.2-1. Old Wooden Wheel courtesy of textures.funpic.de	10
Figure 2.2-2. 0X (radial) and 1X spoke configurations.	11
Figure 2.2-3. 2X, 3X and 4X spoke crossing patterns. (Gavin 1996).....	12
Figure 2.2-4. The loads experienced by modern bicycle wheels. Note a front wheel is shown.	12
Figure 2.2-5. Shows the load distribution through the affected spokes.....	21
Figure 2.2-6. Results from Burgoyne and Dilmaghanian showing agreement with Pippard's theoretical analysis	25
Figure 2.2-7. (<i>Top</i>) Lateral test setup; (<i>Bottom Left</i>) Radial test setup; (<i>Bottom Right</i>) Torsional test setup (Price and Akers 1985).	26
Figure 2.2-8. Results for radial deflection under load from Price and Akers (1985) for 0X, 1X, 2X, 3X, 4X spoke wheels (<i>top</i>) and 3X spoked wheel (<i>bottom</i>) showing that after a certain load (about 1.5 kN in the 3X graph) the rate of change of the deformation decreases with increasing load.	28
Figure 3.3-1. Rim profile used for analysis.	38
Figure 3.3-2. The basic hub used in the analysis.	39
Figure 3.3-3. CAD Models (top left to right) - 20 spoke 2X, 24 spoke 2X and 28 spoke 3X. (Bottom left to right) - 32 spoke 3X, 36 spoke 3X, 48 3X.	40
Figure 3.4-1. 6700R wheel with a spoke angle of 90°	41
Figure 3.4-2. Gradient wheel with unevenly distributed spokes around the rim.	42
Figure 3.4-3. Circuit wheel with a high right hand side hub flange and low left hand side hub flange.....	42
Figure 3.4-4. Fixed support at A, 100 N Radial load at B - along y-axis, and the additional displacement constraint at C to maintain deformation in the plane of the rim as assumed by the theoretical models used in this study.	43
Figure 3.4-5. Fixed Support at A, 100 N Lateral load at B - along z-axis.	44
Figure 3.4-6. Fixed support at A, 100 N Torsional (tangential) load at B - along x-axis.	44
Figure 3.4-7. An example of the mesh used for finite element analysis. <i>Left</i> full wheel. <i>Right</i> Magnification of rim spoke connection. (32 spoke wheel).	46

Figure 3.5-1. The application and deformation of the 44.9 N radial load. *Photo courtesy of Peta Keller (2013)*..... 48

Figure 3.5-2. The application and deformation measurement of the 92.4 N lateral load. *Photo courtesy of Peta Keller (2013)*..... 49

Figure 3.5-3. The application and deformation measurement of the 92.4 N tangential load. *Photo courtesy of Peta Keller (2013)*..... 50

Figure 4.2-1. 20 spoke wheel optimised spoke geometry - (*left*) full wheel; (*centre*) 8 LHS spokes; (*right*) 12 RH spokes. 61

Figure 4.2-2. 24 spoke wheel optimised spoke geometry - (*left*) full wheel; (*centre*) 10 LH spokes; (*right*) 14 RH spokes..... 61

Figure 4.2-3. 28 spoke wheel optimised spoke geometry - (*left*) full wheel; (*centre*) 10 LH spokes; (*right*) 18 RH spokes..... 61

Figure 4.2-4. 32 spoke wheel optimised spoke geometry - (*left*) full wheel; (*centre*) 12 LH spokes; (*right*) 20 RH spokes..... 62

Figure 4.2-5. 36 spoke wheel optimised spoke geometry - (*left*) full wheel; (*centre*) 12 LH spokes; (*right*) 24 RH spokes..... 62

Figure 4.2-6. 48 spoke wheel optimised spoke geometry - (*left*) full wheel; (*centre*) 18 LH spokes; (*right*) 30 RH spokes..... 62

Figure 4.3-1. The maximum principal stress experienced by a 32 3X wheel under a 100 N torsional loading applied at the top centre of the rim aligned along the x-axis. The spokes angled back opposite the load direction experience compressive stress, whereas those angled in the direction of the load experience tensile stress..... 69

Figure 4.3-2. The 20 Opt-1b wheel with a small change to the spoke distribution. Compare to Figure 4.2-1. 70

Figure 4.3-3. The 28 Opt-1b wheel with a small change to the spoke distribution. Compare to Figure 4.2-3. 71

Figure 4.5-1. Wheel used by Goldberg (1984) showing the spokes connected to the tyre bed..... 80

Figure 4.5-2. The rim cross-section of the wheel used by Goldberg (1984). 81

Figure C.1-1. Mesh convergence of the 20 2X wheel. The difference between the total deformation seen at 7.5 mm and 1 mm mesh is very small with a significant reduction in required computational time. 116

Figure C.1-2. Mesh convergence of the 48 3X wheel. The difference between the total deformation seen at 7.5 mm and 1 mm mesh is very small with a significant reduction in required computational time. 117

LIST OF TABLES

Table 2.2-1. The effects of different symmetrical spoke patterns on wheel strength under five loading scenarios (Goldberg 1980).....	14
Table 2.2-2. Comparison between reported and calculated torsional stiffness values (Goldberg 1984). Values in brackets are the equivalent TS values in kg.mm/deg.....	16
Table 2.2-3. The possible E value used in Goldberg's calculations to achieve his published torsional stiffness values. These results were calculated by rearranging Equation 2.1 to solve for E . Initial E value = 10^7 psi.....	17
Table 2.2-4. Comparison table of wheel stiffness data from Price and Akers (1985)....	29
Table 3.4-1. Properties of commercially available wheels used for comparison with optimised geometries.	41
Table 3.4-2. Summary of boundary conditions used in the finite element analysis. The load in each scenario was 100 N.	45
Table 3.4-3. Formulae for the displacements of wired spoked wheels. The full table, including values, can be seen in Appendix D.1. (t_1 and t_2 indicate tensile or compressive stress load respectively).	47
Table 4.1-1. The constant values used throughout the theory and MATLAB® calculations unless otherwise stated.....	51
Table 4.1-2. MATLAB® results for the 20 spoke wheels. The optimised wheel has a spoke ratio of 2:3.....	52
Table 4.1-3. MATLAB® results for the 24 spoke wheels. The optimised wheel has a spoke ratio of 5:7.....	53
Table 4.1-4. MATLAB® results for the 28 spoke wheels. The optimised wheel has a spoke ratio of 5:9.....	54
Table 4.1-5. MATLAB® results for the 32 spoke wheels. The optimised wheel has a spoke ratio of 3:5 (32 Opt) and 1:1 (32 Opt ES).....	55
Table 4.1-6. MATLAB® results for the 36 spoke wheels. The optimised wheel has a spoke ratio of 1:2.....	56
Table 4.1-7. MATLAB® results for the 48 spoke wheels. The optimised wheel has a spoke ratio of 3:5.....	57
Table 4.1-8. The optimised geometries and stiffness values calculated using ' <i>Optimised_wheel_stiffness_Ver_2</i> ' for all total spoke categories.	60

Table 4.3-1. Wheel deformation comparison between theoretical calculations and FEA.	64
Table 4.3-2. Measured wheel deformation under radial, lateral and torsional loading compared to FEA and theoretical values.	65
Table 4.3-3. Simulation results for the 100 N radial load scenario with and without displacement constraints on the rim.....	67
Table 4.3-4. The FEA results of the modified optimised geometry wheels. Note: R - Radial, L - Lateral, T - Torsional, D - Deformation. Theoretical values shown in brackets. * - No additional constraints used.....	71
Table 4.4-1. Radial - no extra constraints, lateral and torsional stiffness of the analysed wheels based on the results of the finite element analysis.	73
Table 4.4-2. Comparison between the results of 'Optimised_wheel_stiffness.m' V1.0, V1.0 multiplied by the dish ratio and the FEA calculated torsional stiffness values. V2.0 wheels not included.....	77
Table 4.5-1. Effective modulus of elasticity, E , values calculated from the results of the finite element analysis.....	79
Table 4.5-2. The new torsional and lateral stiffness values for the V1.0 optimised wheels using the new E value. FEA values are in brackets.	82
Table 5.1-1. The stiffness properties of 20 spoke wheels. <i>Extract from Table 4.4-1.</i> ..	84
Table 5.1-2. The stiffness properties of 24 spoke wheels. <i>Extract from Table 4.4-1.</i> ..	85
Table 5.1-3. The stiffness properties of 28 spoke wheels. <i>Extract from Table 4.4-1.</i> ..	86
Table 5.1-4. The stiffness properties of 32 spoke wheels. <i>Extract from Table 4.4-1.</i> ..	87
Table 5.1-5. The stiffness properties of 36 spoke wheels. <i>Extract from Table 4.4-1.</i> ..	88
Table 5.1-6. The stiffness properties of 48 spoke wheels. <i>Extract from Table 4.4-1.</i> ..	88
Table C.1-1. Mesh Convergence data for the 20 2X wheel.	116
Table C.1-2. Mesh convergence data for the 48 3X wheel.	117
Table D.1-1. Theoretical stress, displacement and bending moment calculations for wire spoked wheels including psi table for radial load scenario $K_1=600$, ϵ (eps)=45°. The highlighted cells in the psi table are for the maximum values. (9 pages - total).....	120
Table D.1-2. Rt1/P, Rt2/P and M0/PR tables for a radial load case calculated using and compared to Pippard and White (1932 p218 & 220).....	129
Table D.1-3. Tangential load scenario calculated using and compared to Pippard and White (1932 p223 & 229).....	130

Table D.1-4. Side load scenario calculated using and compared to Pippard and Francis (1932 p444)..... 130

Table E.1-1. Optimised geometry table for 20 and 24 spoke rear wheels with 55 mm hub. Opt. - Optimal; Stiff. - stiffness; Max - maximum. 132

Table E.1-2. Optimised geometry table for 28 and 32 spoke rear wheels with 55 mm hub..... 132

Table E.1-3. Optimised geometry table for 36 and 48 spoke rear wheels with 55 mm hub..... 133

NOMENCLATURE

- A - Spoke cross-sectional area
- D - Wheel dish. The distance between the centre of the hub flange and the spoke connection on the rim
- D_f - Change in dish (D) due to an applied lateral load
- E - The effective elasticity of the wheel (combination of the hub, the rim and the spokes)
- E_r - The modulus of elasticity of the rim material
- E_s - The modulus of elasticity of the spoke material
- LS - Lateral Stiffness
- N - Total spoke number
- P - Applied load
- psi (ψ) - Angular position from origin
- R_h - Hub radius
- R_r - Rim radius
- R_s - Spoke radius
- S - Calculated spoke length
- T - Spoke Tension
- TS - Torsional Stiffness
- eps (ϵ) - The angle at the rim between the spoke line from the hub and the radial line from the rim connection
- μ - Spoke angle
- μ_f - Change in spoke angle (μ) due to an applied lateral load
- ϕ - Spoke brace/dish angle

GLOSSARY OF TERMS

Clincher Rim	- the rim is designed to hold an inflatable rubber tube underneath a tyre that hooks onto the rim.
Disc Brakes	- are brakes where the stopping force is applied to a disk fixed to the wheel hub via mechanical or hydraulic actuation.
Freehub (body)	- the part installed on the rear wheel hub to hold the gear cassette.
Lacing	- the process by which spokes are joined to the hub and the rim. Once completed, the spokes are said to be laced.
Lateral Stiffness	- the sideways force required to produce unit displacement of the rim with respect to the hub.
Load Affected Zone (LAZ)	- the area over which the applied force acts.
Radial Spoke	- a spoke between the hub and the rim that runs along a straight line passing through the centre of the hub.
Radial Stiffness	- the radial force required to produce a radial displacement of the rim with respect to the hub.
Rim Brakes	- are brakes where the stopping force is applied to the rim by means of rubber pads.
Spoke Angle	- the angle at which a spoke leaves the hub and links to the rim. 0° - radial to 90° - tangential.
Spoke Brace Angle	- the angle of spoke between the hub flange and the rim, also referred to as dish angle.
Spoke Elbow	- the bend near the end of the spoke to enable the spoke to 'hook' onto the hub flange.
Tangential Spoke	- a spoke that leaves the hub flange whose line does not intersect the axis of the hub.
Torsional Stiffness	- the torque required to produce a unit angular rotation of the hub with respect to the rim.
Tubeless Rim	- the rim is designed without spoke holes so when the tyre hooks the rim an airtight seal is created negating the need for an inner tube.

- Tubular Rim** - is constructed such that the one piece tyre-tube combination is glued to the rim.
- Wheel Dish** - the wheel dish is the offset of the spoke connection on the rim to the centre line of the hub flange. No dish means the centreline of the rim is in-line with the centreline of the hub flange.
- Wheel Trueness** - a wheel is true if it is completely round both radially and laterally within a certain tolerance. Once it is outside of this tolerance the wheel is said to be untrue (if laterally displaced) or out of round (if radially displaced).

CHAPTER 1 - BACKGROUND

“The bicycle wheel with tensioned spokes came into use more than a century ago, replacing wooden wheels with thick rigid spokes. It was a major improvement, important to the development of the lightweight bicycle, advancing performance by increasing strength while reducing weight. Today’s elegant, lightweight tensioned wheel can carry loads of more than a hundred times its own weight. Although most people are familiar with the bicycle few understand how its wheels achieve this unusual strength.” (Brandt 1988)

1.1 Outline of the Study

The modern lightweight bicycle wheel has remained relatively unchanged for over 100 years. The need for further investigations into wheel behaviour has been highlighted by Salamon and Oldham (1991), Wilson and Papadopoulos (2004), Price and Akers (1985) and Burrows (2002). The main objective of this study was to develop a method to optimise the geometry of a rear wheel and in doing so limit the possibility of buckling wheel failures.

1.2 Introduction

The bicycle wheel can be considered one of the most important parts of the modern bicycle. Not only do the wheels support the rider's weight but they are also responsible for transferring the power generated by the rider at the cranks, to forward motion on the road. Importantly, there are many ways bicycle wheels can fail as stated by Wilson and Papadopoulos (2004):

1. Rear axle bending or breakage
2. High flange breakage
3. Spoke elbow fatigue
4. Spoke body failure from rubbing
5. Cracks in rims near spoke holes
6. Braking wear through rim sidewalls
7. Lateral buckling due to insufficient torsional stiffness
8. Rim radial untruth
9. Rim denting from penetration

The failure method considered in this study is:

- Lateral buckling of the rim due to insufficient torsional stiffness, poor spoke bracing angle, high spoke tensions and side loads in combination with radial loads

1.3 The Problem

Despite many years of development, bicycle wheels are still prone to failure due to lateral buckling. To be able to re-true a wheel after a buckling failure, people need to have access to expensive equipment (truing stand) and have the skills, and the time available, to fix it properly. As a result, most riders take their buckled wheels to professional mechanics for repair. This can become quite costly depending on what materials are required to re-true the wheel (i.e. new spokes, new rim or just re-tensioning existing spokes).

To be able to design a wheel that is both strong and stiff enough to reduce, or eliminate, lateral buckling while maintaining its light weight and low cost, the designer must understand how a wheel behaves under different load conditions. With an understanding of how the wheel behaves, a method to optimise the stiffness properties of wheels can be developed.

1.4 Spoked Wheel Design Variables

The design of the spoked bicycle wheel depends on a number of different factors. Each of these factors can be altered to achieve the best combination of strength, stiffness, low weight and low cost.

The wheel parameters, with the nomenclature used within this document, affecting the strength and stiffness of the wheel are:

- The total number of spokes used, N

- The rim material modulus of elasticity, E_r
- The spoke material modulus of elasticity, E_s
- The spoke angle, μ
- The spoke brace (dish) angle, ϕ
- The spoke radius, R_s
- The rim radius, R_r
- The hub radius, R_h

The overall stiffness properties of the wheel will change with any of these factors. Other factors in the design of a wheel include what rim profile is used (clincher, tubeless or tubular rim), what material is used for the different components (spokes, rim and hub) and what the wheel will be used for (mountain biking/road racing).

This study focuses on rear bicycle wheels with aluminium clincher rims, aluminium hubs and stainless steel spokes that are commonly used on road bicycles for commuting or recreation. The rear wheel is the primary focus of this investigation because it carries the majority of the rider's weight (approximately 60% under static loading) and it is also subjected to all three load cases (radial, torsional/tangential and lateral).

1.5 Project Objectives

Wheels transfer the energy provided by the rider into forward motion on the road and if they were to fail, the cyclist could be stranded or seriously injured. Therefore, it is important to design a wheel that is both strong, to prevent buckling, and stiff, for the efficient transfer of power.

The research plan was divided into seven subparts:

1. The identified problem is the tendency for wheels to lose their lateral trueness (lateral buckling).
2. Review the relevant literature available on bicycle wheels to gain an understanding of the factors to consider in correcting the problem. This has been grouped into the following sections:
 - i. History of the spoked wheel
 - ii. Theoretical analysis of the spoked wheel
 - a. Radial loading
 - b. Torsional loading
 - c. Lateral loading
 - iii. Existing studies using Finite Element Analysis
 - a. Radial loading
 - b. Torsional loading
 - c. Lateral loading
 - iv. Existing Experimental data
 - v. Identified areas for further studies
3. Develop a MATLAB® model to output wheel design variables for the best possible combination of lateral and torsional stiffness.
4. Develop a mathematical model (spread sheet) based on the existing theory to predict deformations for the analysed load cases.
5. Develop a 3D finite element analysis model to compare the optimised wheel designs to both conventionally spoked wheels and commercially available wheels.

6. If possible, provide a set of guidelines for designing an optimised wheel based on the findings of the analysis.
7. Perform laboratory testing on an existing wheel, and compare the results to an FEA model, in order to ensure that the outcomes of the analysis are reliable.

1.6 Wheel Buckling

Under normal usage conditions, a rear bicycle wheel experiences radial, torsional and lateral loadings which can lead to the wheel losing its trueness or roundness. Radial loading is primarily from the weight of the rider (rider weight is usually distributed approximately 60% rear wheel and 40% front wheel). However, if a rider was to ride off of a gutter, or a step, then the radial load could be multiplied by factors of three or more. This loading would result in the spokes losing tension and the rim buckling in towards the hub (losing its roundness).

Lateral loading is experienced when the bike is inclined from vertical while travelling in a straight line (e.g. out of the saddle climbing and sprinting). If the lateral loads are large enough to cause the spokes to lose tension, the rim is likely to buckle out of the plane of the rim creating a saddle-like deformation. This deformation causes a decrease in the efficiency of power transfer and it adds extra stress to the other spokes which could ultimately lead to spoke breakage and wheel failure.

Torsional loading is the load applied by braking and accelerating the wheel. This type of load is unlikely to cause buckling of the wheel in isolation, but can create a reduction

in spoke tension so when the wheel experiences a simultaneous lateral or radial load, some buckling may occur. Torsional stiffness of a rear wheel is important because with increased stiffness comes increased power transfer efficiency.

1.7 Conclusion

In this dissertation a model has been developed to output the optimised geometry of a spoked rear wheel in order to minimise the occurrence of lateral buckling. The behaviour of the outputted geometry has been compared to commercially available and conventionally spoked wheels using finite element analysis software. By building wheels with geometry optimised for stiffness, it is predicted that the failure of wheels due to lateral and radial buckling can be minimised. Using the optimised spoke geometries for wheels could also result in more people using bicycles as a means of transport because the risks of being stranded, or seriously injured, due to a buckling wheel failure have been reduced.

CHAPTER 2 - LITERATURE REVIEW

2.1 Introduction

The modern bicycle wheel has only changed slightly since pre-tensioned steel spokes were introduced by James Starley in 1871 to replace wooden spokes. Although materials like carbon fibre composites have become popular in recent years, only a few manufacturers have tried redesigning the wheel. According to Burgoyne and Dilmaghanian (1993), it could be assumed that the reason why major redesigns have not eventuated with the introduction of new materials is because the current design is known to work. The following publications have been identified as significant contributions to the current knowledge on spoked wheels.

2.1.1 A note on A.J.S Pippard and his work on the theory of the spoked wheel

Alfred John Sutton Pippard was a civil and aeronautical engineer in the early 1900s. Throughout his career he published eighty papers and five books, with one book, ‘The Analysis of Engineering Structures’ (with J. F. Baker in 1936), becoming a “classic in engineering literature” (Elliot & Fry 1954). His published works were largely based on artillery and aeroplane wheels, but his methods can be applied to any spoked wheel system.

In the following material where Pippard is mentioned, the names of the contributors who worked alongside him have sometimes been omitted. This is in no way meant to disrespect the contributions of his colleagues but is simply used as a convenience.

However, where specific data has been used, the respective contributors have also been cited.

2.2 The Spoked Bicycle Wheel

Despite the evolution in design and the use of modern materials, the basic structure of the modern spoked wheel has remained constant. The basic structure consists of three major components:

1. a hub that houses the bearings and the axle;
2. pre-tensioned spokes that join the hub to the rim; and
3. a rim made of rolled or extruded material.

In their analysis, Salamon and Oldham (1991) recognised that although manufacturers have made significant progress in the design of the wheel, proprietary restrictions limit the amount of publicly available data. Burgoyne and Dilmaghanian (1993) state:

'The basic design has not changed significantly in 100 years; it probably therefore represents a design that cannot be greatly improved upon with existing technology. At the same time, its behaviour is not clearly understood; perhaps it does not matter, since it works.'

2.2.1 History of the Spoked Wheel

(This section has been taken from Burgoyne and Dilmaghanian (1993) with only slight modifications)

Prior to the mid-19th century wheel design was based on a compressed system. The rim, hub and spokes were made of wood and when the tyre was added to the rim compressive pre-stress was generated (Figure 2.2-1).



Figure 2.2-1. Old Wooden Wheel courtesy of textures.funpic.de

In 1871, James Starley developed the first wire spoked wheel ‘the Ariel’. These wheels were radially spoked and tensioned by turnbuckles that rotated the rim around the hub. This resulted in all the spokes becoming inclined in one direction which made the wheel behave differently under acceleration and braking forces. A few years later in 1874, Starley produced the first wheel with half of the spokes inclined in the forward direction and the other half inclined in the rearward direction. This development marked the beginning of the modern bicycle wheel.

The next major step in the evolution of the wheel came with the invention of the pneumatic tyre by Dunlop in 1888. This early tyre system had three components:

1. The inner rubber tube that maintained air pressure
2. A fabric pocket that enclosed the tube and the rim; and
3. An outer rubber layer that protected the fabric layer.

However, this early system made it difficult to fix punctures, and it was not until Welch and Bartlett, in 1890, separately invented systems to allow the tyre to lie wholly on the outer edge of the rim, that the pneumatic tyre became a viable alternative for wheels.

Modern bicycle wheels are now built with a range of spoke patterns radial (0X), cross one (1X), cross two (2X), cross three (3X) and cross four (4X) (Figure 2.2-2 and Figure 2.2-3), with 20 – 48 spokes connecting the hub to the rim.

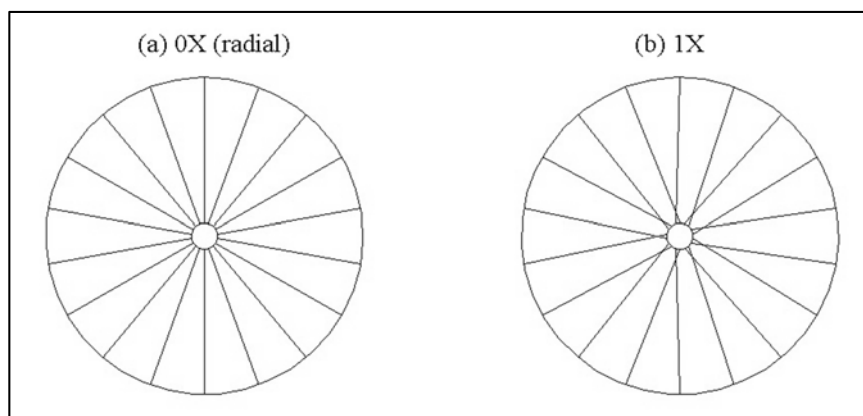


Figure 2.2-2. 0X (radial) and 1X spoke configurations.

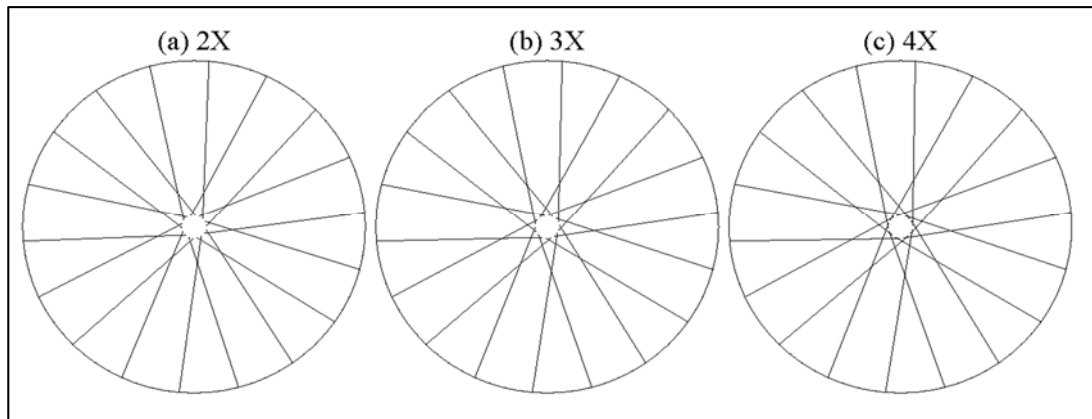


Figure 2.2-3. 2X, 3X and 4X spoke crossing patterns. (Gavin 1996)

Radial spoke patterns are more likely to be used on front wheels since they do not experience significant torque loading (unless hub or disk brakes are used) and according to Burrows (2008), if the wheel is to be used on the rear or with a disk/hub brake, a 3X pattern is best.

The rear wheel is exposed to all of the loading types – radial, torsional (tangential) and lateral loads as shown in Figure 2.2-4.

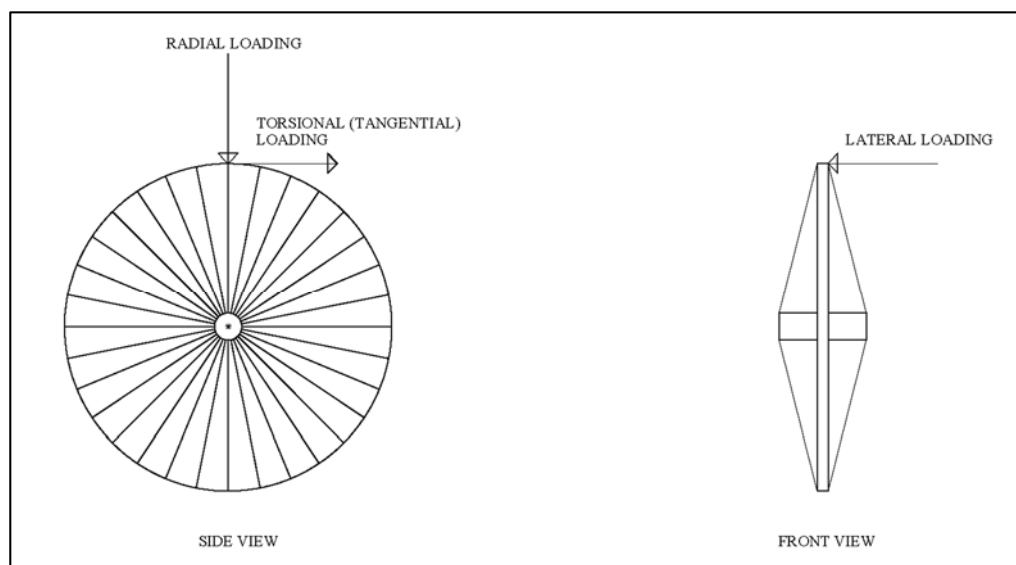


Figure 2.2-4. The loads experienced by modern bicycle wheels. Note a front wheel is shown.

Many types of wheel failures were identified by White and Papadopoulos (Section 1.2).

If a wheel fails during use it could lead to collisions and or cause serious injury to the rider or bystanders.

2.2.2 Theoretical Analysis of the Spoked Wheel

In the early 1930's, Pippard, and his colleagues, White, Baker and Francis, wrote a series of papers on the theories behind spoked wheels under various loads. Pippard consolidated these articles in his 1952 book 'Studies in Elastic Structures'. Pippard's work is considered to be at the forefront of wheel design by Wilson and Papadopoulos (2004) and is used in design analyses by Gavin (1996), Burgoyne and Dilmaghanian (1993) and Salamon and Oldham (1991).

Some of Pippard's works have been validated by Salamon and Oldham (1991), Burgoyne and Dilmaghanian (1993) and Gavin (1996) (Gavin also used Hetenyi's 1979 work on elastic foundations). Gavin (1996) stated that the benefit of using Hetenyi's formula for a flexural beam on an elastic foundation is that it provides a simpler method than that introduced by Pippard. Despite Hetenyi's method being considered less complex, Pippard's formulations have been used in this study to compare the results of the finite element analysis to theoretical values.

Goldberg (1980), aims to present the facts on how different spoke patterns and hub geometries affect the properties of bicycle wheels. These facts were based on his experience as a wheel builder. Table 2.2-1 shows the qualitative wheel strength findings in regards to spoke patterns under five different scenarios.

CHAPTER 2 - LITERATURE REVIEW

2.2 The Spoked Bicycle Wheel

Table 2.2-1. The effects of different symmetrical spoke patterns on wheel strength under five loading scenarios (Goldberg 1980).

Symmetrical Spoking Pattern	Spoke Angle (Z)		Wheel Strength				
	Z, for a 27-inch wheel with 36 spokes and a high flange hub	Z, for a 27-inch wheel with 40 spokes and a high flange hub	Driving torque stiffness	Side Load stiffness	Rim Brakes	Hub brakes	Transmission of Road Shock from rim to axle
0-cross	0°	0°	Weak	Strong	Wheel strength is independent of both flange diameter and spoking pattern	Weak	Transmission of road shock is essentially independent of both flange diameter and spoking pattern
1-cross	22.24°	20.02°					
2-cross	41.11°	39.78°					
3-cross	65.38°	59.07°					
4-cross	85.9°	77.78°	Strong	Weak		Strong	

Goldberg identifies the following points:

- to increase lateral stiffness the bracing angle can be increased,
- radial spoking is excellent for free-rolling (non-drive) wheels,
- radial spokes provide maximum lateral strength but are weak under torsional loads,
- to minimise the breakage of an un-dished wheel, more spokes can be added
- wheels can be strengthened by using heavier spokes,
- when a wheel is dished the spokes on the RHS hold more tension than those on the LHS (typically 1.6 times greater),
- breakage can be reduced by increasing spoke number on drive side, and

- lateral stiffness can be increased by weaving spokes.

In ‘*The Spoking Word*’, Goldberg (1984) proves the above qualitative findings through a series of calculations and experiments. Goldberg uses Equations 2.1 and 2.2 to calculate the torsional and lateral stiffness of symmetrical wheels.

$$Torsional\ Stiffness = \frac{\pi ER_w^2 N A R_h^2 \sin^2 \mu}{180 S^3} \quad (2.1)$$

$$Lateral\ Stiffness = \left(\frac{N}{S^3}\right) ((S^2 + D^2)T + EAD^2) \quad (2.2)$$

When placing Goldberg’s numbers for the variables into Equation 2.1, the values calculated for torsional stiffness are not the same as the values he reported in his 1984 book ‘*The Spoking Word*’. A comparison between the calculated values and those reported by Goldberg has been performed and the results are shown in Table 2.2-2. It can be seen that the reported values and the calculated values are different by an approximate factor of two.

CHAPTER 2 - LITERATURE REVIEW
 2.2 The Spoked Bicycle Wheel

Table 2.2-2. Comparison between reported and calculated torsional stiffness values (Goldberg 1984). Values in brackets are the equivalent TS values in kg.mm/deg.

	E (psi)	Rw (in)	Rh (in)	D (in)	A (in²)
Constant values	1.00E+07	12.15	1.3	1.0	0.00394

Wheel type	N	μ (deg)	S (in)	Reported Value (lb.in/deg)/ (kg.mm/deg)	Calculated Value (lb.in/deg)/ (kg.mm/deg)
0X	36	0	10.8960	0.0	0.0
1X	36	20	10.9831	1087.9 (12560)	545.3 (6296)
2X	36	40	11.2300	3594.4 (41498)	1801.8 (20803)
3X	36	60	11.5982	5922.8 (68381)	2969.0 (34278)
4X	36	80	12.0344	6856.0 (79156)	3436.7 (39678)
5X	48	75	11.9221	9045.0 (104429)	4534.0 (52347)

The discrepancy between the reported values and the calculated values was assessed by solving Equation 2.1 for the effective elasticity modulus, E (a combined modulus used by Goldberg to calculate the stiffness properties). A comparison between the E value stated and the E value required to calculate Goldberg's results is shown in Table 2.2-3. However, the lateral stiffness calculations performed in Goldberg (1984) do use the stated elasticity value 10^7 psi and the calculations performed as part of this investigation matched those Goldberg reported in 1984.

CHAPTER 2 - LITERATURE REVIEW
 2.2 The Spoked Bicycle Wheel

Table 2.2-3. The possible E value used in Goldberg's calculations to achieve his published torsional stiffness values. These results were calculated by rearranging Equation 2.1 to solve for E . Initial E value = 10^7 psi.

Wheel type	N	μ (deg)	S (in)	Reported Value (lb.in/deg)	Calculated E Values (psi)
0X	36	0	10.8960	0.0	-
1X	36	20	10.9831	1087.9	1.99E+07
2X	36	40	11.2300	3594.4	1.99E+07
3X	36	60	11.5982	5922.8	1.99E+07
4X	36	80	12.0344	6856.0	1.99E+07
5X	48	75	11.9221	9045.0	1.99E+07

Price and Akers compared their experimental results to those reported by Goldberg. Their findings showed that the values reported by Goldberg are approximately twice as large as the values they obtained in their experiments. However, both sets of results followed the same pattern. Price and Akers attributed this to the use of the effective elasticity value being 10^7 psi instead of the value of 5×10^6 psi Goldberg had calculated from one of his experiments. However, Table 2.2-2 shows that when performing the calculations using the same values as Goldberg, Goldberg's values are approximately half as large as those he had reported. The values calculated in this study align Goldberg's results with the experimental results for torsional stiffness seen by Price and Akers.

For the lateral stiffness of the wheel, the values calculated using Goldberg's numbers match his reported values but are nearly twice as large as those obtained in the experiments by Price and Akers. In this instance, using the value of the effective elasticity Goldberg calculated from his experiment ($E = 5 \times 10^6$ psi) in Equation 2.2, calculates stiffness values that match the experimental data of Price and Akers.

Even though Goldberg's reported values do not match those of the experimental data obtained by Price and Akers, the results calculated in this study do match these experimental results. It is therefore concluded that Goldberg's equations can still be used to optimise the spoke geometry based on stiffness, but that the values reported will have to be treated with caution. Due to the discrepancy in Goldberg's calculations, this study also includes verification of the effective elasticity modulus by calculating a new E value based on the results of the finite element analysis.

2.2.3 Finite Element Analysis of the Spoked Wheel

2.2.3.1 Introduction

Mariappan, Vijay and Ramamurti (2003), Hartz (2002), Salamon and Oldham (1991) and Brandt (1988) have performed finite element analysis of bicycle wheels using computer software and compared the results to the theoretical values obtained using Pippard's, Hetenyi's formula and experimental results (or a combination of the three) to explain the stiffness properties of the wheel.

2.2.3.2 Analysis by Mariappan, Vijay and Ramamurti

The analysis by Mariappan et.al (2003) was only for the radial load case. They used static and dynamic analysis to find the amount of deformation, stress and the natural frequencies of the wheel. For their model they used the principle of cyclic symmetry to analyse one section of the wheel with the results interpolated for the other sections. This was primarily done to reduce the computational time. The wheel was modelled as 10 identical sections with each section consisting of four spokes joining the hub to the rim.

From their analysis they concluded:

- Cyclic symmetry saves significant computational time.
- Net compression load can lead to catastrophic failure due to buckling.
- Stresses on the rim and axle are much less than that experienced by the spokes.
- If the axle thickness and width is increased, the natural frequency decreases.

2.2.3.3 *Analysis by Hartz*

The goals of the analysis by Hartz (2002) were:

- to determine the accuracy of the published results,
- to determine the benefit of additional nodes on the rim, and
- to analyse the impact of spoke geometries on the effectiveness of the wheel structure.

He used two-dimensional (2D) models in ANSYS® to examine the effects of loading on the rim and spokes. This analysis was performed using point loads on the rim, with the rim modelled as beam elements and the spokes as truss elements. The wheel itself was based on the wheel used in the experimental analysis of Burgoyne and Dilmaghanian (1993) (Section 2.2.4.3).

The results showed that for each wheel model tested:

- The displacements of each model were all similar.
- The strain magnitude was higher than the published data but the difference in magnitude was similar for all spokes.
- The bending analysis showed similar results to the published data.

He concluded that with further adjustments to his ANSYS® model he could match his calculated data to the published data. No articles were found in this literature review that confirmed whether or not this was ever done.

2.2.3.4 Analysis by Salamon and Oldham

Salamon and Oldham (1991) analysed tension and compression spoked wheels using finite element analysis. Their work on tension spokes included a comparison between the stress distributions of radially and tangentially spoked wheels. The tension spoked wheels had a radius of 300 mm and were laced with 32 spokes. The compression spoked wheels had 3, 5, 7 or 9 equally spaced spokes.

Salamon and Oldham concluded that:

- Both tangential and radial spoked wheels have notable structural performance.
- Four or five spokes distribute the load around the structure depending on where on the wheel it was loaded (either directly in line with a spoke or between spokes).

- Maximum radial loads depend on the number of spokes in the load affected zone (LAZ).
- The maximum load a tension wheel can handle is when the tension in the last loaded spoke is equal to zero (the sum of the compression stress caused by loading the wheel is greater than the pre-tension in the spokes the load affects).
- The load is distributed in a ratio of 50:20:5 with 50% of the load carried by the spoke directly in line with the load, 20% on each spoke immediately either side of the loaded spoke and 5% on each of the remaining spokes of the group of five (Figure 2.2-5).

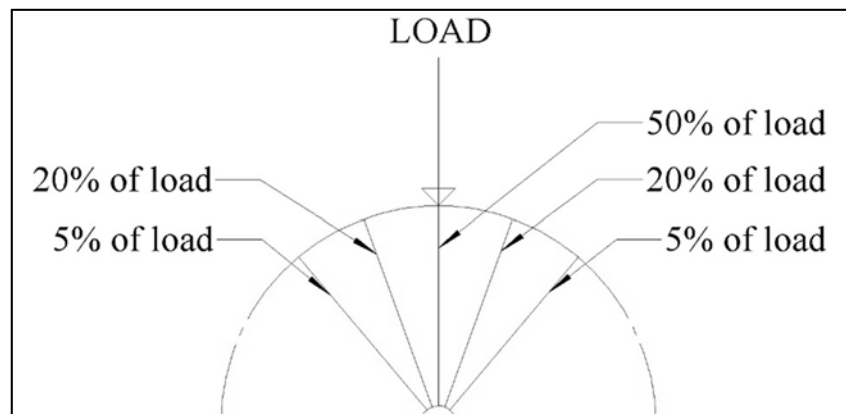


Figure 2.2-5. Shows the load distribution through the affected spokes

- Tangentially spoked wheels performed better under torque loads than radially spoked wheels.
- It is possible for an 8 spoke compression wheel to match the deflection of a 32 spoke tension wheel by manipulating the rim and spoke geometries.

2.2.3.5 *Analysis by Brandt*

Brandt (1988) performed one of the earliest finite element analyses on the bicycle wheel. He based his 2D analysis on the assumption that even though the wheel is a three dimensional (3D) structure, most of the dynamics are 2D, and as a result a 2D model could be analysed with good accuracy. For his analysis he used a 36 spoke wheel with the active nodes at the rim each having 3 degrees of freedom. The results of his analysis showed deflections of the different spokes under radial and torsional loading. In his book, '*The Bicycle Wheel*' (1988) Brandt offers no discussion on these results. However, his computed values have been compared to values obtained experimentally by Goldberg (1984) and Price and Akers (1985), with his values found to be similar to those reported by Price and Akers.

2.2.4 Experimental Studies of the behaviour of a Spoked Bicycle Wheel

2.2.4.1 Introduction

Laboratory, or road testing, of bicycle wheels has been performed and analysed by Gavin (1996), Burgoyne and Dilmaghanian (1993) and Price and Akers (1985). These experiments involved placing strain gauges on spokes and rim sections before loading the wheel using laboratory equipment, or riding the wheel over roads, to identify the maximum strains in the different wheel sections.

2.2.4.2 Investigation by Gavin

Gavin (1996) compared his experimental data to theoretical values calculated from Hetenyi's formula for in-plane deformation of a flexural beam on an elastic foundation because it was simpler to evaluate than Pippard's method. The effects of different

spoke patterns (2X, 3X and 4X) were assessed by lacing these patterns onto similar rims and hubs.

The results of his experiments showed that:

- Under a radial load the 2X pattern is the stiffest and the 4X pattern is the least stiff.
- Under lateral loading, wheels with longer spokes are more flexible, with the 2X pattern exhibiting higher strains.

He concluded that:

- The characteristics of strength, stiffness and low weight are met by pre-tensioned bicycle wheels.
- The rear wheel requires high pre-tension in half the spokes to maintain asymmetry.
- The spoke pattern has its greatest influence under lateral or cornering loads.

2.2.4.3 Investigation by Burgoyne and Dilmaghanian

Burgoyne and Dilmaghanian (1993) ran experiments on wheels with tyres installed. The testing was performed using laboratory equipment on handmade production wheels. The spoke tensions in these wheels were adjusted until the wheel was radially and laterally true. The strains in the spokes and the rim were measured using strain gauges.

Their experiments showed:

- The deformations that were measured match the results of Pippard (Figure 2.2-6) for a wheel under a radial load applied to the rim. Figure 2.2-6 shows the strain in each of the adjacent, measured spokes as the load increases (top) and the strain in spokes as they move away from the area of ground contact (bottom).
- Pippard's analysis is accurate until the spokes lose their pre-tension.
- Only those spokes near the LAZ show significant strains.
- With tyres installed there was only a small pressure difference detected but the peak strain was reduced, due to the expansion of the LAZ.
- Bending moments found closely match those calculated using Hetenyi's and Pippard's formulae.

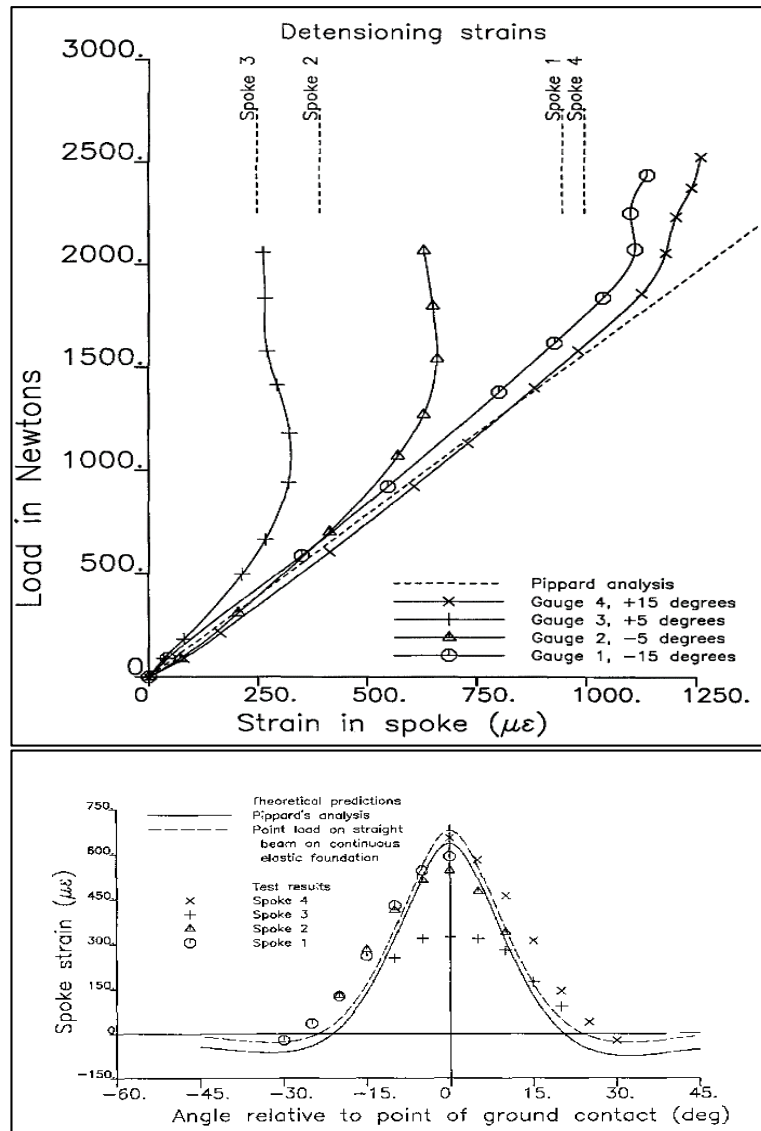


Figure 2.2-6. Results from Burgoyne and Dilmaghanian showing agreement with Pippard's theoretical analysis

Burgoyne and Dilmaghanian concluded:

- that the load is only carried by the spokes near the load (ground force or force applied in a laboratory),
- the rim distributes the load to the spokes by local bending, and
- the spokes near the ground undergo the largest loss of pre-tension with the tension in the spokes outside of the LAZ experiencing very little change.

2.2.4.4 *Investigation by Price and Akers*

Price and Akers (1985) performed laboratory analyses on five differently spoked wheels. They used wheels built from the same materials (a 36 hole hub, 1.8 mm stainless steel spokes and an AVA aluminium rim) using radial, 1X, 2X, 3X and 4X spoking patterns. They ran experiments to analyse the radial, lateral and torsional stiffness of the wheels (Figure 2.2-7).

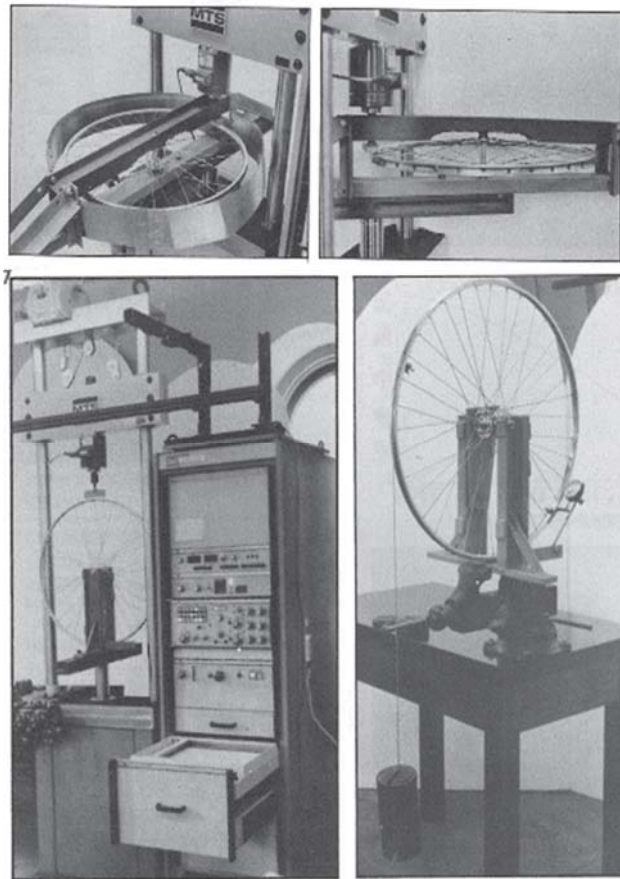


Figure 2.2-7. (Top) Lateral test setup; (Bottom Left) Radial test setup; (Bottom Right) Torsional test setup (Price and Akers 1985).

Their testing showed the following for a wheel under torsional loading:

- A larger hub diameter = less torque load = less tension required per spoke.
- Spoke patterns effect torsional stiffness more than hub diameter.
- The 4X pattern was 23 times stiffer than the radial pattern.

Lateral loading:

- Stiffness is affected by the distance between hub flanges, spoke tension, number of spokes and spoke geometry.
- Distance from flange to rim centreline is most influential (dishing).
- Shorter spokes are slightly stiffer than longer spokes.

Radial loading:

- Is influenced by the number, thickness and tension of spokes.
- Smaller flange hubs lead to an increase in comfort.
- In Figure 2.2-8 the slope of the curve changes with higher loads and this is possibly due to the release of tension from the loaded spokes. For example, the first 0.8 mm deflection was under a load of approximately 1.4 kN, and to deform the wheel 1.6 mm (another 0.8 mm) only took a load of approximately 2.2 kN (another 0.8 kN).
- The LAZ covers 4 spokes.

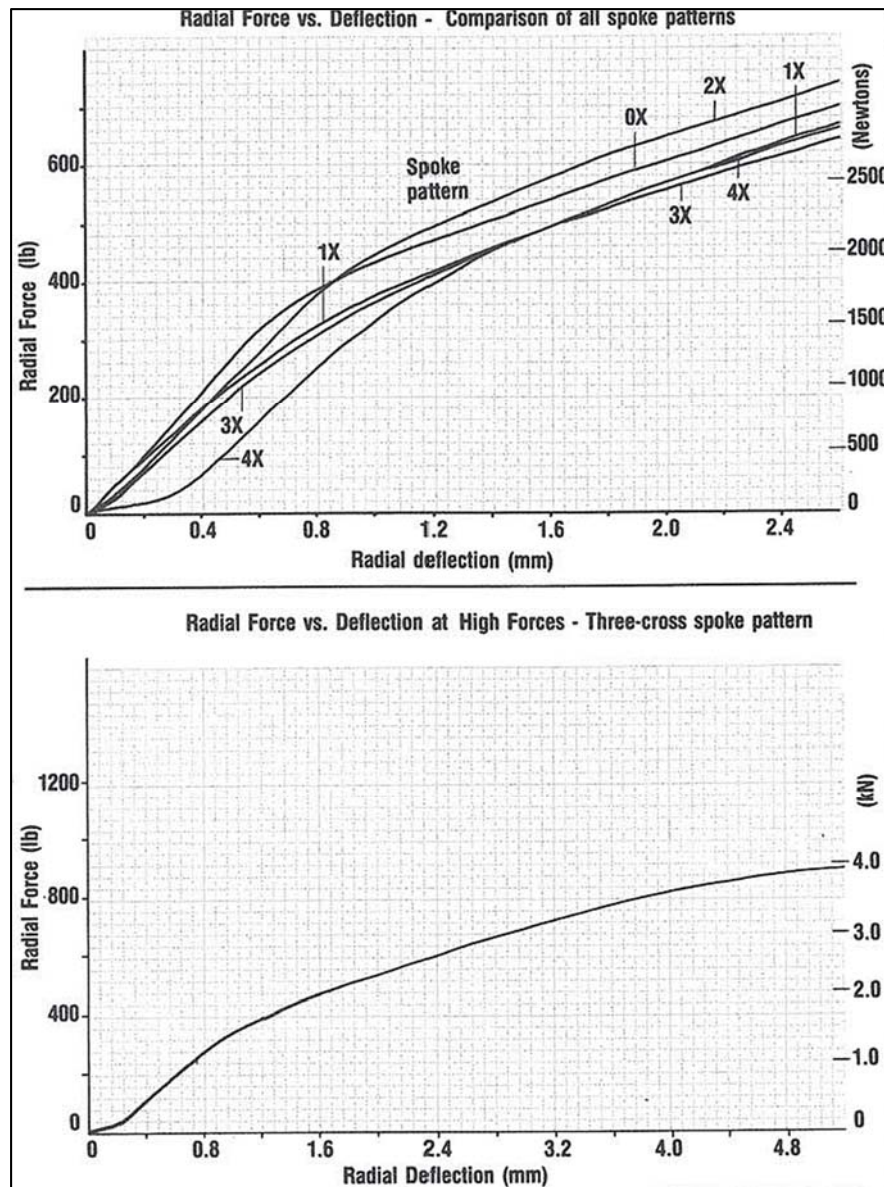


Figure 2.2-8. Results for radial deflection under load from Price and Akers (1985) for 0X, 1X, 2X, 3X, 4X spoke wheels (*top*) and 3X spoked wheel (*bottom*) showing that after a certain load (about 1.5 kN in the 3X graph) the rate of change of the deformation decreases with increasing load.

They concluded that the spoking pattern effects torsional stiffness the most and that shorter spokes increase both radial and lateral stiffness. The results from their study were compared to those seen in Brandt (1988) and Goldberg (1984) and are shown in Table 2.2-4.

Table 2.2-4. Comparison table of wheel stiffness data from Price and Akers (1985)

COMPARISON OF WHEEL STIFFNESS DATA		SPOKE PATTERN					SOURCES OF DATA
		0X	1X	2X	3X	4X	
Torsional Stiffness (inch-lb/degree)	Price & Akers (tests)	143	718	1859	2823	3304	Price & Akers
	Brandt (Calculations)	-	-	-	2118	-	Bicycle Wheel, p.136
	Brandt (finite elements)	-	-	-	2094	-	Bicycle Wheel, Fig. 70, p.144
	Goldberg (Calculations)	0	1088	3594	5923	6856	Spoking Word, Table K-2, p.K-19
Lateral Stiffness (lb/inch)	Price & Akers (tests)	616	656	634	606	576	Price & Akers
	Brandt (tests)	-	-	-	200	-	Bicycle Wheel, Fig.17, p.42
	Goldberg (Calculations)	1430	1401	1325	1222	1115	Spoking Word, Table K-3, p.K-23
Radial Stiffness (lb/inch)	Price & Akers (tests)	13,960	11850	14,130	13,050	11,970	Price & Akers
	Brandt (finite elements)	-	-	-	18,281	-	Bicycle Wheel, Fig.67, p.141
	Goldberg (tests)	14,500	-	-	-	-	Spoking Word, Table G-2, p.G-15

The discrepancy between the experimental values of Price and Akers and the theoretical values reported by Goldberg has been discussed in detail in Section 2.2.2. Price and Akers believed that the discrepancy was due to the effective elasticity value, E , being twice as large in Goldberg's calculations. However, after checking the calculations (Section 2.2.2) this may be the case for the lateral stiffness values only. From Table 2.2-4 it is shown that despite the difference in magnitude the stiffness values show the same pattern of change as the number of cross spokes increase.

2.2.5 Identified areas where further study is required

Further investigations into wheel behaviour that have been identified during the literature review include:

- Comparing the stresses generated at the hub of 28-, 32- and 36-spoke tangentially spoked tension wheels with 3-, 5-, 7-spoked compression wheels in order to understand the load transfer mechanism around the hub (Salamon & Oldham 1991).
- Testing is required to analyse the wheels response to high shock loads (sudden impacts i.e. off of footpaths, potholes, etc.) (Price and Akers 1985)

- Burrows (2008) notes the unreliability of current titanium spokes even though as a spoke material titanium ‘makes sense’. An investigation into why titanium spokes are unreliable is required.
- Wilson and Papadopoulos (2004) identified the following areas for further study:
 - a. To identify whether torsional yield is responsible for a rim to becoming laterally untrue.
 - b. Following the approach of Pippard and Hetenyi a simple formula for tangential load could be derived. They suggest this may warrant more consideration when hub brakes are introduced because current tangential loads do not cause significant changes in spoke tensions.
 - c. Lateral wheel mechanics require more study since lateral stiffness plays an important part in wheel collapse and may be responsible for spoke fatigue.
- Goldberg (1984) states:

‘...it is fruitless to come up with one best possible rear wheel. There are too many variables and the possibilities for spoking are almost limitless.’
- Finite element analysis has been used previously to analyse the wheel but these analyses have only investigated one or two design variables.

2.3 Conclusions from literature

There are still many possible investigations to perform to gain a better understanding of how the wheel works. This study focusses on the optimisation of wheel geometry to improve torsional stiffness and to minimise the risk of lateral buckling failures.

The theoretical analyses performed by Pippard and Goldberg have proven consistent with both experimental and finite element analyses in the past. Therefore this study has adopted these methods to generate the optimal wheel geometry and validate the results of the finite element analysis.

Previous finite element analyses have been performed for the bicycle wheel but these have focussed on 2D analysis and assessed only a few features of the wheel design. In order to validate the merits of the optimised geometries calculated in this study and to add to the available data of existing finite element analyses, the 3D behaviour of bicycle wheels under radial, lateral and torsional load cases has been analysed.

CHAPTER 3 - METHODOLOGY

3.1 Introduction

A significant review of the technical literature pertaining to spoked wheels identified that the majority of studies are over 10 years old and that the most used theoretical analysis is based on the work of Pippard et.al in the 1930s. This study focusses on optimising the lateral and torsional stiffness of spoked wheels to prevent buckling failures while still maintaining efficient power transfer.

MATLAB® and Microsoft Excel® mathematical models were developed to optimise and calculate the theoretical deformations of spoked wheel designs. ANSYS® finite element analysis software was used to analyse these designs under the three common load scenarios. The process involved:

1. Developing and using a MATLAB® script to identify the spoke geometry of wheels with the best possible combination of lateral and torsional stiffness using set criteria.
2. Developing solid models of these geometries using a standard hub and rim profile to enable the comparison between spoke numbers, spoke angle and spoke pattern only.
3. Analysing the models in ANSYS® to verify the stiffness values and check the validity of the effective elasticity, E , value used in Step 1.
4. Comparing the optimised wheels with existing wheels to see if there is any improvement in performance.

5. Summarising the results and, if possible, create a set of guidelines to assist designers with the design of a spoked wheel.

3.2 The Optimisation Method

A MATLAB® script has been produced, based on the work of Goldberg, to determine the geometry of the spokes in the wheel to provide the best combination of torsional and lateral stiffness within some set constraints. The total number of calculations required is dependent upon the step size for each variable within the script. With small step sizes, over 400 million calculations are required. MATLAB® was chosen because it is capable of performing these calculations in an acceptable time period.

The complexity of the required calculations increases when analysing asymmetrical wheels because the variables can be different on each side of the wheel. Goldberg's equations for torsional and lateral stiffness for all wheels are:

$$TS = \frac{\pi * E * R_w^2}{180} \sum_1^N \frac{A * R_h^2 * \sin^2 \mu}{S^3} \quad (3.1)$$

$$LS = \sum_1^N \left\{ \frac{T}{S} + \frac{(T+EA)D^2}{S^3} - \left[\frac{(T+EA)DR_w R_h}{S^3 D_f} \right] [\cos(\mu + \mu_f) - \cos(\mu)] \right\} \quad (3.2)$$

Both of the above equations have the variables:

- A (cross-sectional area of the spoke),
- R_h (the hub radius),
- μ (the spoke angle at the hub) and

- N (the total number of spokes).

The spoke tension, T , the rim radius, R_w , the effective elasticity, E , and the lateral displacement limit, D_f , were all fixed for this analysis. The amount of dish, D , was based on a rear wheel with a 10-speed gear cluster (105 mm total width minus 50 mm freehub body). Goldberg (1984) states that the wind up angle, μ_f , is very small even under extreme conditions and should be considered as zero if the wheel is symmetrical or less than one degree if the wheel is asymmetrical. Version 1.0 of the script developed for optimisation, '*Optimised_wheel_stiffness.m*', is shown in Appendix B.1.

The optimal spoke geometries for wheels containing 20, 24, 28, 32, 36 and 48 spokes were obtained using the code based on Equations 3.1 and 3.2 for a hub width of 55 mm. The maximum possible torsional stiffness was found from Equation 3.1. Dishing of the wheel makes the identification of the maximum lateral stiffness less straightforward. It is assumed in this study that wheel asymmetry makes it necessary to assess the lateral stiffness using two loads; one applied from right to left and another load applied from left to right. The overall lateral stiffness of the wheel was then calculated as an average of these two values.

The optimised geometries were then modelled in CAD and analysed with different load cases in ANSYS®.

3.2.1 How Version 1.0 of the code works

Version 1.0 of the code, '*Optimised_wheel_stiffness.m*', is based on the equations of Goldberg for torsional and lateral stiffness to output the optimised wheel geometry.

The initial cell, ‘%% Set Known Values’, consists of all the variables required to calculate the stiffness values. It is designed to calculate the optimal geometry for a given total spoke number and therefore it prompts the user to enter the total number of spokes required for the analysis. A *for* loop is used to calculate the right hand side (RHS) spoke number based on the spokes required on the left hand side (LHS). For the lateral stiffness calculation, a value for spoke tension is required. Goldberg (1984) states that for a dished wheel the spoke tension on the RHS is approximately 1.6 times greater than the tension on the LHS. However, this difference in spoke tension increases the likelihood of spoke breakage which can be reduced by using thicker spokes or more spokes on the RHS. For this analysis a slightly lower tension ratio of 1.4 has been chosen to reduce the tensile difference between the left and right hand side spokes while also reducing the likelihood of spoke breakage.

The variables R_h , μ and A were initially set to vary between 20 mm and 25 mm, 0° and 90° and 0.785 mm^2 and 2.545 mm^2 (or 1 mm and 1.8 mm spoke diameter) respectively. Initial trials of the code identified that both lateral and torsional stiffness were maximised with the maximum hub flange radius, R_h , and the maximum spoke cross-sectional area, A . Subsequently, those two values were fixed at their maximums for the remainder of the analysis. The change in spoke angle (μ), μ_f , was set arbitrarily at 0.8° for each side.

In the second cell, ‘%% Lateral and Torsional Stiffness’, the code proceeds to calculate the torsional and lateral stiffness by initially calculating the different spoke lengths required for each geometric combination using Equation 3.3 (Goldberg 1984).

$$S = \sqrt{R_w^2 + R_h^2 + D^2 - 2 * R_w * R_h * \cos \mu} \quad (3.3)$$

A nested loop structure is then used to calculate each variable change against every other variable. By changing the number of spokes on the LHS and the spoke angle for the LHS and RHS independently, the stiffness values for a range of combinations are calculated.

For many of the possible geometries the lateral stiffness in one direction was negative while the stiffness under a load from the other direction was positive. The following pattern was noted for all total spoke numbers:

- The magnitude of minimum stiffness (- value) in one direction \approx the magnitude of maximum stiffness (+ value) in the opposite direction.

It was assumed that a negative lateral stiffness meant that the wheel would be unable to stay true in rest conditions, as the higher spoke tension on one side of the wheel would cause it to buckle. Therefore, to find the maximum lateral stiffness of the wheel, only the geometries with a positive lateral stiffness in each load scenario were considered and averaged.

In the third cell, '`% Optimisation loop`', the optimal geometry is found and reported based on the average of the combined maximum percentage of torsional and lateral stiffness. Since the bulk of the analysis time was found to be used to find the maximal stiffness properties, a *while* loop was inserted here so that optimisation process may be repeated using different percentages of maximum stiffness until the results met the needs of the wheel designer.

The percentages are used to specify the minimum requirement of stiffness based on the maximum stiffness values reported previously. For the optimisation process this has been automated to calculate values between 40% - 100% of the desired stiffness parameter. The next step identifies the maximum value of the “non-reduced” stiffness property for geometry that meets the minimum requirements. The code then extracts the indices and uses these to display the optimal geometry in the command window with a series of *fprintf* commands. An example printout of the command window is shown in Appendix B.2.

To ensure that the code is working correctly, the outputted values were directly inputted into a separate code, ‘*Check_Stiffness_Properties.m*’ (Appendix B.3), and the values for torsional, average lateral and left and right side lateral stiffness were compared to those found and reported in the optimisation code. Hand calculations with different geometries were also used to obtain results for spoke length, torsional stiffness and lateral stiffness. The indices of the values and the results of the hand calculations were compared with the results in their respective matrix locations. This process was repeated after script modifications to ensure that the results continued to be indexed correctly.

A timer was included in the code so that the total run-time could be displayed when the code had finished. The initial analysis times ranged from approximately two hours (for 20 spoke wheels) to six hours (for 48 spoke wheels) (using a Pentium Core i7 3.20GHz processor and 18GB of RAM) but after fixing the hub flange radius and the spoke cross-sectional area, this time was reduced to approximately five minutes.

3.3 The CAD models

The CAD models produced for the optimised wheels have the same rim geometry (Figure 3.3-1), spoke material (stainless steel), rim material (aluminium), hub material (aluminium) and hub geometry (Figure 3.3-2) to ensure that any variations seen in the simulations were because of the different spoke geometries and lacing patterns used.

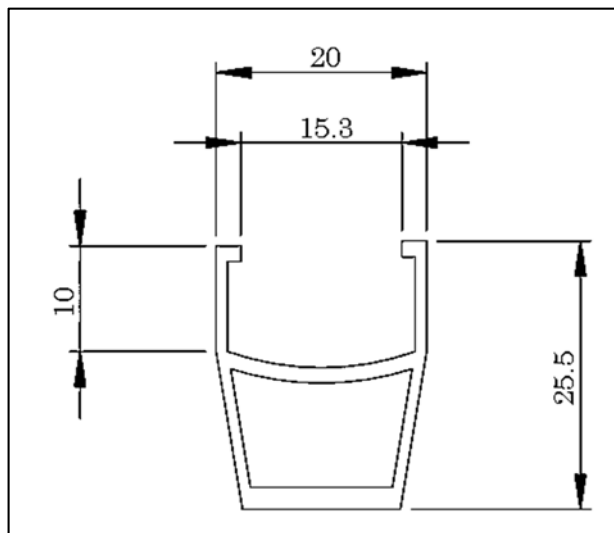


Figure 3.3-1. Rim profile used for analysis.

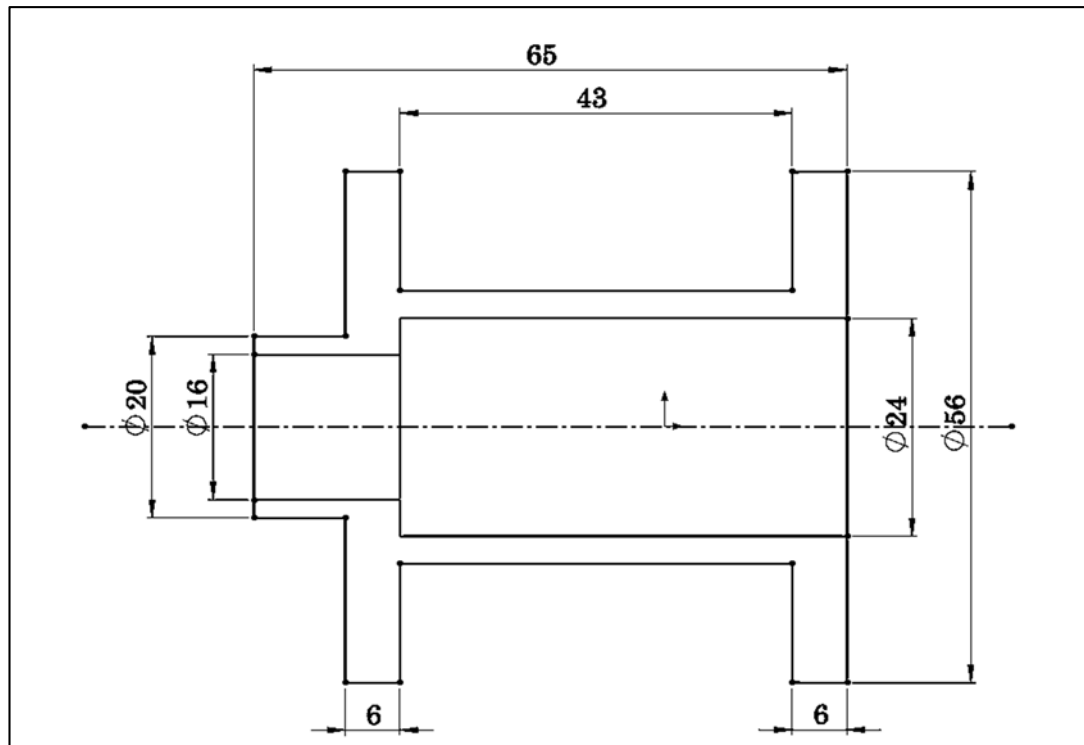


Figure 3.3-2. The basic hub used in the analysis.

For the range of spoke numbers tested, models were created for:

- The calculated optimised spoke geometries for 55 mm hub width.
- Conventional 2X patterns for 20 and 24 spoke wheels, 3X for 28, 32, 36 and 48 spoke wheels (Figure 3.3-3).
- The three commercial wheels described in Table 3.4-1 and shown in Figure 3.4-1, Figure 3.4-2 and Figure 3.4-3.

For the ease of modelling and simulation, the spokes were modelled as straight pull spokes and were attached to the hub and the rim without the use of spoke nipples to avoid using complicated geometry in the simulation software.

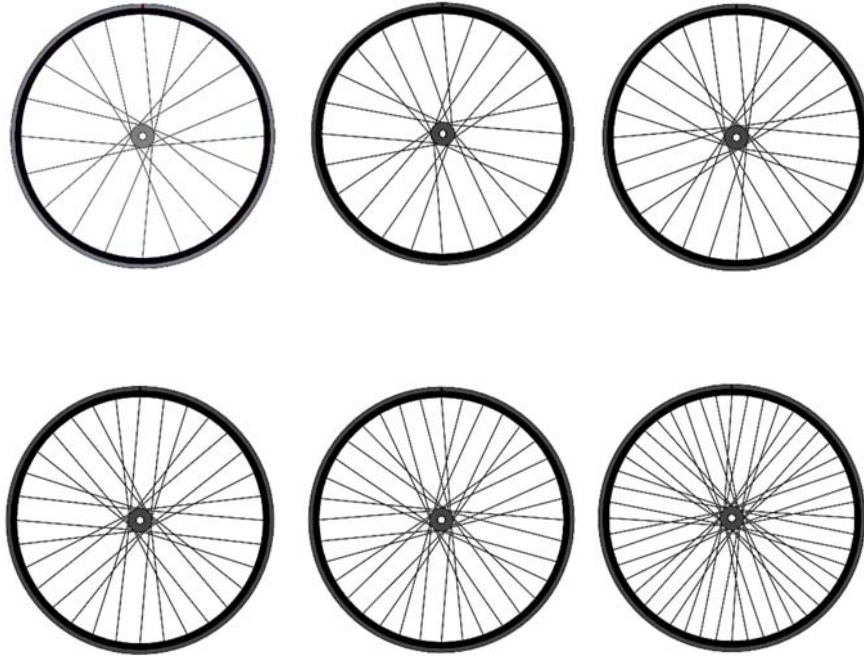


Figure 3.3-3. CAD Models (top left to right) - 20 spoke 2X, 24 spoke 2X and 28 spoke 3X. (Bottom left to right) - 32 spoke 3X, 36 spoke 3X, 48 3X.

3.4 Simulation of the optimised wheel geometries and commercial wheels

ANSYS® is an industry standard program used to perform finite element analysis. For this study, it has been used to perform static structural analysis of the optimised wheel geometries, conventional spoke pattern wheels and three commercially available wheels. Each of the commercial wheels have been designed and sold within the last 10 years and can be considered low profile aluminium clincher wheels with stainless steel spokes. Table 3.4-1 shows their key geometric properties.

CHAPTER 3 - METHODOLOGY

3.4 Simulation of the optimised wheel geometries and commercial wheels

Table 3.4-1. Properties of commercially available wheels used for comparison with optimised geometries.

Wheel	Spoke Number (N)	Rim Radius* (mm)	Hub Radius** (mm)	Spoke Diameter (mm)	Spoke Angle (deg)	Spoke Length (mm)
6700R (Figure 3.4-1)	20	300	24 (R) and 20 (L)	2 (slightly flattened)	90 (L and R)	304 (R) and 306 (L)
Gradient (Figure 3.4-2)	28	305	30 (L and R)	2 (round)	55 (L and R)	283 (R) and 285(L)
Circuit (Figure 3.4-3)	28	291	34 (R) & 20 (L)	2 (round)	0 (L) and 40	265 (L) and 270 (R)

*Measured centre of hub to the bottom of the brake track

** Measured from centre of hub flange hole to base of nipple on the rim



Figure 3.4-1. 6700R wheel with a spoke angle of 90°.

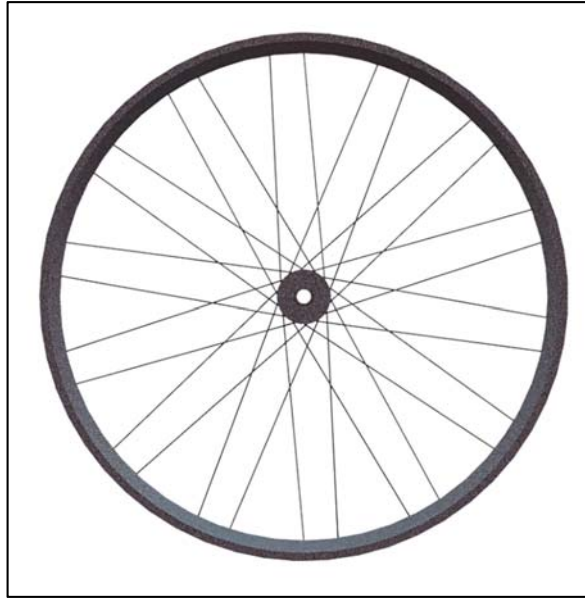


Figure 3.4-2. Gradient wheel with unevenly distributed spokes around the rim.



Figure 3.4-3. Circuit wheel with a high right hand side hub flange and low left hand side hub flange.

3.4.1 Simulation Pre-processing

The CAD models were imported into ANSYS® and the boundary conditions, summarised in Table 3.4-2, were applied. All three load cases had fixed supports

applied to the external hub faces to model the wheel installed in a bicycle frame. A 100 N load was added to a small surface on either the tyre bed or brake track. These surfaces are 0.1 mm thick and cover $1/360^{\text{th}}$ of the rim. The boundary conditions are shown in Figure 3.4-4 for a radial load, Figure 3.4-5 for a lateral load and Figure 3.4-6 for a torsional (tangential) load.

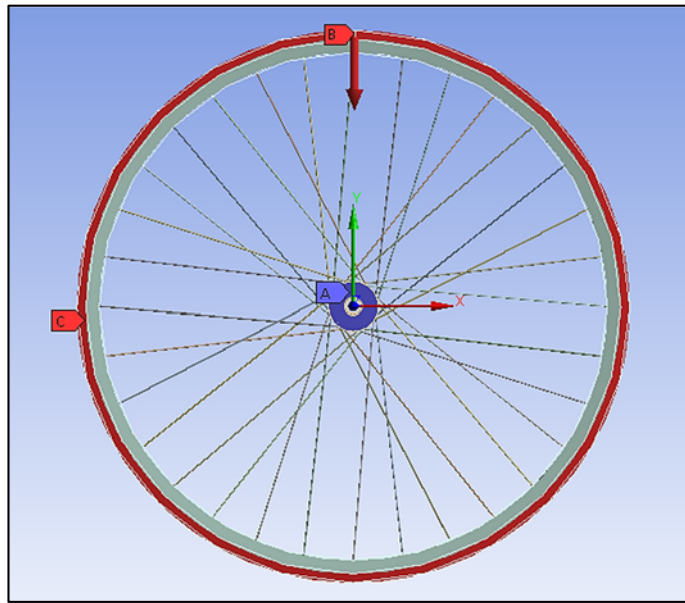


Figure 3.4-4. Fixed support at A, 100 N Radial load at B – along y-axis, and the additional displacement constraint at C to maintain deformation in the plane of the rim as assumed by the theoretical models used in this study.

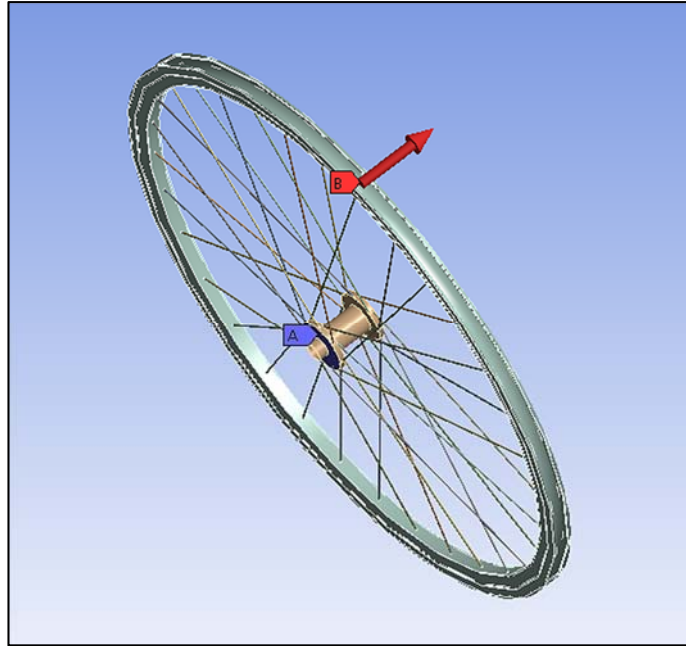


Figure 3.4-5. Fixed Support at A, 100 N Lateral load at B - along z-axis.

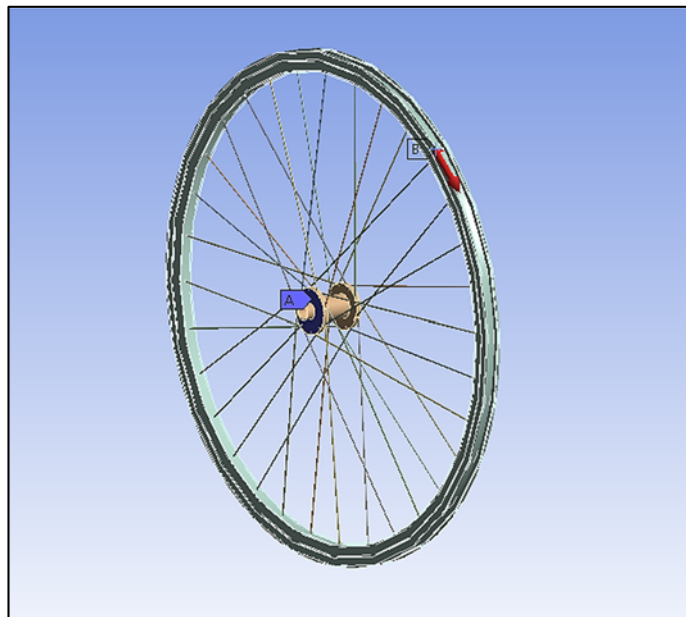


Figure 3.4-6. Fixed support at A, 100 N Torsional (tangential) load at B – along x-axis.

Table 3.4-2. Summary of boundary conditions used in the finite element analysis. The load in each scenario was 100 N.

Load Scenario	Load Location	Load orientation	Fixed Support	Displacement Constraints	
Radial	On the LHS and RHS brake track surface	Y-axis top of wheel towards hub	External Hub faces	For theory comparison: displacement was constrained in x and z directions, y direction free	For laboratory comparison: no displacement constraints were used.
Lateral	On the tyre bed	Z-Axis top of wheel perpendicular to the plane of the rim	External Hub faces	No extra constraint	No extra constraint
Torsional	On the tyre bed	X-Axis top of wheel tangential to surface	External Hub faces	No extra constraint	No extra constraint

Two wheels, out of the twenty-two wheels analysed, were selected to undergo a mesh convergence and quality analysis to identify the best meshing for the models. The results of the convergence analysis are shown in Appendix C.1. The analysis identified a tetrahedral mesh size of 7.5 mm as having acceptable quality and this mesh was applied to the rim and the hub of all of the wheel models. The spokes were meshed independently using ANSYS®'s sweep method to create 50 equal sections along the length of each spoke. An example of the mesh produced is shown in Figure 3.4-7.

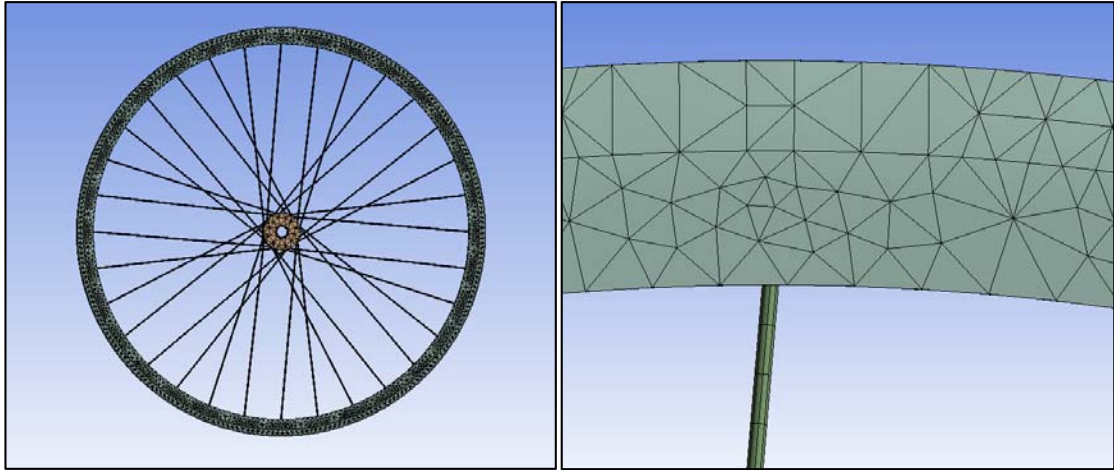


Figure 3.4-7. An example of the mesh used for finite element analysis. *Left* full wheel. *Right* Magnification of rim spoke connection. (32 spoke wheel).

3.4.2 Simulation Post-Processing

The results from the simulation were compared to the values obtained using the theoretical equations developed by Pippard et.al. A spread sheet was used to reproduce the values that were reported in Pippard's articles to ensure that the complex equations had been entered correctly. This process is further explained in the next section and Appendix D.1. The predicted theoretical displacements caused by loading a wire spoked wheel were calculated using the spread sheet and used to assess the accuracy of the values calculated in the finite element analysis.

3.4.2.1 Spread sheet using the Pippard Calculations

In order to use Pippard's theoretical formulae to compare the results of the finite element analysis, a spread sheet was created to reproduce his results for radial, tangential and side loading of wire wheels. For each load scenario, calculations for 70 combinations of K factors and ε values were performed. Appendix D.1 includes an example of the calculations for a wheel with the properties, $K=600$ and $\varepsilon=45^\circ$. Using

CHAPTER 3 - METHODOLOGY

3.4 Simulation of the optimised wheel geometries and commercial wheels

the formulae shown in Table 3.4-3, the displacements for each load scenario were calculated.

The theoretical values compared with the results from the finite element analysis are:

- u – radial displacement of the wheel rim under a radial load;
- v – tangential displacement of the wheel rim under torsional load; and
- w – the side displacement of the wheel rim under lateral load.

Table 3.4-3. Formulae for the displacements of wired spoked wheels. The full table, including values, can be seen in Appendix D.1. (t1 and t2 indicate tensile or compressive stress load respectively).

Parameter Name	Formula	Formula Reference
Displacements for Radial Load		
t1: u	$u = D \cosh(g \cdot \psi) + E \cos(a \cdot \psi) \cosh(b \cdot \psi) + F \sin(a \cdot \psi) \sinh(b \cdot \psi)$	Pippard & White 1932 Eqn 12 & 13
t1: v	$v = -[D/g \cdot \sinh(g \cdot \psi) + (Eb - Fa)/(a^2 + b^2) \cdot \cos(a \cdot \psi) \sinh(b \cdot \psi) + (Ea + Fb)/(a^2 + b^2) \cdot \sin(a \cdot \psi) \cosh(b \cdot \psi)]$	
t2: u	$u = D \cosh(g \cdot \psi) + E \cos(a \cdot \psi) \cosh(b \cdot \psi) + F \sin(a \cdot \psi) \sinh(b \cdot \psi)$	Pippard & White 1932 Eqn 12 & 13
t2: v	$v = -[D/g \cdot \sinh(g \cdot \psi) + (Eb - Fa)/(a^2 + b^2) \cdot \cos(a \cdot \psi) \sinh(b \cdot \psi) + (Ea + Fb)/(a^2 + b^2) \cdot \sin(a \cdot \psi) \cosh(b \cdot \psi)]$	
Displacements for Tangential Load		
u	$u = A \cosh(g \cdot \psi) + B \cos(a \cdot \psi) \sinh(b \cdot \psi) + C \sin(a \cdot \psi) \cosh(b \cdot \psi)$	Pippard & White 1932 Eqn 18 & 19
v	$v = -[A/g \cdot \cosh(g \cdot \psi) + (Bb - Ca)/(a^2 + b^2) \cdot \cos(a \cdot \psi) \cosh(b \cdot \psi) + (Ba + Cb)/(a^2 + b^2) \cdot \sin(a \cdot \psi) \sinh(b \cdot \psi)]$	
Displacements for Lateral Load		
x	$u = G \cosh(g \cdot \psi) + H \cos(a \cdot \psi) \cdot \cosh(b \cdot \psi) + U \sin(a \cdot \psi) \sinh(b \cdot \psi)$	Pippard & Francis 1932
w	$w = R/(n+1) \cdot [(n-g^2)/g^2 \cdot G \cosh(g \cdot \psi) - \cos(a \cdot \psi) \cosh(b \cdot \psi)/(a^2 + b^2)^2 \cdot \{H \cdot ((a^2 + b^2)^2 + n \cdot (a^2 - b^2)) + 2abnU\} - \sin(a \cdot \psi) \sinh(b \cdot \psi)/(a^2 + b^2)^2 \cdot \{U \cdot ((a^2 + b^2)^2 + n \cdot (a^2 - b^2)) - 2abnH\}]$	Pippard & Francis 1932 Eqn. 10

3.5 Laboratory Test Procedure

A 24 spoke front wheel was tested in the laboratory for each of the load cases analysed in this study. The results of these tests were used to establish the accuracy and reliability of the finite element analysis and the theoretical calculations.

The wheel was tested with a 44.9 N, 47.6 N and a 92.4 N static load in the radial, lateral and tangential configurations shown in Figure 3.5-1, Figure 3.5-2 and Figure 3.5-3. For each load case, the hub was fixed in position with no other constraints placed on the wheel. The deflections were measured using a dial gauge with a precision of +/- 0.005 mm.



Figure 3.5-1. The application and deformation of the 44.9 N radial load.

Photo courtesy of Peta Keller (2013).



Figure 3.5-2. The application and deformation measurement of the 92.4 N lateral load. *Photo courtesy of Peta Keller (2013).*



Figure 3.5-3. The application and deformation measurement of the 92.4 N tangential load. *Photo courtesy of Peta Keller (2013).*

CHAPTER 4 - RESULTS AND VALIDATION

4.1 The MATLAB® Optimisation Results

The features that are constant for all of the wheel models (except for the commercial models) are listed in Table 4.1-1 and the summarised outputs from Version 1.0 (V1.0) of the ‘*Optimised_wheel_stiffness.m*’ script, are shown in Table 4.1-2 to Table 4.1-7. An even dished (ED) wheel is included in the tables to highlight the different stiffness properties of front and rear wheels, however, in depth discussion of these results falls outside of the scope of this study. A copy of the full results from V1.0 of the optimisation script can be found in Appendix E.1.

Table 4.1-1. The constant values used throughout the theory and MATLAB® calculations unless otherwise stated.

Constant values	
Spoke Diameter (mm)	1.8
Flange Radius (mm)	25.0
Modulus of Elasticity - Rim (MPa)	69000
Modulus of Elasticity - Spoke (MPa)	193000
Moment of Inertia – Rim - I_{xx} (mm ⁴)	12058
Moment of Inertia – Rim - I_{yy} (mm ⁴)	5570
Hub width (mm)	55
Nomenclature for Wheel Identification	
<i>ED</i> = Evenly dished	
<i>ES</i> = Even spoke numbers LH and RHS	
<i>2X</i> = 2 cross lacing pattern (Figure 2.2-3a)	
<i>3X</i> = 3 cross lacing pattern (Figure 2.2-3b)	

4.1.1 20 Spoke Wheels Optimisation Results and Discussion

Table 4.1-2 displays the MATLAB® calculated values for the 20 spoke wheel models. The 20 Opt has an improved torsional stiffness over the 20 2X and 20 2X ED wheel but its TS is still slightly less than the TS of the 6700R wheel. The 6700R wheel has different hub flange radii, an even number of spokes on both sides and a larger spoke angle than the 20 Opt wheel. These differences in geometry could account for both the slight improvement in torsional stiffness and the similar lateral stiffness values. It is also noted that the LHS and RHS lateral stiffness for the 20 Opt wheel are close in magnitude, whereas the respective stiffness values of the 6700R are quite different. The script also recommended less spokes be used on the LHS of the wheel. In this instance, the spoke ratio between left and right hand sides is 2:3. The suggested spoke angles for the Opt wheel are 72° (LHS) and 78° (RHS).

Table 4.1-2. MATLAB® results for the 20 spoke wheels. The optimised wheel has a spoke ratio of 2:3.

Property	Wheel ID			
	20 2X	20 2X ED	20 Opt	6700R*
Total Number of Spokes (N)	20	20	20	20
Number of Spokes - LHS	10	10	8	10
LHS Spoke angle (μ) (deg)	72	72	72	90
Number of Spokes - RHS	10	10	12	10
RHS Spoke angle (μ) (deg)	72	72	78	90
Torsional Stiffness (N.mm/deg)	12218.0	12229.5	12458.5	12492.2
Total Lateral Stiffness (N/mm)	6.4	6.0	5.9	6.0
LHS Lateral Stiffness (N/mm)	10.6	6.0	7.3	10.1
RHS Lateral Stiffness (N/mm)	2.2	6.0	4.5	1.9

* - Flange radius as per Table 3.4-1

4.1.2 24 Spoke Wheels Optimisation Results and Discussion

Table 4.1-3 displays the MATLAB® results for the comparison of the conventional 2X and even dish (ED) wheels with the 24 Opt wheel. The torsional stiffness of the 24 Opt wheel is much greater than that of the other two wheels while it only has a slightly smaller lateral stiffness. Again, the script recommended different spoke numbers on the LHS and RHS. This time a spoke ratio of 5:7 was recommended. The decrease in overall lateral stiffness of the 24 Opt wheel is likely to be due to how the script identifies possible optimal combinations. Modifying the script in future studies to find all positive values, instead of only those within at least 40% of the maximum, may improve this value for the optimised geometries. The suggested spoke angles for the Opt wheel are 76° (LHS) and 64° (RHS).

Table 4.1-3. MATLAB® results for the 24 spoke wheels. The optimised wheel has a spoke ratio of 5:7.

Property	Wheel ID		
	24 2X	24 2X ED	24 Opt
Total Number of Spokes (N)	24	24	24
Number of Spokes - LHS	12	12	10
LHS Spoke angle (μ) (deg)	60	60	76
Number of Spokes - RHS	12	12	14
RHS Spoke angle (μ) (deg)	60	60	64
Torsional Stiffness (N.mm/deg)	12786.0	12798.4	14164.1
Total Lateral Stiffness (N/mm)	8.0	7.5	7.2
LHS Lateral Stiffness (N/mm)	12.8	7.5	9.7
RHS Lateral Stiffness (N/mm)	3.1	7.5	4.8

4.1.3 28 Spoke Wheels Optimisation Results and Discussion

Table 4.1-4 displays the MATLAB® results of the 28 spoke wheels tested in this study. The results of the Gradient and Circuit wheel need to be considered carefully due to their different hub geometries (refer to Table 3.4-1). The hub flange radius of the

CHAPTER 4 - RESULTS AND VALIDATION

4.1 The MATLAB® Optimisation Results

Gradient wheel is 30 mm compared to the 25 mm radius used on the 3X, ED and Opt wheel and it is this difference that results in the higher torsional stiffness value. The Circuit wheel features a radially spoked LHS with a 20 mm hub flange radius, as well as a 34 mm hub flange radius on the RHS for the angled spokes. The use of radial spokes on the LHS of the Circuit wheel would cause the significant reduction of torsional stiffness as well as cause the increase in lateral stiffness when compared to the other wheels.

Comparing the 3X, ED and Opt wheels with the same hub geometry, the Opt wheel has improved torsional stiffness with a slightly reduced lateral stiffness. The spoke ratio for the 28 Opt wheel is 5:9. The suggested spoke angles for the Opt wheel are both 78°. Also note that due to the radial spokes on the LHS of the Circuit wheel, the LHS and RHS lateral stiffness values appear to be reversed when compared to the other wheels.

Table 4.1-4. MATLAB® results for the 28 spoke wheels. The optimised wheel has a spoke ratio of 5:9.

Property	Wheel ID				
	28 3X	28 3X ED	28 Opt	Gradient*	Circuit*
Total Number of Spokes (N)	28	28	28	28	28
Number of Spokes - LHS	14	14	10	14	14
LHS Spoke angle (μ) (deg)	77.1	77.1	78	55	0
Number of Spokes - RHS	14	14	18	14	14
RHS Spoke angle (μ) (deg)	77.1	77.1	78	55	40
Torsional Stiffness (N.mm/deg)	17575.7	17592.0	17660.3	20130.0	8827.8
Total Lateral Stiffness (N/mm)	8.8	8.2	7.9	9.6	10.1
LHS Lateral Stiffness (N/mm)	14.7	8.2	8.2	16.3	2.4
RHS Lateral Stiffness (N/mm)	2.8	8.3	7.7	2.9	17.7

* - Flange radius as per Table 3.4-1

4.1.4 32 Spoke Wheels Optimisation Results and Discussion

Table 4.1-5 displays the MATLAB® results of the 32 spoke wheels. Two optimised wheels are reported to allow a direct comparison between the values for the unbalanced spoked wheel, the 32 Opt, with the values for the balanced spoked wheel, the 32 Opt ES. Comparing these wheels to the conventionally spoked 32 3X wheel, the Opt ES has reduced torsional stiffness but increased lateral stiffness (the best LS of the three wheels), while the 32 Opt (with a spoke ratio of 3:5) has the best torsional stiffness and less lateral stiffness than the Opt ES and the 3X wheel. The suggested spoke angles for the Opt wheel are 70° (LHS) and 69° (RHS) and for the Opt ES wheel the angles are 55° (LHS) and 78° (RHS).

Table 4.1-5. MATLAB® results for the 32 spoke wheels. The optimised wheel has a spoke ratio of 3:5 (32 Opt) and 1:1 (32 Opt ES).

Property	Wheel ID			
	32 3X	32 3X ED	32 Opt	32 Opt ES
Total Number of Spokes (N)	32	32	32	32
Number of Spokes - LHS	16	16	12	16
LHS Spoke angle (μ) (deg)	67.5	67.5	70	55
Number of Spokes - RHS	16	16	20	16
RHS Spoke angle (μ) (deg)	67.5	67.5	69	78
Torsional Stiffness (N.mm/deg)	18806.2	18824.1	19174.5	17864.2
Total Lateral Stiffness (N/mm)	10.3	9.7	9.4	10.6
LHS Lateral Stiffness (N/mm)	17.0	9.7	10.6	15.6
RHS Lateral Stiffness (N/mm)	3.7	9.8	8.3	5.7

4.1.5 36 Spoke Wheels Optimisation Results and Discussion

Table 4.1-6 displays the MATLAB® results of the 36 spoke wheels. The 36 Opt, with a spoke ratio of 1:2, has the best torsional stiffness but its lateral stiffness is significantly

CHAPTER 4 - RESULTS AND VALIDATION

4.1 The MATLAB® Optimisation Results

lower than the 3X wheel. The suggested spoke angles for the Opt wheel are 76° (LHS) and 80° (RHS).

Table 4.1-6. MATLAB® results for the 36 spoke wheels. The optimised wheel has a spoke ratio of 1:2.

Property	Wheel ID		
	36 3X	36 3X ED	36 Opt
Total Number of Spokes (N)	36	36	36
Number of Spokes - LHS	18	18	12
LHS Spoke angle (μ) (deg)	60	60	76
Number of Spokes - RHS	18	18	24
RHS Spoke angle (μ) (deg)	60	60	80
Torsional Stiffness (N.mm/deg)	19179.0	19197.7	22730.5
Total Lateral Stiffness (N/mm)	11.9	11.2	9.9
LHS Lateral Stiffness (N/mm)	19.2	11.2	9.2
RHS Lateral Stiffness (N/mm)	4.7	11.2	10.8

4.1.6 48 Spoke Wheels Optimisation Results and Discussion

Table 4.1-7 displays the MATLAB® results for the 48 spoke wheels. The Opt wheel has a spoke ratio of 3:5 with the suggested spoke angles of 80° (LHS) and 60° (RHS). The 48 Opt wheel has 150% improvement of TS over the 3X wheel, but the calculated lateral stiffness is only 83% of the 3X wheel's LS.

Table 4.1-7. MATLAB® results for the 48 spoke wheels. The optimised wheel has a spoke ratio of 3:5.

Property	Wheel ID		
	48 3X	48 3X ED	48 Opt
Total Number of Spokes (N)	48	48	48
Number of Spokes - LHS	24	24	18
LHS Spoke angle (μ) (deg)	45	45	80
Number of Spokes - RHS	24	24	30
RHS Spoke angle (μ) (deg)	45	45	60
Torsional Stiffness (N.mm/deg)	18042.2	18060.4	27404.8
Total Lateral Stiffness (N/mm)	16.7	15.7	13.9
LHS Lateral Stiffness (N/mm)	25.0	15.7	16.3
RHS Lateral Stiffness (N/mm)	8.3	15.7	11.8

4.1.7 Conclusions from MATLAB®

The optimised geometries from Version 1.0 of the '*Optimised_Wheel_Stiffness.m*' script show consistently improved torsional stiffness over their conventionally spoked counterparts. However, the 6700R wheel has better torsional and lateral stiffness than the 20 Opt wheel (Table 4.1-2). Assessing all of the data obtained from MATLAB®, it appears the assumption to balance the RH and LH side load stiffness values was unnecessary, with both the conventionally spoked and commercial wheels showing a large difference between lateral stiffness for the alternate LH and RH loads.

The optimisation script also appeared to miss wheel geometries with better stiffness properties. The script was reviewed to identify what caused these misses. On review, changes were made to the script to remove the lateral stiffness assumption (Section 3.2.1) and to locate the optimised geometry slightly differently. The revised script "*Optimised_wheel_stiffness_Ver_2.m*" can be seen in (Appendix F.1).

4.1.7.1 Delta Review of the 'Optimised_wheel_stiffness.m' Versions 1.0 and 2.0

The first change implemented to the script occurs in cell '`%% Lateral and Torsional Stiffness`'. In V2.0, the nested loop, used to calculate the torsional and lateral stiffness values and add them to a matrix, has been changed so that the average lateral stiffness is calculated for all of the possible geometries. Outside of the loop, the values in the *LSave* matrix are now changed to zero if *gLSL* or *gLSR* values are less than one to remove all of the negative and low stiffness values. V2.0 then proceeds to display the maximum lateral and torsional stiffness values in the same way as V1.0.

The next change in the code is in '`%% Optimisation loop`'. Version 2.0 no longer has the option to optimise by a percentage of torsional stiffness. Instead, the designer can continue to optimise the geometry based on the percentage of lateral stiffness that is required. The nested loops that identified the range of variables to recalculate has also been deleted in V2.0.

The method used to identify the optimised geometry in the '`%% Locate and post optimal values`' cell was also changed significantly. The '`%% Locate and post optimal values`' cell in V2.0 changes all of the *LSave* values to zero if they are less than the maximum lateral stiffness, *LSm*, multiplied by the percentage of stiffness required, *LSper*. The code then makes all of the torsional stiffness values equal to zero where *LSave* is equal to zero, so that only the values coinciding with LS values that are greater than the minimum required value, are assessed further. The remaining stiffness values are then converted to a percentage of maximum stiffness and combined in the *Avp* matrix. The maximum value in the *Avp* matrix is then identified and the indices are used to extract the details of the optimal geometries and post them to the MATLAB® command window. The designer is then given the choice to fine tune the selection, by

repeating the process with different *LSper* values, until they find the combination that meets the required specifications.

There were no changes to the arbitrarily set values mentioned in Section 3.2.1.

4.1.7.2 MATLAB® Optimised Geometry Results for V2.0

The identified optimal geometries using '*Optimised_wheel_stiffness_Ver_2*' are shown in Table 4.1-8. Comparing the results to those in Table 4.1-2 to Table 4.1-7:

1. The optimised geometry now has even spoke numbers on both sides.
2. The torsional stiffness is greater than all other comparable wheels (the 28 spoke Gradient wheel has a larger hub flange radius so it has a TS that is still greater than the 28 Opt-V2.0).
3. The lateral stiffness values are closer to the conventionally spoked wheels.
4. The optimised spoke angles are similar for each total spoke number.

The 'V2.0' nomenclature is used to distinguish the optimised geometries calculated from V2.0 of the optimisation script from all of the other geometries in this study.

CHAPTER 4 - RESULTS AND VALIDATION
 4.2 The CAD Models of the optimised geometries

Table 4.1-8. The optimised geometries and stiffness values calculated using 'Optimised_wheel_stiffness_Ver_2' for all total spoke categories.

Property	Wheel ID					
	20 Opt -V2.0	24 Opt -V2.0	28 Opt -V2.0	32 Opt -V2.0	36 Opt -V2.0	48 Opt -V2.0
Total Number of Spokes (N)	20	24	28	32	36	48
Number of Spokes - LHS	10	12	14	16	18	24
LHS Spoke angle (μ) (deg)	77	77	77	77	77	78
Number of Spokes - RHS	10	12	14	16	18	24
RHS Spoke angle (μ) (deg)	81	81	81	81	81	81
Torsional Stiffness (kg.mm/deg)	12610.6	15132.7	17654.9	20177.0	22699.1	30316.5
Total Lateral Stiffness (kg/mm)	6.2	7.5	8.7	10.0	11.2	14.9
LHS Lateral Stiffness (kg/mm)	11.3	13.6	15.8	18.1	20.4	27.1
RHS Lateral Stiffness (kg/mm)	1.1	1.4	1.6	1.8	2.1	2.7

4.2 The CAD Models of the optimised geometries

Figure 4.2-1 to Figure 4.2-6 shows the CAD models of the optimised geometries produced from Version 1.0 of the MATLAB® optimisation script. Each wheel is shown with all spokes, the LHS spoke pattern only, and the RHS spoke pattern only, to highlight the difference in spoke numbers recommended for each side. Due to the uneven distribution of spokes, the spokes could not be patterned in conventional patterns, or alternated from left and right hand sides, around the rim. The spokes were subsequently grouped together to try and distribute the LHS and RHS spokes as evenly as possible around the rim.



Figure 4.2-1. 20 spoke wheel optimised spoke geometry - (*left*) full wheel; (*centre*) 8 LHS spokes; (*right*) 12 RH spokes.



Figure 4.2-2. 24 spoke wheel optimised spoke geometry - (*left*) full wheel; (*centre*) 10 LH spokes; (*right*) 14 RH spokes.



Figure 4.2-3. 28 spoke wheel optimised spoke geometry - (*left*) full wheel; (*centre*) 10 LH spokes; (*right*) 18 RH spokes.



Figure 4.2-4. 32 spoke wheel optimised spoke geometry - (left) full wheel; (centre) 12 LH spokes; (right) 20 RH spokes.



Figure 4.2-5. 36 spoke wheel optimised spoke geometry - (left) full wheel; (centre) 12 LH spokes; (right) 24 RH spokes.



Figure 4.2-6. 48 spoke wheel optimised spoke geometry - (left) full wheel; (centre) 18 LH spokes; (right) 30 RH spokes.

The models of the ‘V2.0’ wheels are not shown since they are quite similar to those shown in Figure 3.3-3 with the same spoke numbers on each side and only small changes in spoke angles that are too difficult to detect in the models.

4.3 The Finite Element Analysis Results

All of the wheels were analysed using ANSYS® Structural Analysis (Section 3.4) to find the deformations that are reported in Table 4.3-1. Table 4.3-1 also includes the comparison between the theoretical values obtained using Pippard's formulae (Table 3.4-3) and the FE analysis. The percentage difference is calculated using Equation 4.1.

$$\% = \frac{|theory\ value - FEA\ value|}{theory\ value} \times 100\% \quad (4.1)$$

The K , ε and Δ values used in the theoretical calculations were calculated using Equations 4.2, 4.3 and 4.4 for a quadruple spoke system where the spokes are not in the plane of the rim (Pippard & White 1932).

$$K' = \frac{2\Delta E_2 R^3 \cos \phi}{E_1 I (1 + \cos^2 \varepsilon \tan^2 \phi)} \quad (4.2)$$

$$K_0^2 = (K'_1 \cos \varepsilon_1 + K'_2 \cos \varepsilon_2) (K'_1 \sec \varepsilon_1 + K'_2 \sec \varepsilon_2) \quad (4.3)$$

$$\tan^2 \varepsilon_0 = \frac{K'_1 \sin \varepsilon_1 \tan \varepsilon_1 + K'_2 \sin \varepsilon_2 \tan \varepsilon_2}{K'_1 \cos \varepsilon_1 + K'_2 \cos \varepsilon_2} \quad (4.4)$$

Where E_2 is the elastic modulus of the spokes, E_1 is the elastic modulus of the rim, I is the second moment of inertia of the rim about its bending axis, R is the rim radius, ε is the spoke angle at the rim, ϕ is the dish angle and the subscripts 1 and 2 (in equations 4.3 and 4.4) refer to the respective LHS and RHS values.

CHAPTER 4 - RESULTS AND VALIDATION

4.3 The Finite Element Analysis Results

Table 4.3-1. Wheel deformation comparison between theoretical calculations and FEA.

Wheel ID	Radial Load			Torsional Load			Lateral Load L to R			Lateral Load R to L		
	Theory	FEA	%	Theory	FEA	%	Theory	FEA	%	Theory	FEA	%
20 2X	0.0109	0.0117	7%	0.2012	0.7958	296%	1.6312	1.9071	17%	1.6312	1.9071	17%
6700R	0.0109	0.0101	7%	0.2224	0.8670	290%	1.6313	1.2824	21%	1.6313	1.2824	21%
20 Opt	0.0109	0.0117	7%	0.2145	0.5850	173%	1.6318	3.4400	111%	1.6318	3.4400	111%
20 Opt-V2	0.0109	0.0117	7%	0.2012	0.7674	281%	1.6312	1.9478	19%	1.6312	1.9478	19%
24 2X	0.0095	0.0113	19%	0.2156	0.6858	218%	1.4186	1.8228	28%	1.4186	1.8228	28%
24 Opt	0.0095	0.0108	14%	0.1797	0.6010	234%	1.4188	1.9939	41%	1.4188	1.9939	41%
24 Opt-V2	0.0095	0.0104	9%	0.1677	0.5238	212%	1.4183	1.6035	13%	1.4183	1.6035	13%
28 3X	0.0085	0.0095	12%	0.1437	0.4132	188%	1.2605	1.4063	12%	1.2605	1.4063	12%
Gradient	0.0085	0.0085	0%	0.1331	0.2568	93%	1.2604	1.1863	6%	1.2604	1.1863	6%
Circuit	0.0085	0.0085	1%	0.3332	0.7474	124%	1.2611	1.2582	0%	1.2611	1.2582	0%
28 Opt	0.0085	0.0097	14%	0.1437	0.3905	172%	1.2611	2.6868	113%	1.2611	2.6868	113%
28 Opt-V2	0.0085	0.0095	12%	0.1437	0.4107	186%	1.2605	1.4136	12%	1.2605	1.4136	12%
32 3X	0.0077	0.0089	16%	0.1391	0.3687	165%	1.1382	1.2259	8%	1.1382	1.2259	8%
32 Opt	0.0077	0.0089	16%	0.1377	0.3229	134%	1.1387	1.5299	34%	1.1387	1.5299	34%
32 ES Opt	0.0077	0.0089	16%	0.1618	0.3860	139%	1.1388	1.2054	6%	1.1388	1.2054	6%
32 Opt-V2	0.0077	0.0089	16%	0.1258	0.3411	171%	1.1381	1.2662	11%	1.1381	1.2662	11%
36 3X	0.0070	0.0084	20%	0.1471	0.3512	139%	1.0404	1.0889	5%	1.0404	1.0889	5%
36 Opt	0.0071	0.0084	19%	0.1118	0.2933	162%	1.0408	1.5895	53%	1.0408	1.5895	53%
36 Opt-V2	0.0070	0.0085	21%	0.1118	0.2945	163%	1.0402	1.1492	10%	1.0402	1.1492	10%
48 3X	0.0057	0.0072	27%	0.1518	0.3513	131%	0.8356	0.8331	0%	0.8356	0.8331	0%
48 Opt	0.0057	0.0073	28%	0.0909	0.2739	201%	0.8357	1.1038	32%	0.8357	1.1038	32%
48 Opt-V2	0.0057	0.0073	28%	0.0839	0.2077	148%	0.8353	0.9160	10%	0.8353	0.9160	10%

4.3.1 Validation of the FE Analysis

Main findings:

- There are inconsistencies in the magnitude of error between the FEA and theoretical results under lateral loading with some of the results closely matching the theoretical values (48 3X, 36 3X and Circuit), while others are out by over 100% (28 Opt and 20 Opt).
- The radial loading response is consistent for all wheel models when the additional displacement constraints are added (refer to Figure 3.4-4).

- The torsional deformation values calculated in this analysis are considerably larger than those predicted by the theory.

To assess the validity of the FEA results especially under torsional load, laboratory testing was performed in accordance with Section 3.5.

4.3.1.1 Laboratory Results and Discussion

Table 4.3-2 shows the data collected from the laboratory testing using the techniques depicted in Figure 3.5-1, Figure 3.5-2 and Figure 3.5-3, compared to the theoretical and FEA predicted values.

The wheel tested was spoked similarly to the 28 spoke Gradient wheel, with the spokes located on the rim in pairs 40 mm apart. The loads used were 44.88 N, 47.56 N and 92.44 N. These were applied at the valve hole in the rim (between the spokes – as opposed to directly on the spokes) of the wheel when it was fixed at the hub (Section 3.5).

Table 4.3-2. Measured wheel deformation under radial, lateral and torsional loading compared to FEA and theoretical values.

Load Type	Deformation (mm)								
	Load (4.575kg/44.88N)			Load (4.848kg/47.56N)			Load (9.423kg/92.44N)		
	Lab	FEA	Theory	Lab	FEA	Theory	Lab	FEA	Theory
Lateral	0.920	0.5915	0.7517	0.970	0.6268	0.7966	1.910	1.2183	1.5483
Radial	0.024	0.0202	0.0051	-	0.0214	0.0054	0.042	0.0415	0.0105
Torsional	0.530	0.6045	0.2565	-	0.6406	0.2718	1.150	1.2452	0.5283

4.3.1.2 Discussion of the Lateral Loading test

The simulation and theoretical results for the lateral load cases were within 25% of each other with the theory predicting a greater deformation than the FEA model. Both of these values were within 35% of the laboratory result with the theoretical value more accurate than the FEA value. Considering that the rim cross-section in the simulation is based on Figure 3.3-1 and that it is likely to be different from the real cross-section of the rim, variations between all of the results are likely. However, the results are still within acceptable limits, even with the estimated geometry of the rim, so it was concluded that both the simulation and theoretical calculations provide adequate predictions of the deformation seen under lateral loading for this analysis.

4.3.1.3 Discussion of the Radial Loading test

The radial load deformations of the test wheel were predicted better by the FEA model (without the additional displacement constraints) than the theoretical model, with the variance being 16% for the 44.88 N load and only 2% for the 92.44 N load. The 400% difference between the theory and the laboratory deformations could not be readily explained. After re-examining the literature, it was noted that Pippard had made the simplifying assumptions that deformations only occur within the plane of the rim whereas in the laboratory test, the wheel was fixed in all directions at the hub but the rim was free to move in any direction when loaded. It was concluded that for the purposes of this study, the deformation under radial loading is predicted better by the FEA model without the additional constraints applied (Table 3.4-2) than by the theoretical equations.

As a result of the laboratory testing, the initial simulations for the radial load case were repeated without the additional constraints. The new deformations are shown in Table

CHAPTER 4 - RESULTS AND VALIDATION

4.3 The Finite Element Analysis Results

4.3-3. The original values are included for a comparison. The deformations seen in the unconstrained analysis are approximately three to seven times greater than the deformations seen in the constrained analysis.

Table 4.3-3. Simulation results for the 100 N radial load scenario with and without displacement constraints on the rim.

* - no displacement constraints.

Wheel ID	Radial Load	
	FEA	FEA*
20 2X	0.0117	0.0717
6700R	0.0101	0.0522
20 Opt	0.0117	0.2221
20 Opt-V2.0	0.0117	0.0721
24 2X	0.0113	0.0820
24 Opt	0.0106	0.0394
24 Opt-V2.0	0.0095	0.0583
28 3X	0.0095	0.0421
Gradient	0.0085	0.0505
Circuit	0.0085	0.0340
28 Opt	0.0097	0.2324
28 Opt-V2.0	0.0085	0.0424
32 3X	0.0089	0.0379
32 Opt	0.0089	0.0665
32 ES Opt	0.0089	0.0364
32 Opt-V2.0	0.0077	0.0383
36 3X	0.0084	0.0350
36 Opt	0.0084	0.0579
36 Opt-V2.0	0.0070	0.0360
48 3X	0.0072	0.0280
48 Opt	0.0073	0.0308
48 Opt-V2.0	0.0057	0.0287

4.3.1.4 Discussion of the Torsional Loading test

Deformations measured in the laboratory for the torsional load cases were greater than 200% of the predicted theoretical values while the FEA predicted values were within 8 – 14%. The difference between the FEA, laboratory results and the results of the theoretical calculation can be attributed to the assumptions made by Pippard for a torsional loading scenario. By assuming the spokes could be replaced by a thin disk, Pippard managed to simplify his equations. However, by making this assumption some shear force resistance has been added (imagine trying to twist a solid plate compared to a latticed disk) causing a reduction in the magnitude of the predicted deformations.

The conditions of the FE analysis were also changed to see if the large discrepancy between the theoretical and FEA/laboratory results could be resolved. Changes made to the simulation included:

- adding extra constraints to prevent out of plane deformation,
- changing the load location from at the spokes to between spokes,
- changing how the spokes were patterned; and
- changing the load surface area from 1% of the rim circumference to up to 10% of the rim circumference.

However, these changes did not lead to any significant improvement in the correlation between the theoretical and FEA results.

It was also noted that the simulation showed tensile and compressive principal stresses on the pulling spokes (spokes angled with the load direction) and the pushing spokes

(angled against the load direction) respectively. This is the expected behaviour (Figure 4.3-1) and provided further evidence of the correct setup of the FEA model.

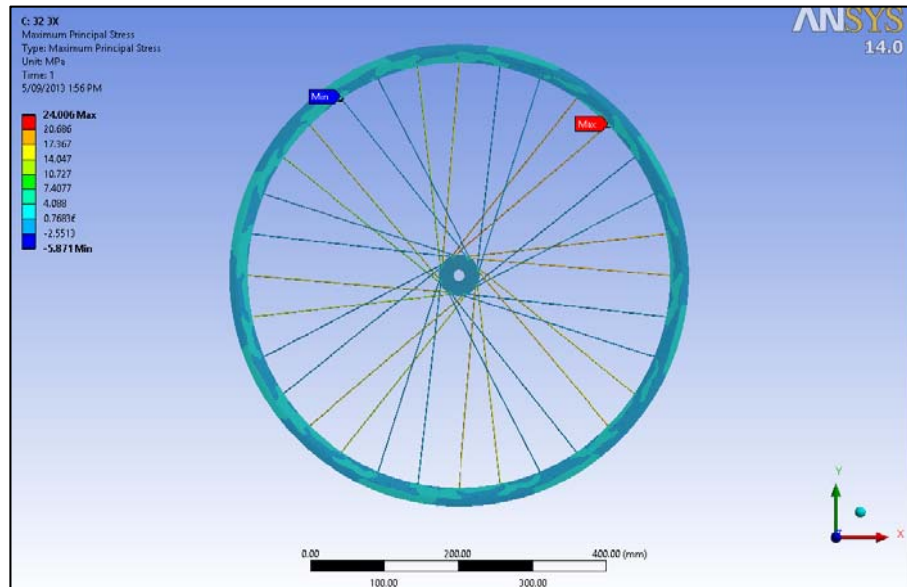


Figure 4.3-1. The maximum principal stress experienced by a 32 3X wheel under a 100 N torsional loading applied at the top centre of the rim aligned along the x-axis. The spokes angled back opposite the load direction experience compressive stress, whereas those angled in the direction of the load experience tensile stress.

It was concluded that the applicability of the chosen theoretical equations to the torsional loading scenario is questionable. Investigations as to why this is the case can be performed as part of any future work. However, because of the close correlation between the FEA results and the laboratory measured values (Table 4.3-2), it has been concluded that the FEA results for torsional deformation are reliable enough for the purposes of this study.

4.3.1.5 Investigation of the FE analysis of the 20 Opt and 28 Opt wheels

Of all the wheels simulated, the V1.0 optimised wheels (unbalanced spoke arrangement i.e. more spokes on one side than the other) showed a greater variation between predicted and simulated values. Two wheels in particular, the 20 Opt and 28 Opt, initially had a variation greater than 100% for the lateral load scenario. As part of the investigation into why the results for these wheels were so different, the wheels were remodelled in CAD using the same spoke angles but a slightly different spoke distribution around the rim (Figure 4.3-2 and Figure 4.3-3). They were then reanalysed in ANSYS® with the results shown in Table 4.3-4.

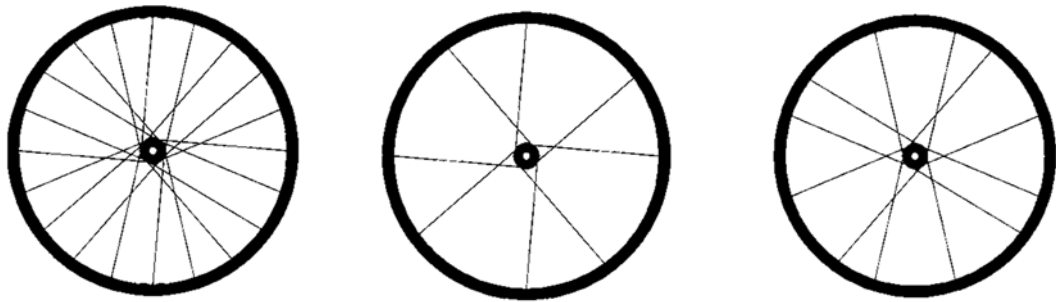


Figure 4.3-2. The 20 Opt-1b wheel with a small change to the spoke distribution. Compare to Figure 4.2-1.

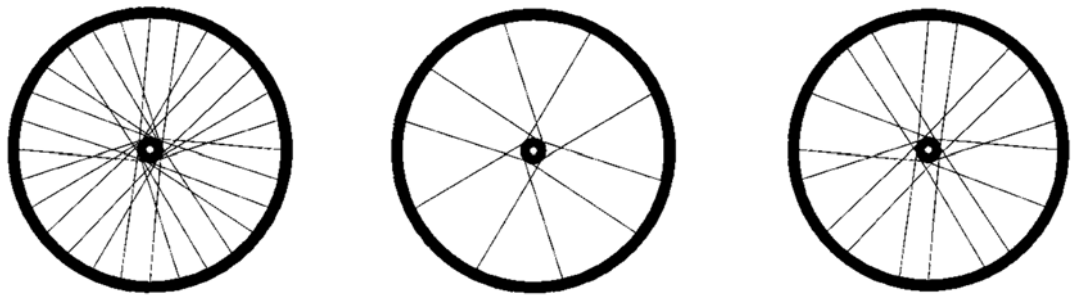


Figure 4.3-3. The 28 Opt-1b wheel with a small change to the spoke distribution. Compare to Figure 4.2-3.

Table 4.3-4. The FEA results of the modified optimised geometry wheels. Note: R – Radial, L – Lateral, T – Torsional, D – Deformation. Theoretical values shown in brackets. * - No additional constraints used.

Wheel ID	Radial		Lateral	Torsional
	RD* (mm)	RD (mm)	LD (mm)	TD (mm)
20 Opt-1b	0.0679	0.0114 (0.0109)	2.1280 (1.6318)	0.7027 (0.2145)
28 Opt-1b	0.0285	0.0096 (0.0085)	1.6047 (1.2611)	0.4339 (0.1437)

Changing the spoke pattern in the CAD models significantly improved the correlation between FEA and theoretical values. The radial deformations (with additional displacement constraints in the FEA) came to within 5% and 1% of the theory for the 20 Opt-1b and 28 Opt-1b wheel respectively. The lateral deformation came back to within 30% for both wheels. The torsional deformation only changed slightly and the large difference between the FEA and theoretical values remained.

The differences between the theoretical and FEA values for the torsional load scenario range between 93% and 300% and the applicability of the theoretical results to the torsional load case has been discussed previously in Section 4.3.1.4.

4.4 Radial, Lateral and Torsional Stiffness values calculated from the FE Analysis

The radial, lateral and torsional stiffness values that were calculated from the FEA results are shown in Table 4.4-1. The stiffness values are compared to the values published by Price and Akers for a 36 spoke wheel, and to the results published online by Roues Artisanales.

Table 4.4-1. Radial – no extra constraints, lateral and torsional stiffness of the analysed wheels based on the results of the finite element analysis.

Wheel ID	Radial Stiffness	Lateral Stiffness	Torsional Stiffness
	kg/mm	kg/mm	kg.mm/deg
20 2X	142	5.3	17841
6700R	195	7.9	16663
20 Opt	46	3.0	24695
20 Opt-V2.0	141	5.2	18501
20 Opt-1b	150	4.8	20559
24 2X	124	5.6	21064
24 Opt	259	5.1	24036
24 Opt-V2.0	175	6.4	27580
28 3X	242	7.2	34967
Gradient	202	8.6	56247
Circuit	300	8.1	19329
28 Opt	44	3.8	36991
28 Opt-V2.0	240	7.2	35172
28 Opt-1b	357	6.4	33297
32 3X	269	8.3	39186
32 Opt	153	6.7	44744
32 ES Opt	280	8.5	37426
32 Opt-V2.0	266	8.1	42350
36 3X	291	9.4	41139
36 Opt	176	6.4	49256
36 Opt-V2.0	283	8.9	49049
48 3X	364	12.2	41118
48 Opt	331	9.2	52749
48 Opt-V2.0	355	11.1	69568

The radial and lateral stiffness values were calculated by dividing the load (in kilograms) by the deformation in either the radial or lateral direction. The torsional stiffness value was calculated by dividing the applied moment (in kg.mm) by the deformation (in degrees).

The torsional deformation (in mm) was converted to degrees by using a conversion factor:

$$\text{Rim circumference at centroid (mm)} = 2\pi * 295.27 \text{ mm}$$

$$\text{Circumference (mm)} = 1855.24 \text{ mm}$$

$$\frac{\text{mm}}{\text{deg}} = \frac{\text{circumference}}{360} = 5.153 \frac{\text{mm}}{\text{deg}}$$

4.4.1 Acceptance of the calculated radial stiffness values

The radial stiffness values for the wheels in Table 4.4-1 agree closely with the results published by Roues Artisanales (2008) which found that it takes approximately 150-250 kg to deform a standard wheel radially 1 mm. Although the wheels were not identified by total spoke number, the wheel models tested by Roues Artisanales were high-end road racing or training wheels which typically have total spoke counts between 16 and 32 spokes. The comparison of the 36 spoke wheel tested by Price and Akers (radial stiffness values ranging from 210 and 250 kg/mm) to the 36 spoke dished wheels analysed in this study (radial stiffness values ranging from 176 to 290 kg/mm), also validate the results of the unconstrained radial FEA model because the stiffness values are of similar magnitude.

It was concluded that based on the close correlation between the existing published values and the values calculated from the FEA, the radial stiffness values in Table 4.4-1 can be used to compare the wheels analysed in this study.

4.4.2 Acceptance of the calculated lateral stiffness values

Roues Artisanales (2008) also tested lateral wheel stiffness and found that it takes approximately 2–6 kg to cause a lateral deformation of 1 mm. The 2 kg/mm stiffness value was for a wheel with spokes that were bonded to the hub and the rim and therefore it did not have any pre-tensioned spokes. The lateral stiffness values reported by Price and Akers for a 36 spoke, evenly dished wheel (Table 2.2-4) were between 10.3 and 11.2 kg/mm and these values are similar to the 36 spoke, dished rear wheels analysed in this study (6.4 to 9.4 kg/mm). The MATLAB® calculated values are also within 1 to 4 kg/mm of the FEA values (Table 4.1-2 to Table 4.1-7). This can be attributed to the value selected for the change in spoke angle, μ_f , which, when changed to other values (from the arbitrarily set 0.8 for both sides) resulted in the lateral stiffness value ranging from 11.1 kg/mm to as low as 7.6 kg/mm for a 28 spoke wheel. Changes in spoke distribution around the rim can also affect lateral stiffness by 60 to 70% as demonstrated in the 20 Opt and 28 Opt wheels.

It was concluded that the lateral stiffness values calculated from the FEA results can be used to accurately assess the differences between the lateral stiffness of the wheels tested in this study because the calculated stiffness values compare well to those obtained experimentally in other studies.

4.4.3 Acceptance of the calculated torsional stiffness values

The torsional stiffness values based on the FEA results are typically 1.5 to 2 times the torsional stiffness values calculated in the MATLAB® analysis. The FEA results still rank the wheels in the same order as the MATLAB® results and this correlation is considered satisfactory for the requirements of this study.

Three analyses were performed to try and identify the cause of this discrepancy between the TS values.

Test one tested the sensitivity of the MATLAB® calculations to changes in the arbitrarily set values in the code. This test showed that changing the arbitrary values had very little effect on the calculated TS values and it was concluded that these values were not the cause of the discrepancy.

Test two changed the effective modulus of elasticity, E , and it was found that by doubling the E value used in the code, the torsional stiffness values calculated from FEA results were closely matched to the MATLAB® values. This aligns with the E value calculated in Table 2.2-2 of 1.99×10^9 psi (13986 kg/mm^2) (NB – 6895 kg/mm^2 was originally used in the code). However, using this larger value for E also increases the lateral stiffness values so that they no longer closely matched the FEA results. It was concluded that the chosen value of E was not the cause of the discrepancy between the MATLAB® and FEA results.

Test three was done by multiplying the MATLAB® results for torsional stiffness by the dish ratio (ratio of the LHS:RHS dish magnitude in mm – in the case of the 55 mm hub this was 32/17 or 1.88). After applying this ratio to the TS equation, the average ratio between the MATLAB® to FEA results became 0.98 (Table 4.4-2). To confirm that the dish ratio is an important factor for torsional stiffness, further investigations using a variety of different dish ratios could be performed as part of any future studies.

CHAPTER 4 - RESULTS AND VALIDATION

4.4 Radial, Lateral and Torsional Stiffness values calculated from the FE Analysis

Table 4.4-2. Comparison between the results of ‘*Optimised_wheel_stiffness.m*’ V1.0, V1.0 multiplied by the dish ratio and the FEA calculated torsional stiffness values. V2.0 wheels not included.

Wheel ID	Torsional Stiffness				
	Original MATLAB -TS	MATLAB x Dish Ratio (32/17)-TS	FEA-TS	Ratio (FEA/ Original MATLAB)	Ratio (FEA/ (M x DR)
20 2X	12218	22999	17841	1.46	1.28
6700R	12492	23515	16663	1.33	1.41
20 Opt	12459	23451	24695	1.98	0.95
24 2X	12786	24068	21064	1.65	1.14
24 Opt	14164	26662	24036	1.70	1.11
28 3X	17575	33084	34967	1.99	0.95
Gradient	20130	37892	56247	2.79	0.67
Circuit	8827.8	16617	19329	2.19	0.86
28 Opt	17660	33243	36991	2.09	0.90
32 3X	18806	35400	39186	2.08	0.90
32 Opt	19175	36093	44744	2.33	0.81
32 ES Opt	16918	33627	37426	2.10	0.90
36 3X	19179	36102	41139	2.15	0.88
36 Opt	22731	42787	49256	2.17	0.87
48 3X	18042	33962	41118	2.28	0.83
48 Opt	27405	51586	52749	1.92	0.98
20 Opt-1b	12459	23452	20559	1.65	1.14
28 Opt-1b	17660	33242	33297	1.89	1.0
Average				1.99	0.98

The results of the two wheel models that were re-tested (the 20 Opt and the 28 Opt) with a slightly different lacing pattern are shown in (Table 4.4-1). The results suggest that when a wheel is laced differently, the stiffness properties can vary greatly even with the same number of total spokes. Goldberg (1984) found a similar trend (Table 2.2-2) where the torsional stiffness varied between 0.0 lb.in/deg to 3400 lb.in/deg (0 to 39250 kg.mm/deg) for the 0X (radial) and the 4X spoking patterns in a 36 spoke wheel.

Goldberg’s published data (from 1984) was based on evenly dished wheels with even spoke numbers on the left and right hand side. Therefore, it is possible that the dishing

of the wheel, or the unequal spoke distribution seen in this study, could have an unforeseen influence on the overall TS value. The variation in stiffness between spoke patterns (up to a factor of six between 1X and 4X patterns - Table 2.2-1) may also contribute to the discrepancy seen in this study. Regardless of the magnitude of the stiffness value the wheels are ranked in the same order in both sets of data (FEA and MATLAB®).

After consideration of the above information, it was concluded that the FEA calculated stiffness values for TS can be used to compare the behaviour of the wheel models in this study, however, further investigations to identify the cause of the discrepancy between the results are recommended in the future.

4.5 The Effective Modulus of Elasticity

The effective modulus of elasticity, E , used in '*Optimised_wheel_stiffness.m*' Versions 1.0 and 2.0, was based on the value 10^7 psi (6895 kg/mm^2) used by Goldberg (Section 2.2.2). The discrepancy between Goldberg's published values and those calculated as part of this study using his equations, is highlighted in Table 2.2-2. This discrepancy created a need to validate the applicability of using Goldberg's value in the MATLAB® code.

Values for the maximum principal stresses and maximum principal strains under a 100 N radial load were obtained by finite element analysis for a random sample of wheels. These stress and strain values were then used to calculate an average effective modulus value. The results are shown in Table 4.5-1.

Table 4.5-1. Effective modulus of elasticity, E , values calculated from the results of the finite element analysis.

Wheel Assessed	Maximum Principal Stress (MPa)	Maximum Principal Strain	Calculated E Value (MPa) (stress/strain)	Calculated E Value (kg/mm ²)
20 Opt-1b	7.1677	8.72E-05	82214	8381
24 Opt	7.5778	8.68E-05	87324	8902
Circuit	7.7715	8.91E-05	87256	8895
28 3X	6.8925	7.70E-05	89558	9129
32 Opt	6.6237	7.62E-05	86901	8858
36 3X	5.5723	6.45E-05	86347	8802
48 3X	4.7827	6.12E-05	78205	7972
Average			85401	8705

The results of this assessment suggest that the effective modulus of elasticity, E , should be 8705 kg/mm², or 1.2×10^7 psi, for the particular wheels used in this analysis. In his 1984 book, Goldberg refers to a rim comprising of the tyre bed only (Figure 4.5-1 and Figure 4.5-2) whereas this study uses the hollow ‘box’ cross-section shown in Figure 3.3-1 which could increase the E value. The use of the hollow ‘box’ cross-section is validated because it has been used for many years to increase the stiffness of wheels by increasing the inertia about the bending axis. Therefore it is probable that the different cross-section used in this study has caused the increase in the effective modulus.

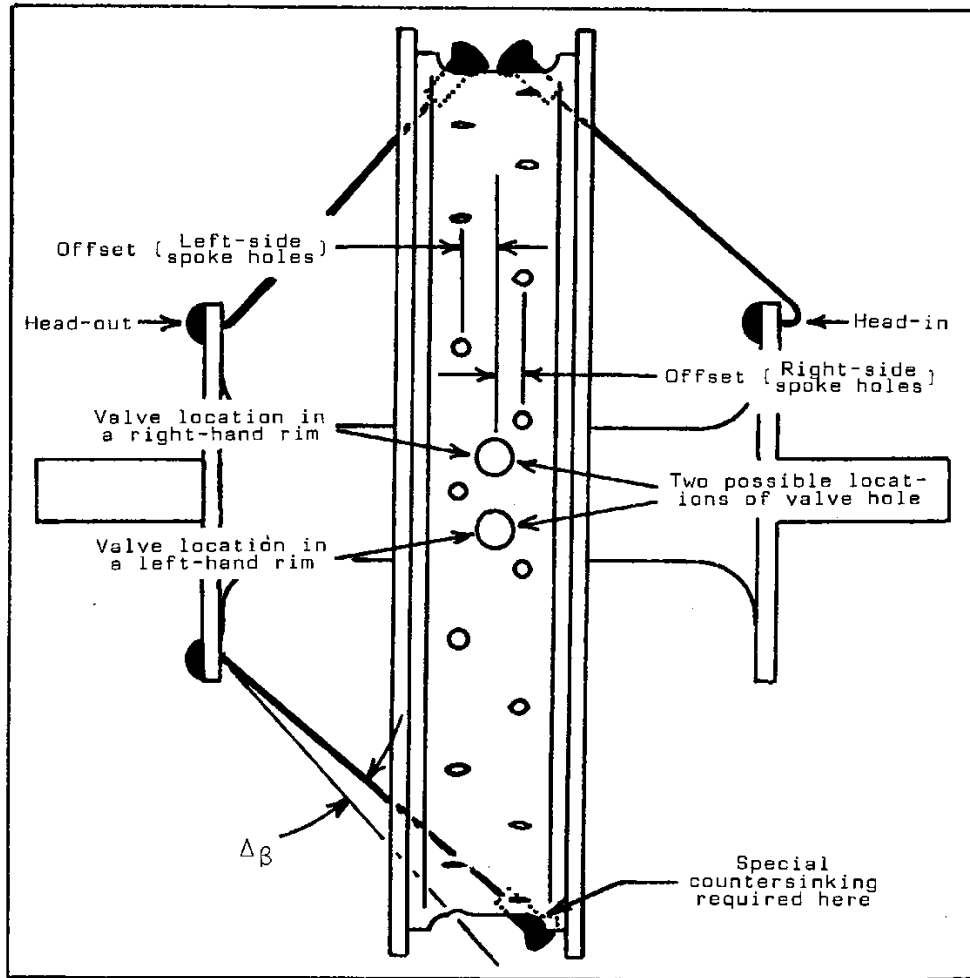


Figure 4.5-1. Wheel used by Goldberg (1984) showing the spokes connected to the tyre bed.

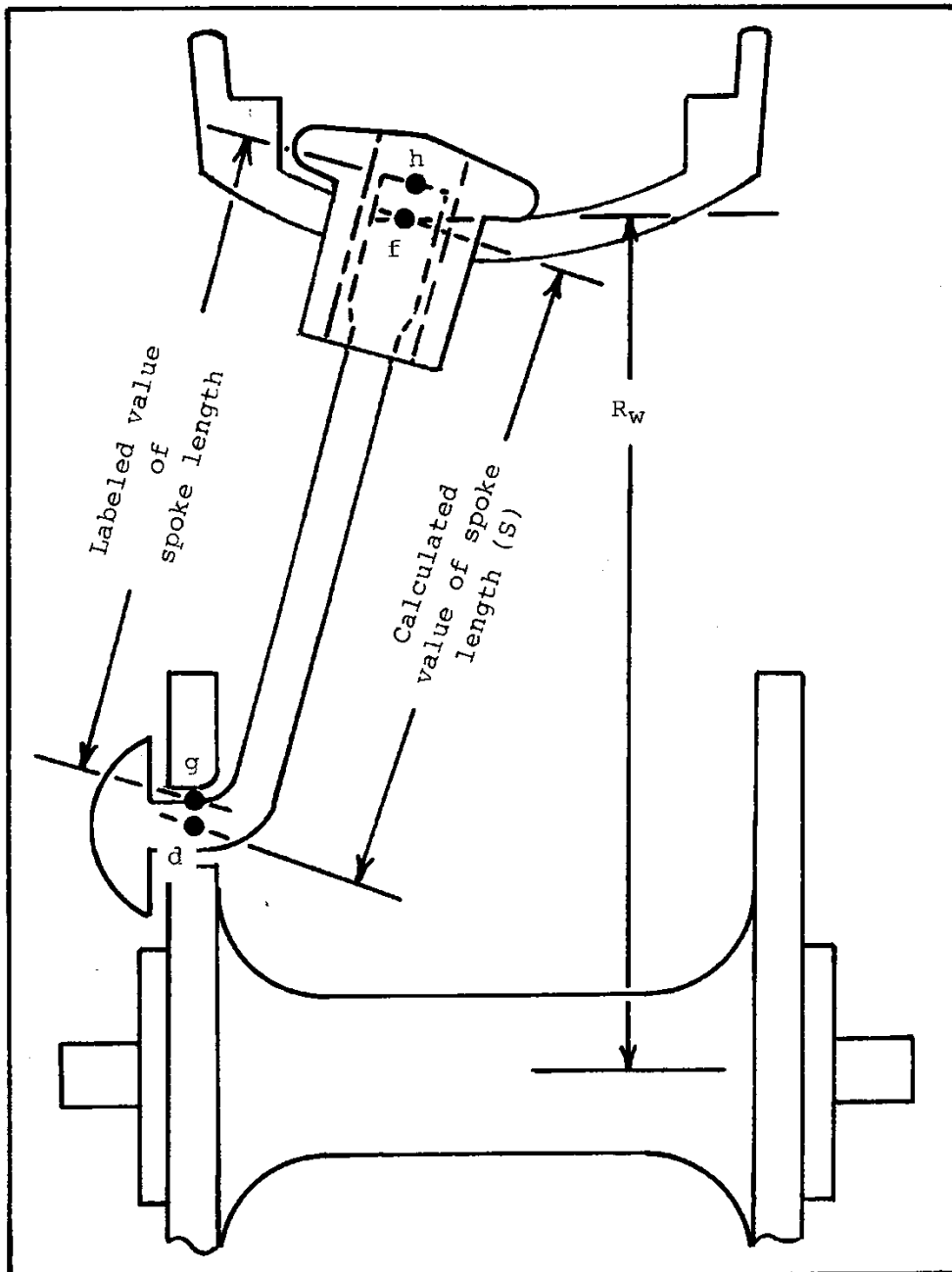


Figure 4.5-2. The rim cross-section of the wheel used by Goldberg (1984).

The stiffness values for the optimised wheels were re-calculated using the new effective modulus (Table 4.5-2). The change in modulus slightly improved the correlation of the FEA and MATLAB® TS values. However, the new modulus value also made the correlation between the FEA and MATLAB® LS values slightly worse.

Table 4.5-2. The new torsional and lateral stiffness values for the V1.0 optimised wheels using the new E value. FEA values are in brackets.

Wheel ID	TS (kg.mm/deg)	LS (kg/mm)
20 Opt-1b	15729 (20559)	6.9 (4.8)
24 Opt	17882 (24036)	8.5 (5.1)
28 Opt-1b	22296 (33297)	9.2 (6.4)
32 Opt	24208 (44744)	11.0 (6.7)
36 Opt	28697 (49256)	11.6 (6.4)
48 Opt	34599 (52749)	16.4 (9.2)

It was concluded that changing the effective modulus from 6895 kg/mm^2 to 8705 kg/mm^2 only has a small effect on the correlation between the FEA and MATLAB® results and because of this, the initial value (6895 kg/mm^2) will stay in the code for the purposes of this study.

CHAPTER 5 - DISCUSSION

5.1 Discussion of the Stiffness values calculated from the FEA results

For each total spoke number, the 'V2.0' wheel has a better torsional stiffness than the conventionally spoked wheels for wheels with a 25 mm hub flange radius. The V2.0 wheels also have an equal number of spokes on each side. The only wheels that had a slightly greater TS than the V2.0 geometries are the 20 Opt, the 20 Opt-1b, the 28 Opt and the Gradient wheels. However, the 20 and 28 Opt wheels performed poorly under radial and lateral loads and can be considered the weakest wheels in their respective categories. The results of the 20 Opt and 28 Opt wheels were discussed in Section 4.3.1.5.

Before using any of the calculated wheel geometries in this study, it is recommended that further computational investigations into the wheels' behaviour are performed. This should be done by applying loads to different areas of the rim to ensure that the wheels will perform consistently during use. It is also recommended that prototype testing be carried out:

1. to ensure the spokes can be laced as required for the outputted spoke angles; and
2. to ensure that the wheels do perform in a similar way to the simulated models.

The specific geometries of each wheel model can be found in Table 4.1-2 to Table 4.1-8.

5.1.1.1 20 Spoke Wheel Models

Table 5.1-1 shows the stiffness properties of the analysed wheels with 20 spokes. The remodelled 20 Opt-1b has a slightly better radial stiffness, a significantly better torsional stiffness and a slightly lower lateral stiffness when compared to the 20 Opt-V2.0. However, due to the similarity between the V2.0 and the 2X model, the performance of the V2.0, in the absence of any further investigations, can be assessed as being more consistent around the rim, and also as a safer option, than the Opt-1b. Based on this analysis, it is concluded that a wheel built with V2.0 geometry would provide the optimal stiffness properties for a 20 spoke wheel.

Table 5.1-1. The stiffness properties of 20 spoke wheels. *Extract from Table 4.4-1.*

Wheel ID	Radial Stiffness	Lateral Stiffness	Torsional Stiffness
	kg/mm	kg/mm	kg.mm/deg
20 Opt-1b*	150	4.8	20559
20 Opt-V2.0	141	5.2	18501
20 2X	142	5.3	17841
6700R	195	7.9	16663
20 Opt	46	3.0	24695

5.1.1.2 24 Spoke Wheel Models

Table 5.1-2 shows the stiffness properties of the analysed wheels with 24 spokes. The 24 Opt-V2.0 model significantly outperformed the 24 2X and 24 Opt in the lateral and torsional stiffness analysis. The V2.0's radial stiffness, while better than the stiffness of

the 24 2X, is significantly less than the stiffness of the 24 Opt. However, it is still within acceptable limits at 175 kg/mm. Based on this analysis, it is concluded that the V2.0 wheel geometry is the optimal geometry for a 24 spoke wheel.

Table 5.1-2. The stiffness properties of 24 spoke wheels. *Extract from Table 4.4-1.*

Wheel ID	Radial Stiffness	Lateral Stiffness	Torsional Stiffness
	kg/mm	kg/mm	kg.mm/deg
24 Opt-V2.0	175	6.4	27580
24 Opt	259	5.1	24036
24 2X	124	5.6	21064

5.1.1.3 28 Spoke Wheel Models

Table 5.1-3 shows the stiffness properties of the analysed wheels with 28 spokes.

The commercial Gradient wheel has the maximum torsional and lateral stiffness of all of the 28 spoke wheels tested, but has an uneven spoke distribution around the rim and a significantly larger hub flange radius than the other wheels making it quite different to the other wheels in this category. This result confirms that by increasing the hub flange radius significant stiffness improvements can be made.

The Circuit wheel has the second best radial stiffness and worst torsional stiffness due to the 'hi-low' hub flange arrangement and the radial spoke pattern on the LHS.

Of the four models analysed that have the same hub geometry, the V2.0 and the 3X model were closely matched with the 3X having a slightly better radial stiffness than the V2.0, the V2.0 having a slightly improved torsional stiffness, and both models

displaying similar lateral stiffness. The Opt-1b has the best radial stiffness, but lower lateral and torsional stiffness, while the Opt wheel performs poorly under lateral and radial loading, but has the best torsional stiffness. The differences seen between the Opt and the Opt-1b highlight the importance spoke patterns play in determining the overall stiffness of the wheel.

Based on the outcomes of this study it is recommended that the 28 Opt-V2.0 geometry be considered as the optimal geometry for a 28 spoke wheel due to the slight increase in torsional stiffness over the 28 3X. Again, before using any of these geometries, further computational and experimental testing is recommended.

Table 5.1-3. The stiffness properties of 28 spoke wheels. *Extract from Table 4.4-1.*

Wheel ID	Radial Stiffness	Lateral Stiffness	Torsional Stiffness
	kg/mm	kg/mm	kg.mm/deg
Gradient	202	8.6	56247
28 Opt-V2.0	240	7.2	35172
28 3X	242	7.2	34967
28 Opt-1b	357	6.4	33297
Circuit	300	8.1	19329
28 Opt	44	3.8	36991

5.1.1.4 32 Spoke Wheel Models

Table 5.1-4 shows the stiffness properties of the analysed wheels with 32 spokes. In this category, four wheel models each having the same hub and rim cross-section were analysed. The 32 Opt and the 32 Opt ES geometries were calculated using V1.0 of the MATLAB® script (Appendix B.1), while the V2.0 geometry was calculated using V2.0

(Appendix F.1). The radial and lateral stiffness values of the 32 Opt were significantly worse than the other three wheels but it has the best torsional stiffness.

Based on this analysis, the best all-round rear wheel is considered to be the 32 V2.0 because of its slightly higher torsional stiffness than the 32 3X. However, if radial and lateral stiffness were a priority for the wheel, then the best wheel would be the 32 ES Opt even though it has the worst TS of the four wheels tested.

Table 5.1-4. The stiffness properties of 32 spoke wheels. *Extract from Table 4.4-1.*

Wheel ID	Radial Stiffness	Lateral Stiffness	Torsional Stiffness
	kg/mm	kg/mm	kg.mm/deg
32 Opt-V2.0	266	8.1	42350
32 3X	269	8.3	39186
32 ES Opt	280	8.5	37426
32 Opt	153	6.7	44744

5.1.1.5 36 Spoke Wheel Models

Table 5.1-5 shows the stiffness properties of the analysed wheels with 36 spokes. Both of the optimised wheels, 36 Opt and 36 Opt-V2.0, have significantly improved torsional stiffness over the 36 3X. Of the two optimised wheels, it is the V2.0 that has the significantly better radial and lateral stiffness, with only a small reduction in torsional stiffness from the Opt model. Based on this analysis, the use of the V2.0 geometry for a 36 spoke wheel is recommended to obtain the best combination of stiffness properties.

Table 5.1-5. The stiffness properties of 36 spoke wheels. *Extract from Table 4.4-1.*

Wheel ID	Radial Stiffness	Lateral Stiffness	Torsional Stiffness
	kg/mm	kg/mm	kg.mm/deg
36 Opt-V2.0	283	8.9	49049
36 Opt	176	6.4	49256
36 3X	291	9.4	41139

5.1.1.6 48 Spoke Wheel Models

Table 5.1-6 shows the stiffness properties of the analysed wheels with 48 spokes. Both of the optimised wheels, 48 Opt and 48 Opt-V2.0, have improved torsional stiffness over the 48 3X. Of the two optimised wheels, it is the V2.0 that has the significantly better torsional stiffness and a slight improvement on the radial and lateral stiffness. Based on this analysis, this study recommends the use of the V2.0 geometry for a 48 spoke wheel for the optimal combination of stiffness properties.

Table 5.1-6. The stiffness properties of 48 spoke wheels. *Extract from Table 4.4-1.*

Wheel ID	Radial Stiffness*	Lateral Stiffness	Torsional Stiffness
	kg/mm	kg/mm	kg.mm/deg
48 Opt-V2.0	355	11.1	69568
48 Opt	331	9.2	52749
48 3X	364	12.2	41118

5.2 Discussion of the MATLAB® Optimisation Results

Refer back to Section 4.1 for the discussion on the main findings from the MATLAB® Optimisation process.

CHAPTER 6 - SUMMARY AND DESIGN RECOMMENDATIONS

6.1 Project Summary

This study set out to gain a better understanding of how the spoked wheel works under different load scenarios and to produce a MATLAB® script to find the best possible spoke geometry for a rear bicycle wheel. The developed script, '*Optimised_wheel_stiffness_Ver_2*', successfully identifies the optimised geometry of the rear spoked bicycle wheels in this study and can be easily adapted to identify the optimal geometry for any wire spoked wheel. Goldberg believed that the one best possible rear wheel design did not exist because there are simply too many variables and spoking possibilities. The conclusions of this study reinforce that belief. However, a method to design the best possible wheel given certain hub and rim geometries has been developed.

The modelling and testing of the wheel models in ANSYS® resulted in the variation of stiffness properties depending on how the spokes were distributed around the rim, even with all of the other geometric features remaining the same. Most of the optimised models using script V2.0, consistently performed at the same standard (for radial and lateral stiffness) or slightly better than conventionally spoked wheels (for torsional stiffness).

The features that were common to all total spoke numbers form part of the design recommendations and are made only for the wheels that have similar properties to those tested in this study.

6.2 Design Recommendations

The following generalisations can be made to assist in determining the starting point of rear wheel design:

1. The thicker the spoke the stiffer the wheel.
2. The larger the hub flange the stiffer the wheel.
3. Lateral stiffness increases with hub width (for a particular spoke number) and as total spoke number increases.
4. Torsional stiffness decreases slightly with hub width for the same number of total spokes. Therefore, the smaller the spoke dish/brace angle the greater the torsional stiffness will be.
5. Torsional stiffness increases with total spoke number and depends more on spoke angle than whether the spokes are on the LHS or RHS of the wheel.
6. Radial stiffness is determined by the number of spokes in the load affected zone that have less dish (i.e. if more spokes in the LAZ are from the RHS the wheel will deform less than if the same amount of spokes were on the LHS). This leads to the recommendation of equal spoke numbers for each side with LHS and RHS spokes alternating around the rim.

7. A wheel deforms the same amount under a lateral load of the same magnitude regardless of direction. This could allow for more spokes to be placed on the RHS for improved radial stiffness to decrease the pre-tension differential. However, this solution is not recommended due to the reasoning provided in Point 6.
8. To get the best possible combination of radial, lateral and torsional stiffness the spoke angles on each side of the wheel need to be slightly different. The V2.0 models performed consistently well for all spoke numbers tested. Common features of these wheels included:
 - i. LHS spoke angle of 77° (20 to 36 spokes) and 78° (48 spokes)
 - ii. RHS spoke angle of 81° for all wheels
 - iii. Equal numbers of spokes on the LHS and RHS

CHAPTER 7 - CONCLUSIONS AND FURTHER WORK

7.1 Conclusions

This study showed that by making minor changes to the spoke angles on both sides of the wheel, a significant increase in torsional stiffness can be achieved while maintaining the majority of the wheel's radial and lateral stiffness.

The '*Optimised_wheel_stiffness_Ver_2.m*' code developed in this study was successful in outputting geometry that had significant performance benefits over conventional spoking patterns. The one, best rear wheel was unable to be identified but the code has managed to improve the stiffness properties if the total number of spokes to be use is known. Adaptation of the script for different spoke diameters and hub flange radii can be done easily and should also result in the optimal spoking geometry for these wheels.

The finite element analysis identified short-comings in the use of the existing theoretical models for the prediction of deformation under different loads.

- The unconstrained FEA model accurately predicted the deformations seen in the laboratory testing for all three load cases whereas the theoretical model only accurately predicted the lateral load deformations.
- Additional displacement constraints had to be added to the radial load FEA model in order for the resulting deformations to match the theoretical

predictions. These “constrained” deformations were approximately 400% less than the deformations in both the laboratory test and the “unconstrained” FEA models.

- A number of changes were applied to the torsional load FEA model but none of these changes resulted in a better correlation to the theoretical model.

The general guidelines that were developed in this study can be used as a starting point for wheel design. However, the specific spoke angles of the optimised wheel models (77° LHS and 81° RHS) do not apply to all wheels and should not be used unless the rim and hub geometries are similar to the wheels analysed in this study.

7.2 Recommendations for Further Work

This study was undertaken with the aim of providing guidelines for the optimised design of spoked bicycle wheels. It was discovered that there is more to wheel design than finding the best combination of torsional and lateral stiffness. In order to produce more reliable guidelines, it is recommended that the following investigations be performed as part of any future studies:

1. Investigate the effects dishing has on the torsional stiffness calculated using Equation 3.1.
2. Change the spoke patterns used on the optimised wheels in this study while maintaining all the other features to see what effect this has on the stiffness of the wheels.

3. Test the wheels analysed in this study with loads applied at different areas of the rim to see if they perform consistently. This could highlight problems with the models that have uneven spoke numbers on either side, as they may be stronger at some points but weaker in others.
4. Based on the evidence in this study, a new method for theoretically calculating the behaviour of wheels under torsion and under radial loading is required since both the laboratory test, and the unconstrained FEA showed a large deviation from the values calculated using Pippard's equations.
5. Repeat the analysis performed in this study to confirm that the developed script outputs the optimal spoke geometries for wheels with different hub geometries and spoke diameters.

{This page is left intentionally blank}

APPENDICES

APPENDIX A. PROJECT SPECIFICATION

APPENDIX A PROJECT SPECIFICATION

UNIVERSITY OF SOUTHERN QUEENSLAND
FACULTY OF HEALTH, ENGINEERING AND SCIENCES

ENG 4111/4112 Research Project
PROJECT SPECIFICATION

FOR: **JASON KELLER**

SUPERVISORS: Ray MALPRESS

ENROLMENT: ENG4111 – S1, EXT, 2013;
ENG4112 – S2, EXT, 2013

PROJECT AIM: This project seeks to investigate the forces experienced on bicycle wheels during operation, develop a mathematical and a 3D finite element analysis model to calculate the deformations of the wheel under these different forces, investigate the effects of spoke patterns, spoke geometry, rim geometry on the rim deflections under these different load cases in order to produce guidelines for the production of an optimised bicycle wheel.


PROGRAMME:

1. Research the background information relating to wheel design for strength and stiffness
2. Develop a MATLAB model to optimise wheel geometries based on the torsional and lateral stiffness equations used by Goldberg
3. Develop an Excel Spread sheet based on Pippard's work for wire wheels under radial, torsional and side loading
4. Based on the optimised designs in number 2, develop CAD models for 20, 24, 28, 32, 36 and 48 spoked wheels for testing in ANSYS.
5. Run Simulations on the optimised wheels in ANSYS to verify the data and compare to theoretical values.
6. Perform a laboratory experiment to validate results.
7. Produce a set of guidelines for the optimised wheel design based upon results

As time permits:

8. Produce CAD models of existing similar wheel designs to check their performance against the optimised wheels
9. Build and test a prototype wheel with optimised spoke pattern and geometries to correlate computational data with laboratory testing (unlikely due to funding I would imagine)

AGREED:

_____  (Student) 22/04/2013
_____ (Supervisor 1) ___/___/2013
_____ (Supervisor 2) ___/___/2013

APPENDIX B. MATLAB® SCRIPTS

B.1 Optimised_wheel_stiffness.m - V1.0

```
% Goldberg Optimisation Calculations for Torsional and Lateral
Stiffness
%
% This code will output the optimised geometry for wire spoked wheels
% based on the calculated Torsional and Lateral Stiffness using the
% equations formulated by Goldberg (1984).
%
% For my project it will be used to find the optimised geometry of
% 20, 24, 28, 32, 36 and 48 spoke wheels
%
clc; clear all; close all;
% Display start time
disp('Geometry Optimisation for Wire Spoked Wheels')
disp('_____')
Start_time=datestr(now,0);
disp('Analysis Start:')
fprintf(Start_time)
disp(' ')
disp('-----')
disp('----')
%% Nomenclature
%      Rw      - Radius rim (mm)
%      Rh      - Radius hub (mm)
%      mu      - Spoke angle (radians)
%      gS      - Calculated spoke length (mm)
%      E       - Effective Elasticity (hub/rim/spoke combination) -
kg/mm^2
%      Spd     - Spoke diameter
%      gA      - Cross-sectional area of spoke - (mm^2)
%      muf     - Torque induced wind-up angle (between 0 and 1
degree)
%      N       - Total number of spokes (NL - spokes LHS; NR - spokes
RHS)
%      gLS     - L and R for load coming from the LHS or RHS of the
rim
%              respectively
%      D       - amount of dish in mm
%      df/Df   - change in dish cause by applied force (mm)
%      Defrat  - change in dish of rim due to load (mm)
%      LS      - lateral stiffness (kg/mm)
%      gTS     - torsional stiffness (kg.mm/deg)
%      T       - spoke tension (kg)
%      Trm     - tension ratio (RHS tension:LHS tension)
%
%% Set Known Values - all of these are used in Torsional and Lateral
stiffness
E=6895;
% value 1e7 psi used by Goldberg converted
disp('Please enter the total number of spokes to be used in the
wheel')
N=input...
('Total spoke number (minimum 8 spokes): ');
while N<8;
    disp('Total spoke count must be greater than or equal to 8!')
    N=input...
('Total spoke number (minimum 8 spokes): ');
end
% Set spokes for LHS of wheel - NL (minimum 4 spokes on each side
```

APPENDIX B MATLAB® SCRIPTS

B.1 Optimised_wheel_stiffness.m - V1.0

```
NL=4:2:N-4;
% Calculate respective spokes on RHS (Total spokes - LHS spokes)
% Set up matrix to improve calculation time
NR=N-NL;
% Wheel radii - rim and hub
Rw=300;
Rh=25;%input('Enter hub flange radius (both sides) (mm): ');
% Syntax [dish LHS;dish RHS] 10sp freehub length - 45mm RHS, distance
between
% dropouts 130mm - allow 10mm clearance LHS measured centre of flange
to
% centre of rim
D=[32;17];
% Spoke angle
muD=0:1:90;
mu=muD.*pi/180;
% Spoke diameter
Spd=1.8;%input('Enter the spoke diameter (mm): ');
% Spoke cross-sectional area
gA=1/4*pi*Spd.^2;
% LHS Spoke tension
T=45.36;
% 100 lb (Goldberg) converted;
% RHS Multiplication factor
Trm=1.4;
T(2)=Trm*T(1);
% Load from right to left (limiting deflection 2mm)- Defrat -
deflection ratio (small % of dish)
df=input('Enter allowable deflection (mm): ');
Defrat=D(2)/df;
DfR=D(2)/Defrat;
DfL=-DfR;
% Load from left to right - proportional deflected equivalent to DfR
xl=Defrat*D(1)/D(2);
DfLl=D(1)/xl;
DfRl=-DfLl;
% Wind up angle (default value: typically less than 1%)
mufL=0.8*pi/180;
mufR=0.8*pi/180;
%
%% Lateral and Torsional Stiffness
% Calculate spoke length for different hub radius, dish and spoke
angle mu;
% syntax [mu value, dish value, Rh value]
gS=zeros(length(mu),2,length(Rh)); % Preallocation to improve speed
for n=1:length(Rh)
    for i=1:length(mu);
        gS(i,1,n)=sqrt(Rw.^2+Rh(n).^2+D(1).^2-
2.*Rw.*Rh(n).*cos(mu(i)));
        gS(i,2,n)=sqrt(Rw.^2+Rh(n).^2+D(2).^2-
2.*Rw.*Rh(n).*cos(mu(i)));
    end
end
%
% Calculate Torsional stiffness depending on N, A, mu, D, Rh and NL/NR
disp('-----')
disp('Identifying the maximum torsional and lateral stiffness
possible')
disp('Please be patient - analysis may take up to 4 hours...')
% Preallocate matrix to reduce computation time
gTS=zeros(length(mu),length(NL),length(mu),length(Rh)...
,length(Rh),length(gA),length(gA));
```

APPENDIX B MATLAB® SCRIPTS
 B.1 Optimised_wheel_stiffness.m - V1.0

```

gLSR=gTS;
gLSL=gTS;
LSave=gTS;
% Create loop - LSave is calculated only when gLSR and gLSL are
positive
for j=1:length(NL);
% Changes spokes LHS - NL
    for k=1:length(mu);
% Changes spoke angle LHS - mu
        for l=1:length(mu);
% Changes spoke angle RHS - mu
            for m=1:length(Rh);
% Changes hub radius LHS - Rh
                for n=1:length(Rh);
% Changes hub radius RHS - Rh
                    for o=1:length(gA);
% Changes spoke cross-sectional area LHS - gA
                        for p=1:length(gA);
% Changes spoke cross-sectional area RHS - gA
                            % Goldberg's equation for Torsional
                            % Stiffness

gTS(k,j,l,m,n,o,p)=(pi.*E.*Rw.^2)./180)...
                    .* (NL(j).*gA(o).*Rh(m).^2.*...
                    (sin(mu(k))).^2./(gS(k,1,m).^3)...
                    +NR(j).*gA(p).*Rh(n).^2.*...
                    (sin(mu(l))).^2./(gS(1,2,n).^3));
                    % Lateral stiffness for any wheel

gLSR(k,j,l,m,n,o,p)=(NL(j).*(T(1)./gS(k,1,m)...
                    +((T(1)+E.*gA(o)).*D(1).^2)...
                    ./ (gS(k,1,m).^3)-((T(1)+E.*gA(o))...
                    .*D(1).*Rw.*Rh(m))...
                    ./ (gS(k,1,m).^3.*DfL)...
                    .* (cos(mu(k)+mufL)-cos(mu(k))))...
                    +NR(j).*(T(2)./gS(1,2,n)...
                    +((T(2)+E.*gA(p)).*D(2).^2)...
                    ./ (gS(1,2,n).^3)-...
                    ((T(2)+E.*gA(p)).*D(2)...
                    .*Rw.*Rh(n))./(gS(1,2,n).^3.*DfR)...
                    .* (cos(mu(l)+mufR)-cos(mu(l)))))/2;

gLSL(k,j,l,m,n,o,p)=(NL(j).*(T(1)./gS(k,1,m)...
                    +((T(1)+E.*gA(o)).*D(1).^2)...
                    ./ (gS(k,1,m).^3)-((T(1)+E.*gA(o))...
                    .*D(1).*Rw.*Rh(m))...
                    ./ (gS(k,1,m).^3.*DfL1)...
                    .* (cos(mu(k)+mufL)-cos(mu(k))))...
                    +NR(j).*(T(2)./gS(1,2,n)...
                    +((T(2)+E.*gA(p)).*D(2).^2)...
                    ./ (gS(1,2,n).^3)-...
                    ((T(2)+E.*gA(p)).*D(2)...
                    .*Rw.*Rh(n))./(gS(1,2,n).^3.*DfR1)...
                    .* (cos(mu(l)+mufR)-cos(mu(l)))))/2;
                    % Calculate average LS only if both values
are
                    % positive
                    if (gLSL(k,j,l,m,n,o,p)>0)...
                        && (gLSR(k,j,l,m,n,o,p)>0)

LSave(k,j,l,m,n,o,p)=(gLSL(k,j,l,m,n,o,p)...
                    +gLSR(k,j,l,m,n,o,p))./2;
                    end

```


APPENDIX B MATLAB® SCRIPTS
B.1 Optimised_wheel_stiffness.m - V1.0

```

end
end
end
end
end
end
%% Find maximum combined lateral stiffness
% Locate maximum combined lateral stiffness in LSave
LSav=LSave;
% Use a factor of 0.4 to create balanced lateral stiffness
LSave(gLSL<0.40*max(LSav(:)))=0;
LSave(gLSR<0.40*max(LSav(:)))=0;
[max_LS,lposition]=max((LSave(:)));
[h,i,j,k,l,m,n]=ind2sub(size(LSave),lposition);
% Create Geometry matrix for maximum lateral stiffness
% syntax [NL,NR,mu-LHS,mu-RHS,Rh-LHS,Rh-RHS,gA-LHS,gA-RHS]
gLSgeo=[NL(i),NR(i),muD(h),muD(j),Rh(k),Rh(l),Spd(m),Spd(n)];
% Maximum Lateral stiffness
LSm=max_LS;
% Convert to imperial units - compare with recorded results
LSmimp=LSm*2.2*25.4;
% Print to command window
fprintf('\nThe geometry of maximum lateral stiffness - %2.0f spoked
wheel:\n\n',N)
fprintf('Number of spokes LHS:           %2.0f spokes.\n',gLSgeo(1))
fprintf('Number of spokes RHS:           %2.0f spokes.\n',gLSgeo(2))
fprintf('Spoke angle LHS:                   %2.0f degrees.\n',gLSgeo(3))
fprintf('Spoke angle RHS:                   %2.0f degrees.\n',gLSgeo(4))
fprintf('Hub Radius LHS:                    %2.1f mm.\n',gLSgeo(5))
fprintf('Hub Radius RHS:                    %2.1f mm.\n',gLSgeo(6))
fprintf('Spoke Diameter LHS:                %1.1f mm.\n',gLSgeo(7))
fprintf('Spoke Diameter RHS:                %1.1f mm.\n\n',gLSgeo(8))
fprintf('The maximum lateral stiffness - %2.0f spoked wheel:      %4.1f
kg/mm.\n',N,LSm)
fprintf('Lateral Stiffness (imperial):              %4.1f
lb/in.\n\n',LSmimp)
%% Find maximum torsional stiffness
% Locate maximum torsional stiffness in gTS
[max_TS,tposition]=max((gTS(:)));
[a,b,c,d,e,f,g]=ind2sub(size(gTS),tposition);
% Create Geometry matrix for maximum torsional stiffness
% syntax [NL,NR,mu-LHS,mu-RHS,Rh-LHS,Rh-RHS,gA-LHS,gA-RHS]
gTSgeo=[NL(b),NR(b),muD(a),muD(c),Rh(d),Rh(e),Spd(f),Spd(g)];
% Maximum torsional stiffness
TSm=max_TS;
% Convert to imperial units - compare with reported values
TSmimp=TSm*2.2/25.4;
% Print to command window
fprintf('The geometry of maximum torsional stiffness - %2.0f spoked
wheel:\n\n',N)
fprintf('Number of spokes LHS:           %2.0f spokes.\n',gTSgeo(1))
fprintf('Number of spokes RHS:           %2.0f spokes.\n',gTSgeo(2))
fprintf('Spoke angle LHS:                   %2.0f degrees.\n',gTSgeo(3))
fprintf('Spoke angle RHS:                   %2.0f degrees.\n',gTSgeo(4))
fprintf('Hub Radius LHS:                    %2.1f mm.\n',gTSgeo(5))
fprintf('Hub Radius RHS:                    %2.1f mm.\n',gTSgeo(6))
fprintf('Spoke Diameter LHS:                %1.1f mm.\n',gTSgeo(7))
fprintf('Spoke Diameter RHS:                %1.1f mm.\n\n',gTSgeo(8))
%
fprintf('The maximum torsional stiffness - %2.0f spoked wheel:
%4.1f kg.mm/deg.\n',N,TSm)
```

APPENDIX B MATLAB® SCRIPTS
B.1 Optimised_wheel_stiffness.m - V1.0

```
fprintf('Maximum torsional stiffness (imperial):                %4.1f\n',TSmimp)\nlb.in/deg.\n\n',TSmimp)\ndisp('Please review data before continuing...')\n%\n% End time - Stops time after longest part of the program\nInt_time=datestr(now,0);\ndisp('First Analysis Completed:')\nfprintf(Int_time)\nfprintf('\n')\n% Repeat Optimisation loop until results are accepted\nwhile true\n    Q1=...\n        input('\nDo you wish to continue optimisation?\nEnter ''1''\nfor yes or ''2'' for no: '); \n    while Q1<1 || Q1>2 || Q1>1 && Q1<2\n        disp('Error: Please select either 1 or 2')\n        Q1=...\n            input('\nDo you wish to continue optimisation?\nEnter\n''1'' for yes or ''2'' for no: ');\n    end\n    if Q1==1;\n        %% Optimisation loop\n        disp('-----')\n        disp('Find optimal combination depending on requirements:')\n        disp('-----')\n        %\n        % Identifies where the differences in geometry occurs and\n        iterates changes\n        % of parameters until torsional stiffness reaches TSper of\n        maximum\n        % or LSper of maximum lateral stiffness.\n        %\n        % Torsional stiffness is more important in a rear wheel due to\n        transferring\n        % the loads from the rider to the wheel. To favour lateral\n        stiffness\n        % choose Q2=1 and LSper required or reduce TSper in Q2=2.\n        %\n        % Input percentages to keep.\n        Q2=input...\n            ('Press ''1'' to optimise by lateral stiffness or\n''2''\nto optimise by torsional stiffness: ');\n        while Q2<1 || Q2>2 || Q2>1 && Q2<2\n            disp('Error: Please select either 1 or 2')\n            Q2=input...\n                ('Press ''1'' to optimise by lateral stiffness or\n''2''\nto optimise by torsional stiffness: ');\n        end\n        if Q2==1;\n            LSper=0.4:0.01:1;\n            LSp=zeros(length(LSper),1);\n            LSopt=LSp;\n            TSopt=LSp;\n            TSp=LSp;\n            Avp=LSp;\n        elseif Q2==2;\n            TSper=0.4:0.01:1;\n            LSp=zeros(length(TSper),1);\n            LSopt=LSp;\n            TSopt=LSp;\n            TSp=LSp;\n        end\n    end\nend
```

```
        Avp=LSp;
    end
    % Setup the following loop depending on difference between
torsional and
    % lateral stiffness indices. Reduces the required calculations
to find
    % optimal geometry
    if (a<h)
        uu=a:h;
    elseif (a==h)
        uu=a;
    elseif (a>h)
        uu=h:a;
    end
    if (b<i)
        tt=b:i;
    elseif (b==i)
        tt=b;
    elseif (b>i)
        tt=i:b;
    end
    if (c<j)
        vv=c:j;
    elseif (c==j)
        vv=c;
    elseif (c>j)
        vv=j:c;
    end
    if (d<k)
        ww=d:k;
    elseif (d==k);
        ww=d;
    elseif (d>k);
        ww=k:d;
    end
    if (e<l)
        xx=e:l;
    elseif (e==l)
        xx=e;
    elseif (e>l)
        xx=l:e;
    end
    if (f<m)
        yy=f:m;
    elseif (f==m)
        yy=f;
    elseif (f>m)
        yy=m:f;
    end
    if (g<n)
        zz=g:n;
    elseif (g==n)
        zz=g;
    elseif (g>n)
        zz=n:g;
    end
    % Loop to calculate optimal values for torsional and lateral
    % stiffness. Only calculates for geometry between maxima, also
a
    % factor of 0.4 is multiplied to LSm to maintain balance
    % between the LHS and RHS lateral stiffness
    for t=tt;
% Changes spokes LHS - NL
```

APPENDIX B MATLAB® SCRIPTS
 B.1 Optimised_wheel_stiffness.m - V1.0

```

    for u=uu;
% Changes spoke angle LHS - mu
        for v=vv;
% Changes spoke angle RHS - mu
            for w=ww;
% Changes hub radius LHS - Rh
                for x=xx;
% Changes hub radius RHS - Rh
                    for y=yy;
% Changes spoke cross-sectional area LHS - gA
                        for z=zz;
% Changes spoke cross-sectional area RHS - gA
                            if Q2==1;
                                for i1=1:length(LSper);
                                    % Find values above
LSpers*LSm
                                        if
LSave(u,t,v,w,x,y,z)>=LSm*LSper(i1);
TSos(u,t,v,w,x,y,z)=gTS(u,t,v,w,x,y,z);
                                                LSo(u,t,v,w,x,y,z)...
=LSave(u,t,v,w,x,y,z);
                                        elseif
LSave(u,t,v,w,x,y,z)<LSm*LSper(i1);
                                        end
                                end
                            elseif Q2==2;
                                for j1=1:length(TSper);
                                    % Finds values above
TSpers*TSm
                                        if
gTS(u,t,v,w,x,y,z)>=TSm*TSper(j1);
                                                LSo(u,t,v,w,x,y,z)...
=LSave(u,t,v,w,x,y,z);
                                        elseif
gTS(u,t,v,w,x,y,z)<TSper(j1)*TSm
                                        end
                                end
                            end
                        end
                    end
                end
            end
        end
    end
end
%% Locate and post optimal values
if Q2==1;
    LSol=LSo;
    % Change all lower values to Inf and find minimum
    for i1=1:length(LSper);
        LSo(LSol<LSm.*LSper(i1))=Inf;
        % TS is maximum when LS is minimum
        [opt_LS,position]=min((LSo(:)));
        [aa,bb,cc,dd,ee,ff,gg]=ind2sub(size(LSo),position);
        % Get values for lateral and torsional stiffness
        LSopt(i1)=opt_LS;
        % Returns infinity values back to zero
        if LSopt(i1)==Inf;

```

```

        LSopt(i1)=0;
    end
    LSp(i1)=LSopt(i1)./LSm*100;
    TSopt(i1)=TSo(aa,bb,cc,dd,ee,ff,gg);
    % Returns infinity values back to zero
    if TSopt(i1)==Inf;
        TSopt(i1)=0;
    end
    TSp(i1)=TSopt(i1)./TSm*100;
    Avp(i1)=(LSp(i1)+TSp(i1))./2;

Optgeo(i1)={[NL(bb),NR(bb),muD(aa),muD(cc),Rh(dd),Rh(ee),Spd(ff),Spd(gg)]};

    end
    [~,pos]=max(Avp);
    Optg=cell2mat(Optgeo(pos));
    LSop=LSopt(pos);
    LSpe=LSp(pos);
    TSop=TSopt(pos);
    TSpe=TSp(pos);
    % Plot LSopt and TSopt
    figure('Name','Lateral Stiffness Optimisation');
    plotyy(LSper*100,LSopt,LSper*100,TSopt);
    [AX,H1,H2] =
plotyy(LSper*100,LSopt,LSper*100,TSopt,'plot');
    set(get(AX(1),'Ylabel'),'String','Lateral Stiffness
(kg/mm)');
    set(get(AX(2),'Ylabel'),'String','Torsional Stiffness
(kgmm/deg)');
    set(AX(1),'XGrid','on','YGrid','on');
    xlabel('Minimum percent of Lateral stiffness maintained
(%)');

    title('Lateral Stiffness Optimisation')
    % Plot Average Percent stiffness
    figure('Name','Combined Average');
    plot(LSper*100,Avp);
    grid on;
    axis([40 100 0 100]);title('Combined Average Stiffness %')
    xlabel('Minimum percent of lateral stiffness maintained
(%)');

    ylabel('Combined average (%)');
elseif Q2==2;
    % Find position of optimal LS - when TS
    % is minimal
    TSol=TSo;
    for j1=1:length(TSper);
        % Change all lower values to Inf and find minimum
        TSo(TSol<TSper(j1)*TSm)=Inf;
        % Find position
        [opt_TS,position]=min((TSo(:)));
        [aa,bb,cc,dd,ee,ff,gg]=ind2sub(size(TSo),position);
        LSopt(j1)=LSo(aa,bb,cc,dd,ee,ff,gg);
        % Returns infinity values back to zero
        if LSopt(j1)==Inf;
            LSopt(j1)=LSm;
        end
        LSp(j1)=LSopt(j1)./LSm*100;
        TSopt(j1)=opt_TS;
        % Returns infinity values back to zero
        if TSopt(j1)==Inf;
            TSopt(j1)=0;
        end
        TSp(j1)=TSopt(j1)./TSm*100;

```

APPENDIX B MATLAB® SCRIPTS
 B.1 Optimised_wheel_stiffness.m - V1.0

```

    Avp(j1)=(LSp(j1)+TSp(j1))./2;

Optgeo(j1)=[NL(bb),NR(bb),muD(aa),muD(cc),Rh(dd),Rh(ee),Spd(ff),Spd(g
g)]];

    end
    [~,pos]=max(Avp);
    Optg=cell2mat(Optgeo(pos));
    LSop=LSpopt(pos);
    LSpe=LSp(pos);
    TSop=TSopt(pos);
    TSpe=TSp(pos);
    % Plot LSopt and TSopt
    figure('Name','Torsional Stiffness Optimisation');
    plotyy(TSper*100,LSopt,TSper*100,TSopt);
    [AX,H1,H2] =
plotyy(TSper*100,LSopt,TSper*100,TSopt,'plot');
    set(get(AX(1),'Ylabel'),'String','Lateral Stiffness
(kg/mm)');
    set(get(AX(2),'Ylabel'),'String','Torsional Stiffness
(kgmm/deg)');
    set(AX(1),'XGrid','on','YGrid','on');
    xlabel('Minimum percent of Torsional stiffness maintained
(%)');
    title('Torsional Stiffness Optimisation')
    % Plot Average Percent stiffness
    figure('Name','Combined Average');
    plot(TSper*100,Avp);
    grid on; title('Combined Average Stiffness %')
    axis([40 100 0 100]);
    xlabel('Minimum percent of torsional stiffness maintained
(%)');
    ylabel('Combined average (%)');
    end
    % Display results for optimal geometry
    disp('-----')
    disp(' ')
    fprintf('The optimal geometry of a %2.0f spoked wheel
is:\n\n',N)
    fprintf('Number of spokes LHS:           %2.0f
spokes.\n',Optg(1))
    fprintf('Number of spokes RHS:          %2.0f
spokes.\n',Optg(2))
    fprintf('Spoke angle LHS:              %2.0f
degrees.\n',Optg(3))
    fprintf('Spoke angle RHS:              %2.0f
degrees.\n',Optg(4))
    fprintf('Hub Radius LHS:                %2.1f mm.\n',Optg(5))
    fprintf('Hub Radius RHS:                %2.1f mm.\n',Optg(6))
    fprintf('Spoke Diameter LHS:           %1.1f mm.\n',Optg(7))
    fprintf('Spoke Diameter RHS:           %1.1f
mm.\n\n',Optg(8))
    fprintf('Stiffness Properties for the above geometry:\n')
    fprintf('The optimal torsional stiffness - %2.0f spoked wheel:
%4.1f kg.mm/deg (%2.0f%% of max).\n',N,TSop,TSpe)
    fprintf('Torsional Stiffness (imperial):
%4.1f lb.in/deg.\n',TSop*2.2/25.4)
    fprintf('The optimal lateral stiffness - %2.0f spoked wheel:
%4.1f kg/mm (%2.0f%% of max).\n',N,LSop,LSpe)
    fprintf('Lateral Stiffness (imperial):
%3.1f lb/in.\n',LSop*2.2*25.4)
    %% Complete Q1 loop - Re: Continue to Optimisation
    end

```

```
    if Q1==2;
        break
    end
end
%% Display Run time
% End timer
disp('-----')
% Display end time
disp('Analysis Completed:')
end_time=datestr(now,0);
fprintf(end_time)
fprintf('\n\n')
disp('Code written by Jason Keller as part of ENG4111 and ENG4112
Research Project')
disp('Student ID: 0050093222 University of Southern Queensland -
BENG(Mechanical)')
disp('_____')
_____')
```

B.2 Example of Optimisation Results

Geometry Optimisation for Wire Spoked Wheels

Analysis Start:

21-May-2013 11:16:16

Please enter the total number of spokes to be used in the wheel
Total spoke number (minimum 8 spokes): 20
Enter allowable deflection (mm): 1.2

Identifying the maximum torsional and lateral stiffness possible
Please be patient - analysis may take up to 4 hours...

The geometry of maximum lateral stiffness - 20 spoked wheel:

Number of spokes LHS:	16 spokes.
Number of spokes RHS:	4 spokes.
Spoke angle LHS:	0 degrees.
Spoke angle RHS:	0 degrees.
Hub Radius LHS:	25.0 mm.
Hub Radius RHS:	25.0 mm.
Spoke Diameter LHS:	1.8 mm.
Spoke Diameter RHS:	1.8 mm.

The maximum lateral stiffness - 20 spoked wheel: 9.0 kg/mm.
Lateral Stiffness (imperial): 505.7 lb/in.

The geometry of maximum torsional stiffness - 20 spoked wheel:

Number of spokes LHS:	4 spokes.
Number of spokes RHS:	16 spokes.
Spoke angle LHS:	83 degrees.
Spoke angle RHS:	83 degrees.

APPENDIX B MATLAB® SCRIPTS
B.2 Example of Optimisation Results

Hub Radius LHS: 25.0 mm.
Hub Radius RHS: 25.0 mm.
Spoke Diameter LHS: 1.8 mm.
Spoke Diameter RHS: 1.8 mm.

The maximum torsional stiffness - 20 spoked wheel: 12732.7 kg.mm/deg.
Maximum torsional stiffness (imperial): 1102.8 lb.in/deg.

Please review data before continuing...
First Analysis Completed:
21-May-2013 11:16:26

Do you wish to continue optimisation?
Enter '1' for yes or '2' for no: 1

Find optimal combination depending on requirements:

Press '1' to optimise by lateral stiffness or
'2' to optimise by torsional stiffness: 1

The optimal geometry of a 20 spoked wheel is:

Number of spokes LHS: 8 spokes.
Number of spokes RHS: 12 spokes.
Spoke angle LHS: 72 degrees.
Spoke angle RHS: 78 degrees.
Hub Radius LHS: 25.0 mm.
Hub Radius RHS: 25.0 mm.
Spoke Diameter LHS: 1.8 mm.
Spoke Diameter RHS: 1.8 mm.

Stiffness Properties for the above geometry:

The optimal torsional stiffness - 20 spoked wheel: 12458.5 kg.mm/deg (98% of max).
Torsional Stiffness (imperial): 1079.1 lb.in/deg.
The optimal lateral stiffness - 20 spoked wheel: 5.9 kg/mm (65% of max).
Lateral Stiffness (imperial): 328.7 lb/in.

Do you wish to continue optimisation?
Enter '1' for yes or '2' for no: 1

Find optimal combination depending on requirements:

Press '1' to optimise by lateral stiffness or
'2' to optimise by torsional stiffness: 2

The optimal geometry of a 20 spoked wheel is:

Number of spokes LHS: 8 spokes.
Number of spokes RHS: 12 spokes.

APPENDIX B MATLAB® SCRIPTS

B.2 Example of Optimisation Results

Spoke angle LHS: 47 degrees.
Spoke angle RHS: 81 degrees.
Hub Radius LHS: 25.0 mm.
Hub Radius RHS: 25.0 mm.
Spoke Diameter LHS: 1.8 mm.
Spoke Diameter RHS: 1.8 mm.

Stiffness Properties for the above geometry:

The optimal torsional stiffness - 20 spoked wheel: 10823.0 kg.mm/deg (85% of max).

Torsional Stiffness (imperial): 937.4 lb.in/deg.

The optimal lateral stiffness - 20 spoked wheel: 6.2 kg/mm (68% of max).

Lateral Stiffness (imperial): 345.1 lb/in.

Do you wish to continue optimisation?

Enter '1' for yes or '2' for no: 2

Analysis Completed:

21-May-2013 11:17:22

Code written by Jason Keller as part of ENG4111 and ENG4112 Research Project
Student ID: 0050093222 University of Southern Queensland - BENG(Mechanical)

B.3 Check_Stiffness_Properties.m

```
%% Goldberg Optimisation Calculations for Torsional and Lateral
Stiffness
%
% This code is used to check the results of the Wheel_Optimisation.m
code
%
% clc; clear all; close all;
% Start timer
tic;
% Display start time
disp('Goldberg Stiffness for wheels')
formatOut = 'mm/dd/yy HH:MM:SS';
Start_time=datestr(now,formatOut);
disp('Start time')
fprintf(Start_time)
disp(' ')
disp('-----')
disp('----')
% Nomenclature
%      Qn      - Total applied torque
%      Rw      - Radius rim (inch)
%      Rh      - Radius hub (inch)
%      mu      - Spoke angle
%      Tq      - Torque induced tension for each spoke
%      S       - Calculated spoke length (in)
%      E       - Effective Elasticity of hub/rim/spoke combination
%      Spr     - Spoke radius
%      A       - Cross-sectional area of spoke
%      muq     - Torque induced wind-up angle - less than 1 degree so
%              ignored
%      N       - Total number of spokes (NL - spokes LHS; NR - spokes
RHS)
%
% Set Known Values - all of these are used in Torsion and Lateral
stiffness
E=6895;
N=input('Enter total spoke number: ');
NL=input('Enter the number of spokes on LHS: ');
% Set up NR - note cannot have negative number of spokes - RHS is
drive
% side, spoke number from all on RHS to all on LHS
NR=N-NL;
Rw=300;
D=[37;17];
muD(1)=input('Enter spoke angle LHS (degrees): ');
muD(2)=input('Enter spoke angle RHS (degrees): ');
mu=muD.*pi/180;
Rh(1)=25;%input('Enter hub radius LHS: ');
Rh(2)=25;%input('Enter hub radius RHS: ');
Spd(1)=1.8;%input('Spoke diameter LHS: ');
Spd(2)=1.8;%input('Spoke diameter RHS: ');
gA=1/4.*pi*Spd.^2;
%
%% Torsional Stiffness
% Calculate spoke length - imperial units
%
% Calculate spoke length for different hub radius, dish and spoke
angle mu;
```

APPENDIX B MATLAB® SCRIPTS

B.3 Check_Stiffness_Properties.m

```

gS(1)=sqrt(Rw.^2+Rh(1).^2+D(1).^2-2.*Rw.*Rh(1).*cos(mu(1)));
gS(2)=sqrt(Rw.^2+Rh(2).^2+D(2).^2-2.*Rw.*Rh(2).*cos(mu(2)));
%
% Print Left and right spoke lengths
disp('Spoke lengths:')
fprintf('Left side spoke length:  %3.1f mm.\n',gS(1))
fprintf('Right side spoke length: %3.1f mm.\n\n',gS(2))
%
% Goldberg's equation for Torsional Stiffness
gTS=((pi.*E.*Rw.^2)/180).*(NL.*gA(1).*Rh(1).^2.*(sin(mu(1))).^2./(gS(
1).^3)...
    +NR.*gA(2).*Rh(2).^2.*(sin(mu(2))).^2./(gS(2).^3));
fprintf('Total torsional stiffness: %4.1f kg.mm/deg.\n',gTS);
%
%% Lateral Stiffness
% Spoke tension
T(1)=46.36;
T(2)=1.4*T(1);
% Load right to left
df=1.2;%input('\nEnter allowable deflection (mm): ');
Defrat=D(2)/df;
DfR=D(2)/Defrat;
DfL=-DfR;
% Load left to right
xl=D(1)*Defrat/D(2);
DfLl=D(1)/xl;
DfRl=-DfLl;
% Wind up angle
mufL=0.8*pi/180;
mufR=0.8*pi/180;
%% Need to change the following for matrix calculations
% Calculated change in spoke length under side load F - load from RHS
% shortens LHS
gSf(1)=(D(1).*DfL-Rw.*Rh(1).*(cos(mu(1)+mufL)-cos(mu(1))))./gS(1);
gSf(2)=(D(2).*DfR-Rw.*Rh(2).*(cos(mu(2)+mufR)-cos(mu(2))))./gS(2);
% Change in spoke tension
gTf(1)=E.*gA(1).*gSf(1)./gS(1);
gTf(2)=E.*gA(2).*gSf(2)./gS(2);
% Lateral force under a side load for RHS only - also valid for LHS
gVfR=(T./gS(2)).*DfR+(D(2).*T./(gS(2).^2)).*gSf(2)+(D(2)./gS(2)).*gTf(
2);
% Calculate the force required to deflect the wheel D/1000
F=N*(gVfR);
% Lateral stiffness of any wheel
% Load from LHS
gLSL=(NL.*(T(1)./gS(1)+((T(1)+E.*gA(1)).*D(1).^2)/(gS(1).^3)-...
    ((T(1)+E.*gA(1)).*D(1).*Rw.*Rh(1))/(gS(1).^3.*DfLl)...
    .*(cos(mu(1)+mufL)-cos(mu(1))))...
    +NR.*(T(2)./gS(2)+((T(2)+E.*gA(2)).*D(2).^2)/(gS(2).^3)-...
    ((T(2)+E.*gA(2)).*D(2).*Rw.*Rh(2))/(gS(2).^3.*DfRl)...
    .*(cos(mu(2)+mufR)-cos(mu(2)))))/2;
% Load from RHS
gLSR=(NL.*(T(1)./gS(1)+((T(1)+E.*gA(1)).*D(1).^2)/(gS(1).^3)-...
    ((T(1)+E.*gA(1)).*D(1).*Rw.*Rh(1))/(gS(1).^3.*DfL)...
    .*(cos(mu(1)+mufL)-cos(mu(1))))...
    +NR.*(T(2)./gS(2)+((T(2)+E.*gA(2)).*D(2).^2)/(gS(2).^3)-...
    ((T(2)+E.*gA(2)).*D(2).*Rw.*Rh(2))/(gS(2).^3.*DfR)...
    .*(cos(mu(2)+mufR)-cos(mu(2)))))/2;
LS=(gLSR+gLSL)/2;
fprintf('Total lateral stiffness:           %4.1f kg/mm.\n',LS)
fprintf('Lateral stiffness (load from left):  %4.1f kg/mm.\n',gLSL)
fprintf('Lateral stiffness (load from right): %4.1f kg/mm.\n',gLSR)
%% Display End time

```

APPENDIX B MATLAB® SCRIPTS
B.3 Check_Stiffness_Properties.m

```
% Display End time
formatOut = 'mm/dd/yy HH:MM:SS';
End_time=datestr(now,formatOut)
% End timer
toc;
```

APPENDIX C. ANSYS® PRE-PROCESSING

C.1 Mesh Convergence

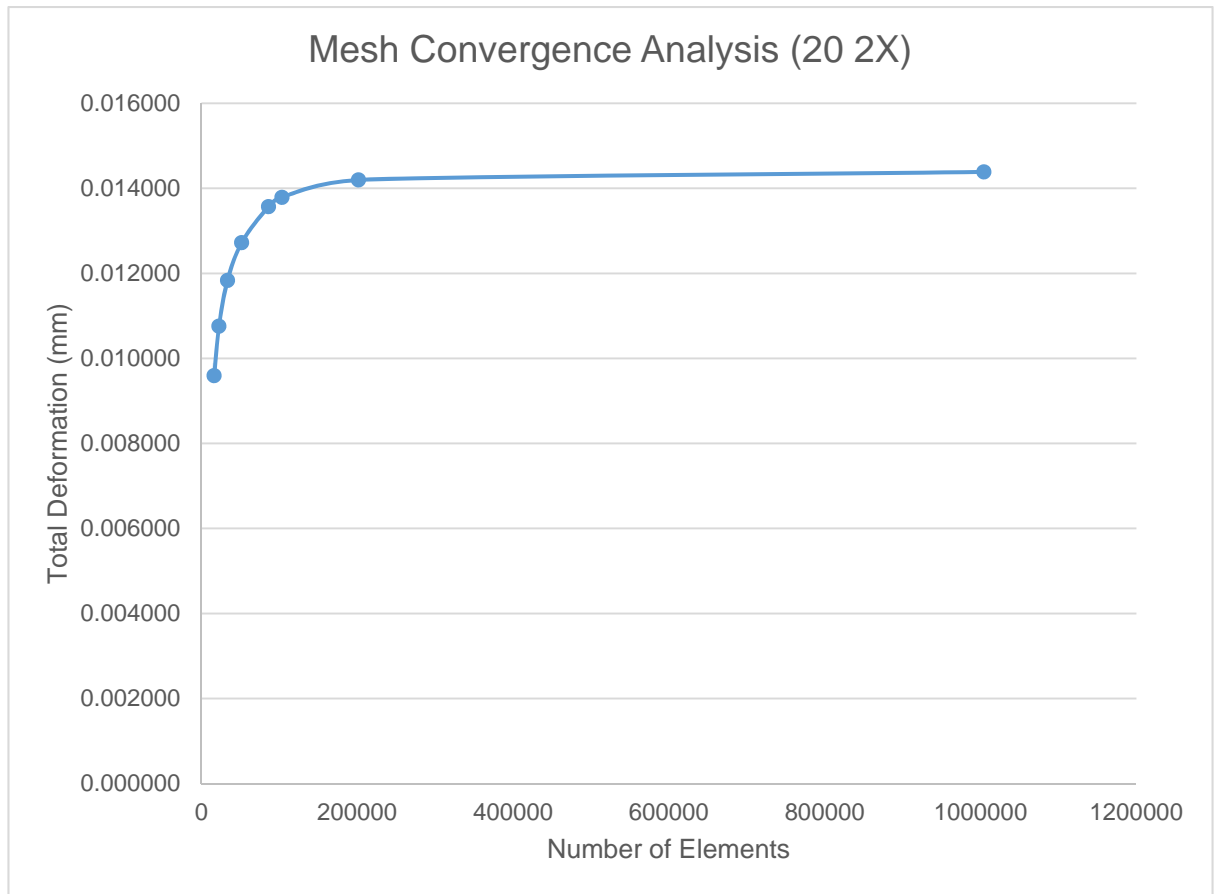


Figure C.1-1. Mesh convergence of the 20 2X wheel. The difference between the total deformation seen at 7.5 mm and 1 mm mesh is very small with a significant reduction in required computational time.

Table C.1-1. Mesh Convergence data for the 20 2X wheel.

Mesh size (mm)	Elements	Total Deformation (mm)	Element Quality	Skewness
50	16514	0.009594	0.220	0.770
25	22548	0.010758	0.217	0.796
15	33615	0.011833	0.286	0.779
10	51791	0.012724	0.375	0.728
7.5	86164	0.013570	0.544	0.561
5	103491	0.013789	0.546	0.572
2	201655	0.014197	0.687	0.411
1	1004193	0.014386	0.764	0.334

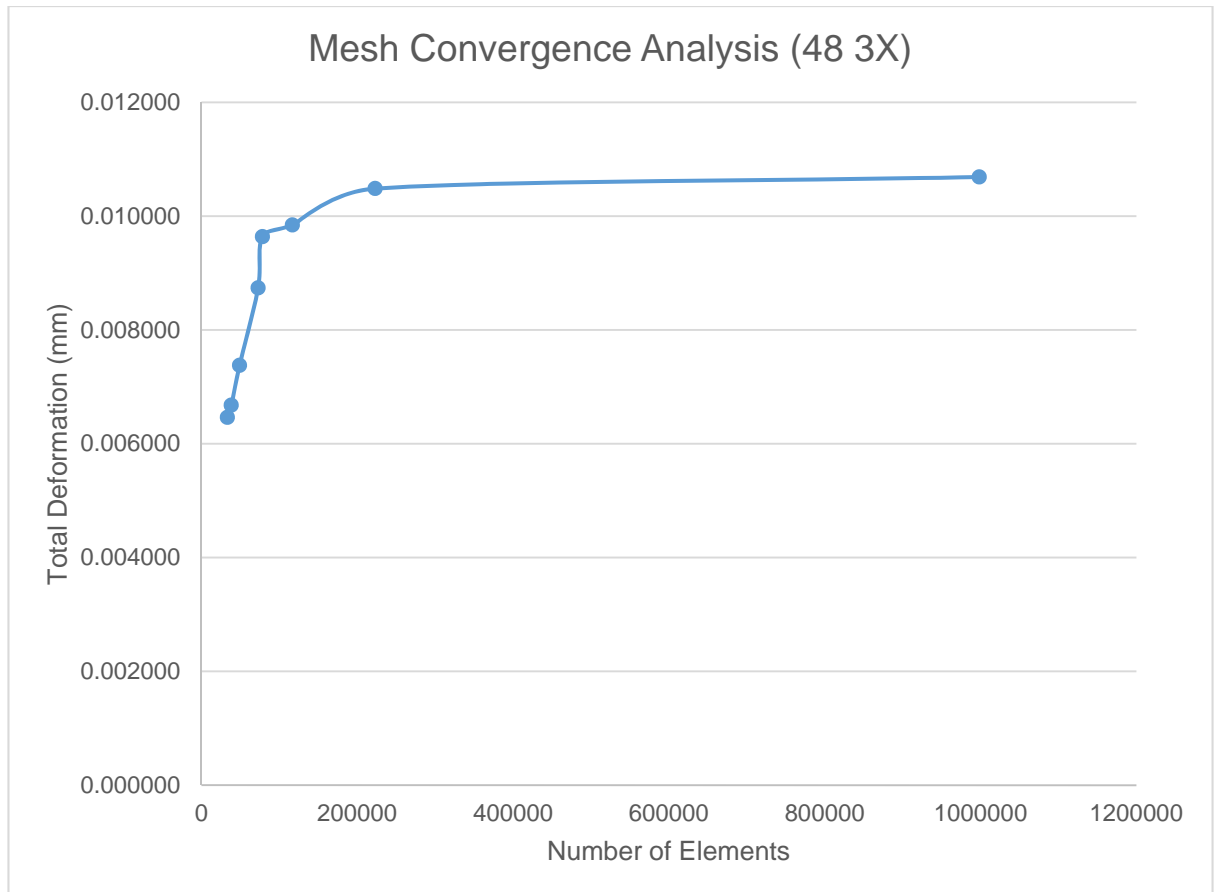


Figure C.1-2. Mesh convergence of the 48 3X wheel. The difference between the total deformation seen at 7.5 mm and 1 mm mesh is very small with a significant reduction in required computational time.

Table C.1-2. Mesh convergence data for the 48 3X wheel.

Mesh size (mm)	Elements	Total Deformation (mm)	Element Quality	Skewness
50	33375	0.006463	0.237	0.724
25	38463	0.006677	0.253	0.735
15	49111	0.007379	0.310	0.720
10	72849	0.008740	0.402	0.665
7.5	78352	0.009638	0.433	0.645
5	116872	0.009846	0.525	0.569
2	222969	0.010485	0.667	0.418
1	998260	0.010688	0.747	0.353

**APPENDIX D. THEORETICAL
CALCULATIONS**

D.1 An example of Pippard's Calculations

Table D.1-1 outlines the method used to obtain the theoretical values of stress, displacement and bending moments for wire spoked wheels. The table is based on one combination of K_1 and ϵ but was used for 70 combinations in total in order to validate the equations by matching the outputted values with those published by Pippard and White in the 1930s. Using the calculation methods available today, namely Microsoft Excel®, the accuracy of the calculations has been improved and although most values match those of Pippard and White, some values are quite different. This is assumed to be caused by the rounding of figures used in the 1930s when computational calculations were not available. Therefore, the values calculated in Excel® and shown in Table D.1-2, Table D.1-3 and Table D.1-4 can be used to calculate stresses and bending moments for the different load cases, if K_1 and ϵ are known.

APPENDIX D THEORETICAL CALCULATIONS

D.1 An example of Pippard's Calculations

Table D.1-1. Theoretical stress, displacement and bending moment calculations for wire spoked wheels including psi table for radial load scenario K1=600, ε (eps)=45°. The highlighted cells in the psi table are for the maximum values. (9 pages - total)

Constants	E1 (rim)	I (rim)	E2 (spokes)	R (rim)	R0 (hub)	N	L	as (Spoke Radius 0.9)	ar (cross-sectional area rim)	P (applied force)	K1	eps	delta
	69000	40000	207000	300	30	24	270	2.545	1	1000	600	45	0.5

Radial, Tangential and Lateral Load Values for M, Q, X, Y, alpha, beta and gamma

Name	Value	Formula	Reference
M	353.59	$M=1/27 + (K1sec(eps)/6)*(2-sin^2(eps))$	
Q	1716.62	$Q=sqrt(K1/27*[K1^2 cos^3(eps)+K1*(2-sin^2(eps))*(7+2/4*tan^2(eps))] + sec(eps)^2)$	
X	1.6574	$X=(M+Q)^{1/3} + (M-Q)^{1/3}$	Pippard & White 1932 p212 Eqn 11
Y	23.8325	$Y=(M+Q)^{1/3} - (M-Q)^{1/3}$	
a	3.3308	$a=sqrt((X^2/4+2Y^3+4Y+2Y^2/4)^{1/2} - (X/2+2/3)/2)$	
b	3.0982	$b=sqrt(((X/2+2Y^3+4Y+2Y^2/4)/2 - (X/2+2/3)/2)$	
g	0.9954	$g=(X-2/3)^{1/2}$	
Values for Tangential and Radial Load			
Z	1.62E-04	$Z=P*K1/(12*sqrt(3)*delta*E2*Q)$	Pippard & White 1932 p214
A	2.95E-04	$A=Z*2*ab*sinh(g*pi)$	
B	1.60E-07	$B=Z*((2*ab*cos(a*pi)*sinh(b*pi) - (a^2-b^2+g^2)*sin(a*pi)*cosh(b*pi))/(cosh^2(b*pi) - cos^2(a*pi)))$	For tangential: Pippard & White 1932 p221
C	3.67E-07	$C=Z*((a^2-b^2+g^2)*cos(a*pi)*sinh(b*pi) + 2*ab*sin(a*pi)*cosh(b*pi))/(cosh^2(b*pi) - cos^2(a*pi))$	
D	2.93E-04	$D=Z*2*ab*g*sinh(g*pi)$	
E	1.72E-06	$E=Z*((b*(a^2+b^2-g^2)*sin(a*pi)*cosh(b*pi) + a*(a^2+b^2+g^2)*cos(a*pi)*sinh(b*pi))/(cosh^2(b*pi) - cos^2(a*pi)))$	For radial: Pippard & White 1932 p214
F	6.03E-07	$F=Z*((a*(a^2+b^2+g^2)*sin(a*pi)*cosh(b*pi) - b*(a^2+b^2-g^2)*cos(a*pi)*sinh(b*pi))/(cosh^2(b*pi) - cos^2(a*pi)))$	

APPENDIX D THEORETICAL CALCULATIONS
D.1 An example of Pippard's Calculations

Radial Load				
By calculating u and v from 0 to pi the angles of maximum tension and compression were found to be: (t1 - tension; t2 - compression)				
	psi at max t1 (deg)	psi at max t2 (deg)	178	
t1: u	0.0020	$u = D \cosh(g^*psi) + E \cos(a^*psi) \cosh(b^*psi) + F \sin(a^*psi) \sinh(b^*psi)$		
t1: v	-0.0018	$v = -\{D/g^* \sinh(g^*psi) + (Eb-Fa)/(a^2 + b^2) * \cos(a^*psi) \sinh(b^*psi) + [Ea + Fb]/(a^2 + b^2) * \sin(a^*psi) \cosh(b^*psi)\}$		
t1	1.3117	$t1 = E2 * \text{delta} / R * (u + v) \tan(\epsilon ps)$		Pippard & White 1932 p213 Eqn 12 & 13
t2: u	-0.0083	$u = D \cosh(g^*psi) + E \cos(a^*psi) \cosh(b^*psi) + F \sin(a^*psi) \sinh(b^*psi)$		Pippard & White 1932 p211 Eqn 7
t2: v	-0.0003	$v = -\{D/g^* \sinh(g^*psi) + (Eb-Fa)/(a^2 + b^2) * \cos(a^*psi) \sinh(b^*psi) + [Ea + Fb]/(a^2 + b^2) * \sin(a^*psi) \cosh(b^*psi)\}$		Pippard & White 1932 p213 Eqn 12 & 13
t2	-2.7483	$t2 = E2 * \text{delta} / R * (u + v) \tan(\epsilon ps)$		Pippard & White 1932 p211 Eqn 7
Rt1/P	0.3935	$R * t1 / P$		Pippard and White 1932 p218
Rt2/P	-0.8245	$R * t2 / P$		
M	0.0749	$M/PR = 1 / \{ (g^* \text{sqrt}(3) Q) * [2abg(g^2 + 1) \coth(g^*pi) + (a \sinh(2^*b^*pi))^2 * (a^2 + b^2) * (a^2 + b^2 - 1) - g^2(3b^2 - a^2 + 1)] - b \sin(2^*a^*pi) \} \{ (a^2 + b^2) * (a^2 + b^2 + 1) + g^2(3a^2 - b^2 - 1) \} / \{ \cosh(2^*b^*pi) - \cos(2^*a^*pi) \}$		Pippard & White 1932 p 219-20 Eqn 16
Tangential Load				
By calculating u and v from 0 to pi the angle of maximum force was found to be:				
	psi	Modified R	200.00	$R = (K1.E1.I) / (2.\text{delta}.E2)^{1/3}$
u	0.0021	$u = A \cosh(g^*psi) + B \cos(a^*psi) \sinh(b^*psi) + C \sin(a^*psi) \cosh(b^*psi)$		
v	-0.0025	$v = -\{A/g^* \cosh(g^*psi) + (Bb-Ca)/(a^2 + b^2) * \cos(a^*psi) \sinh(b^*psi) + (Ba + Cb)/(a^2 + b^2) * \sin(a^*psi) \cosh(b^*psi)\}$		Pippard & White 1932 p221 Eqn 18 & 19
t1	1.5740	$t1 = E2 * \text{delta} / R * (u + v) \tan(\epsilon ps)$		Pippard & White 1932 p211 Eqn 7
t2	-0.1414	$t2 = E2 * \text{delta} / R * (u + v) \tan(\epsilon ps)$		Pippard and White 1932 p223
Rtmax/P	0.4722	$R \tan(\epsilon ps)$		
Using Fig.16 Pippard & White 1932 p 227, psi at max moment when K1=600:				
M	-0.0071	$M/(PR) = E1.I/(P.R^3) [A(g^2 + 1) \sinh(g^*psi) + \{(b^2 - a^2 + 1)B + 2abC\} \cos(a^*psi) \sinh(b^*psi) + \{(b^2 - a^2 + 1)C - 2abB\} \sin(a^*psi) \cosh(b^*psi)]$		Pippard & White 1932 p224 Eqn. 20; Table V p229

APPENDIX D THEORETICAL CALCULATIONS

D.1 An example of Pippard's Calculations

Lateral/Side Load						
Parameters specific for Lateral Load: (Pippard & Francis 1932 p441 Eqn. 11)						
Z	3.34E-05	$Z=PR^2(n+1)/(6*\text{sqrt}(3)*E*I*Q)$	n	1	$n=\tan^2(\text{eps})/2$	$K2=KL/\text{sec}(\text{eps})$
G	6.02E-05	$G=Z*(2abg/\text{sinh}(g*\text{pi}))$	Pippard & Francis 1932 p440			
H	3.53E-07	$H=-Z*(a(a^2+b^2+g^2)\cos(a*\text{pi})\text{sinh}(b*\text{pi})+b(a^2+b^2-g^2)\sin(a*\text{pi})\cosh(b*\text{pi}))/(\cosh^2(b*\text{pi})-\cos^2(a*\text{pi}))$	Pippard & Francis 1932 p439			
U	1.24E-07	$U=-Z*(a(a^2+b^2+g^2)\sin(a*\text{pi})\cosh(b*\text{pi})-b(a^2+b^2-g^2)\cos(a*\text{pi})\sinh(b*\text{pi}))/(\cosh^2(b*\text{pi})-\cos^2(a*\text{pi}))$	psi	180	phi	5
Calculating x and w for all psi the maximum value is at:						
x	-0.0017	$x=\text{Gcosh}(g*\text{psi})+\text{Hcos}(a*\text{psi})\cosh(b*\text{psi})+\text{Usin}(a*\text{psi})\sinh(b*\text{psi})$	mod R	906.418393	Pippard & Francis 1932 p439	
w	1.0547	$w=R/(n+1)*[(n-g^2)/g^2*\text{Gcosh}(g*\text{psi})-\cos(a*\text{psi})\cosh(b*\text{psi})/(a^2+b^2)^2*H*((a^2+b^2)^2+n*(a^2-b^2))+2abnU]-\sin(a*\text{psi})\sinh(b*\text{psi})/(a^2+b^2)^2*[U*((a^2+b^2)^2+n*(a^2-b^2))-2abnH]$	Pippard & Francis 1932 p438 Eqn. 10			
t	10.4958	$t=\text{delta}*E*2*\text{ntan}(\text{phi})/(R*(1+\cos^2(\text{eps})\tan^2(\text{phi})))$	Pippard & Francis 1932 p438 Eqn. 6			
Rsin(phi)/P	0.8292	$R*\text{r}*\text{sin}(\text{phi})/P$	Pippard & Francis 1932 p444: Table I			

APPENDIX D THEORETICAL CALCULATIONS

D.1 An example of Pippard's Calculations

PSI Table @ K1=600, $\epsilon=45^\circ$						
psi	u	v	t1	t2	Rt1/P	Rt2/P
0.0000	3.0533	0.0000	3.0533	3.0533	0.0305	0.0305
0.0175	3.0538	-0.0533	3.1071	3.0005	0.0311	0.0300
0.0349	3.0552	-0.1066	3.1618	2.9486	0.0316	0.0295
0.0524	3.0576	-0.1599	3.2175	2.8976	0.0322	0.0290
0.0698	3.0609	-0.2133	3.2742	2.8475	0.0327	0.0285
0.0873	3.0651	-0.2668	3.3319	2.7983	0.0333	0.0280
0.1047	3.0703	-0.3203	3.3907	2.7500	0.0339	0.0275
0.1222	3.0765	-0.3740	3.4504	2.7025	0.0345	0.0270
0.1396	3.0835	-0.4277	3.5113	2.6558	0.0351	0.0266
0.1571	3.0915	-0.4816	3.5732	2.6099	0.0357	0.0261
0.1745	3.1005	-0.5357	3.6361	2.5648	0.0364	0.0256
0.1920	3.1103	-0.5898	3.7002	2.5205	0.0370	0.0252
0.2094	3.1211	-0.6442	3.7653	2.4769	0.0377	0.0248
0.2269	3.1328	-0.6988	3.8316	2.4340	0.0383	0.0243
0.2443	3.1454	-0.7536	3.8990	2.3918	0.0390	0.0239
0.2618	3.1589	-0.8086	3.9675	2.3503	0.0397	0.0235
0.2793	3.1733	-0.8639	4.0372	2.3094	0.0404	0.0231
0.2967	3.1886	-0.9194	4.1080	2.2692	0.0411	0.0227
0.3142	3.2047	-0.9752	4.1799	2.2296	0.0418	0.0223
0.3316	3.2218	-1.0312	4.2530	2.1905	0.0425	0.0219
0.3491	3.2397	-1.0876	4.3273	2.1520	0.0433	0.0215
0.3665	3.2584	-1.1443	4.4028	2.1141	0.0440	0.0211
0.3840	3.2780	-1.2014	4.4794	2.0767	0.0448	0.0208
0.4014	3.2985	-1.2588	4.5572	2.0397	0.0456	0.0204
0.4189	3.3197	-1.3165	4.6363	2.0032	0.0464	0.0200
0.4363	3.3418	-1.3747	4.7165	1.9672	0.0472	0.0197
0.4538	3.3647	-1.4332	4.7979	1.9315	0.0480	0.0193
0.4712	3.3884	-1.4921	4.8805	1.8963	0.0488	0.0190
0.4887	3.4128	-1.5515	4.9643	1.8614	0.0496	0.0186
0.5061	3.4381	-1.6112	5.0493	1.8268	0.0505	0.0183
0.5236	3.4641	-1.6715	5.1356	1.7926	0.0514	0.0179
0.5411	3.4909	-1.7322	5.2230	1.7587	0.0522	0.0176
0.5585	3.5184	-1.7933	5.3117	1.7250	0.0531	0.0173
0.5760	3.5466	-1.8550	5.4016	1.6916	0.0540	0.0169
0.5934	3.5756	-1.9171	5.4927	1.6584	0.0549	0.0166

APPENDIX D THEORETICAL CALCULATIONS

D.1 An example of Pippard's Calculations

PSI Table @ K1=600, ε=45°						
psi	u	v	t1	t2	Rt1/P	Rt2/P
0.6109	3.6052	-1.9798	5.5851	1.6254	0.0559	0.0163
0.6283	3.6356	-2.0430	5.6786	1.5927	0.0568	0.0159
0.6458	3.6667	-2.1067	5.7735	1.5600	0.0577	0.0156
0.6632	3.6985	-2.1710	5.8695	1.5276	0.0587	0.0153
0.6807	3.7310	-2.2358	5.9669	1.4952	0.0597	0.0150
0.6981	3.7642	-2.3012	6.0655	1.4630	0.0607	0.0146
0.7156	3.7981	-2.3672	6.1653	1.4309	0.0617	0.0143
0.7330	3.8327	-2.4338	6.2665	1.3989	0.0627	0.0140
0.7505	3.8680	-2.5010	6.3690	1.3670	0.0637	0.0137
0.7679	3.9040	-2.5688	6.4728	1.3351	0.0647	0.0134
0.7854	3.9407	-2.6373	6.5780	1.3034	0.0658	0.0130
0.8029	3.9781	-2.7064	6.6845	1.2717	0.0668	0.0127
0.8203	4.0163	-2.7762	6.7924	1.2401	0.0679	0.0124
0.8378	4.0552	-2.8466	6.9018	1.2086	0.0690	0.0121
0.8552	4.0950	-2.9177	7.0127	1.1773	0.0701	0.0118
0.8727	4.1356	-2.9895	7.1251	1.1460	0.0713	0.0115
0.8901	4.1770	-3.0621	7.2391	1.1149	0.0724	0.0111
0.9076	4.2193	-3.1354	7.3547	1.0840	0.0735	0.0108
0.9250	4.2626	-3.2094	7.4719	1.0532	0.0747	0.0105
0.9425	4.3069	-3.2841	7.5910	1.0227	0.0759	0.0102
0.9599	4.3522	-3.3597	7.7119	0.9925	0.0771	0.0099
0.9774	4.3986	-3.4361	7.8347	0.9626	0.0783	0.0096
0.9948	4.4463	-3.5133	7.9596	0.9330	0.0796	0.0093
1.0123	4.4952	-3.5913	8.0865	0.9039	0.0809	0.0090
1.0297	4.5455	-3.6702	8.2157	0.8754	0.0822	0.0088
1.0472	4.5973	-3.7500	8.3473	0.8474	0.0835	0.0085
1.0647	4.6507	-3.8307	8.4814	0.8200	0.0848	0.0082
1.0821	4.7058	-3.9123	8.6181	0.7934	0.0862	0.0079
1.0996	4.7627	-3.9949	8.7576	0.7677	0.0876	0.0077
1.1170	4.8215	-4.0786	8.9001	0.7430	0.0890	0.0074
1.1345	4.8825	-4.1633	9.0458	0.7193	0.0905	0.0072
1.1519	4.9458	-4.2490	9.1949	0.6968	0.0919	0.0070
1.1694	5.0116	-4.3359	9.3475	0.6757	0.0935	0.0068
1.1868	5.0800	-4.4240	9.5040	0.6560	0.0950	0.0066
1.2043	5.1513	-4.5133	9.6645	0.6380	0.0966	0.0064

APPENDIX D THEORETICAL CALCULATIONS

D.1 An example of Pippard's Calculations

PSI Table @ $K1=600, \epsilon=45^\circ$						
psi	u	v	t1	t2	Rt1/P	Rt2/P
1.2217	5.2256	-4.6038	9.8294	0.6218	0.0983	0.0062
1.2392	5.3032	-4.6957	9.9989	0.6075	0.1000	0.0061
1.2566	5.3844	-4.7889	10.1733	0.5954	0.1017	0.0060
1.2741	5.4693	-4.8837	10.3529	0.5856	0.1035	0.0059
1.2915	5.5583	-4.9799	10.5381	0.5784	0.1054	0.0058
1.3090	5.6516	-5.0777	10.7293	0.5739	0.1073	0.0057
1.3265	5.7494	-5.1772	10.9266	0.5723	0.1093	0.0057
1.3439	5.8522	-5.2784	11.1307	0.5738	0.1113	0.0057
1.3614	5.9603	-5.3815	11.3418	0.5788	0.1134	0.0058
1.3788	6.0738	-5.4865	11.5603	0.5873	0.1156	0.0059
1.3963	6.1932	-5.5935	11.7868	0.5997	0.1179	0.0060
1.4137	6.3189	-5.7027	12.0216	0.6161	0.1202	0.0062
1.4312	6.4511	-5.8142	12.2652	0.6369	0.1227	0.0064
1.4486	6.5902	-5.9279	12.5181	0.6622	0.1252	0.0066
1.4661	6.7365	-6.0442	12.7808	0.6923	0.1278	0.0069
1.4835	6.8905	-6.1631	13.0537	0.7274	0.1305	0.0073
1.5010	7.0525	-6.2848	13.3373	0.7677	0.1334	0.0077
1.5184	7.2229	-6.4094	13.6322	0.8135	0.1363	0.0081
1.5359	7.4019	-6.5370	13.9389	0.8649	0.1394	0.0086
1.5533	7.5901	-6.6678	14.2579	0.9223	0.1426	0.0092
1.5708	7.7876	-6.8020	14.5896	0.9856	0.1459	0.0099
1.5882	7.9949	-6.9397	14.9346	1.0552	0.1493	0.0106
1.6057	8.2123	-7.0811	15.2934	1.1312	0.1529	0.0113
1.6232	8.4401	-7.2264	15.6665	1.2136	0.1567	0.0121
1.6406	8.6785	-7.3758	16.0542	1.3027	0.1605	0.0130
1.6581	8.9278	-7.5294	16.4572	1.3983	0.1646	0.0140
1.6755	9.1882	-7.6875	16.8757	1.5007	0.1688	0.0150
1.6930	9.4599	-7.8502	17.3101	1.6097	0.1731	0.0161
1.7104	9.7431	-8.0178	17.7608	1.7253	0.1776	0.0173
1.7279	10.0378	-8.1904	18.2281	1.8474	0.1823	0.0185
1.7453	10.3440	-8.3682	18.7123	1.9758	0.1871	0.0198
1.7628	10.6619	-8.5515	19.2134	2.1104	0.1921	0.0211
1.7802	10.9912	-8.7405	19.7317	2.2508	0.1973	0.0225
1.7977	11.3319	-8.9353	20.2672	2.3967	0.2027	0.0240
1.8151	11.6837	-9.1361	20.8198	2.5476	0.2082	0.0255

APPENDIX D THEORETICAL CALCULATIONS

D.1 An example of Pippard's Calculations

PSI Table @ K1=600, ε=45°						
psi	u	v	t1	t2	Rt1/P	Rt2/P
1.8326	12.0462	-9.3432	21.3894	2.7031	0.2139	0.0270
1.8500	12.4192	-9.5566	21.9758	2.8625	0.2198	0.0286
1.8675	12.8019	-9.7767	22.5787	3.0252	0.2258	0.0303
1.8850	13.1940	-10.0036	23.1975	3.1904	0.2320	0.0319
1.9024	13.5945	-10.2373	23.8318	3.3572	0.2383	0.0336
1.9199	14.0026	-10.4781	24.4808	3.5245	0.2448	0.0352
1.9373	14.4174	-10.7261	25.1436	3.6913	0.2514	0.0369
1.9548	14.8377	-10.9814	25.8192	3.8563	0.2582	0.0386
1.9722	15.2623	-11.2441	26.5064	4.0181	0.2651	0.0402
1.9897	15.6895	-11.5142	27.2037	4.1753	0.2720	0.0418
2.0071	16.1179	-11.7918	27.9097	4.3262	0.2791	0.0433
2.0246	16.5457	-12.0768	28.6225	4.4689	0.2862	0.0447
2.0420	16.9708	-12.3693	29.3402	4.6015	0.2934	0.0460
2.0595	17.3912	-12.6692	30.0604	4.7220	0.3006	0.0472
2.0769	17.8044	-12.9763	30.7808	4.8281	0.3078	0.0483
2.0944	18.2079	-13.2906	31.4986	4.9173	0.3150	0.0492
2.1118	18.5990	-13.6119	32.2108	4.9871	0.3221	0.0499
2.1293	18.9745	-13.9398	32.9143	5.0348	0.3291	0.0503
2.1468	19.3314	-14.2741	33.6055	5.0573	0.3361	0.0506
2.1642	19.6662	-14.6144	34.2806	5.0517	0.3428	0.0505
2.1817	19.9751	-14.9604	34.9356	5.0147	0.3494	0.0501
2.1991	20.2545	-15.3115	35.5660	4.9430	0.3557	0.0494
2.2166	20.5001	-15.6672	36.1673	4.8328	0.3617	0.0483
2.2340	20.7075	-16.0269	36.7344	4.6806	0.3673	0.0468
2.2515	20.8724	-16.3898	37.2622	4.4826	0.3726	0.0448
2.2689	20.9898	-16.7552	37.7450	4.2346	0.3774	0.0423
2.2864	21.0548	-17.1222	38.1770	3.9326	0.3818	0.0393
2.3038	21.0623	-17.4898	38.5521	3.5725	0.3855	0.0357
2.3213	21.0069	-17.8570	38.8639	3.1498	0.3886	0.0315
2.3387	20.8830	-18.2227	39.1057	2.6603	0.3911	0.0266
2.3562	20.6850	-18.5856	39.2705	2.0994	0.3927	0.0210
2.3736	20.4071	-18.9443	39.3513	1.4628	0.3935	0.0146
2.3911	20.0433	-19.2974	39.3407	0.7459	0.3934	0.0075
2.4086	19.5877	-19.6434	39.2311	-0.0557	0.3923	-0.0006
2.4260	19.0342	-19.9806	39.0147	-0.9464	0.3901	-0.0095

APPENDIX D THEORETICAL CALCULATIONS

D.1 An example of Pippard's Calculations

PSI Table @ K1=600, ε=45°						
psi	u	v	t1	t2	Rt1/P	Rt2/P
2.4435	18.3767	-20.3072	38.6839	-1.9305	0.3868	-0.0193
2.4609	17.6093	-20.6214	38.2307	-3.0121	0.3823	-0.0301
2.4784	16.7259	-20.9212	37.6471	-4.1953	0.3765	-0.0420
2.4958	15.7207	-21.2045	36.9253	-5.4838	0.3693	-0.0548
2.5133	14.5881	-21.4692	36.0573	-6.8811	0.3606	-0.0688
2.5307	13.3225	-21.7130	35.0355	-8.3905	0.3504	-0.0839
2.5482	11.9188	-21.9335	33.8522	-10.0147	0.3385	-0.1001
2.5656	10.3722	-22.1282	32.5004	-11.7560	0.3250	-0.1176
2.5831	8.6784	-22.2947	30.9730	-13.6163	0.3097	-0.1362
2.6005	6.8334	-22.4302	29.2636	-15.5968	0.2926	-0.1560
2.6180	4.8340	-22.5323	27.3663	-17.6983	0.2737	-0.1770
2.6354	2.6777	-22.5981	25.2757	-19.9204	0.2528	-0.1992
2.6529	0.3625	-22.6248	22.9874	-22.2623	0.2299	-0.2226
2.6704	-2.1123	-22.6098	20.4975	-24.7221	0.2050	-0.2472
2.6878	-4.7468	-22.5502	17.8034	-27.2970	0.1780	-0.2730
2.7053	-7.5397	-22.4432	14.9035	-29.9829	0.1490	-0.2998
2.7227	-10.4887	-22.2861	11.7973	-32.7748	0.1180	-0.3277
2.7402	-13.5901	-22.0762	8.4861	-35.6662	0.0849	-0.3567
2.7576	-16.8385	-21.8108	4.9723	-38.6493	0.0497	-0.3865
2.7751	-20.2272	-21.4876	1.2604	-41.7148	0.0126	-0.4171
2.7925	-23.7476	-21.1040	-2.6436	-44.8516	-0.0264	-0.4485
2.8100	-27.3893	-20.6579	-6.7314	-48.0472	-0.0673	-0.4805
2.8274	-31.1397	-20.1473	-10.9924	-51.2870	-0.1099	-0.5129
2.8449	-34.9841	-19.5704	-15.4137	-54.5545	-0.1541	-0.5455
2.8623	-38.9056	-18.9257	-19.9799	-57.8313	-0.1998	-0.5783
2.8798	-42.8845	-18.2120	-24.6725	-61.0965	-0.2467	-0.6110
2.8972	-46.8987	-17.4285	-29.4701	-64.3272	-0.2947	-0.6433
2.9147	-50.9231	-16.5749	-34.3483	-67.4980	-0.3435	-0.6750
2.9322	-54.9299	-15.6511	-39.2788	-70.5810	-0.3928	-0.7058
2.9496	-58.8879	-14.6577	-44.2302	-73.5456	-0.4423	-0.7355
2.9671	-62.7628	-13.5960	-49.1668	-76.3588	-0.4917	-0.7636
2.9845	-66.5168	-12.4676	-54.0492	-78.9844	-0.5405	-0.7898
3.0020	-70.1086	-11.2750	-58.8336	-81.3837	-0.5883	-0.8138
3.0194	-73.4933	-10.0215	-63.4717	-83.5148	-0.6347	-0.8351
3.0369	-76.6219	-8.7111	-67.9108	-85.3331	-0.6791	-0.8533

APPENDIX D THEORETICAL CALCULATIONS

D.1 An example of Pippard's Calculations

PSI Table @ $K1=600, \epsilon=45^\circ$						
psi	u	v	t1	t2	Rt1/P	Rt2/P
3.0543	-79.4418	-7.3487	-72.0931	-86.7906	-0.7209	-0.8679
3.0718	-81.8963	-5.9402	-75.9561	-87.8365	-0.7596	-0.8784
3.0892	-83.9245	-4.4925	-79.4320	-88.4170	-0.7943	-0.8842
3.1067	-85.4613	-3.0136	-82.4478	-88.4749	-0.8245	-0.8847
3.1241	-86.4377	-1.5126	-84.9252	-87.9503	-0.8493	-0.8795
3.1416	-86.7802	0.0000	-86.7802	-86.7802	-0.8678	-0.8678
Maxima					0.3935	0.0506
Minima					-0.8678	-0.8847

APPENDIX D THEORETICAL CALCULATIONS

D.1 An example of Pippard's Calculations

Table D.1-2. Rt1/P, Rt2/P and M0/PR tables for a radial load case calculated using and compared to Pippard and White (1932 p218 & 220)

	Rt1/P	Epsilon (rad)									
		0.000	0.175	0.349	0.524	0.785	1.047	1.309	1.484	1.570	1.571
KI	0	0.1592	0.1592	0.1592	0.1592	0.1592	0.1592	0.1592	0.1592	0.1591	--
	10	0.1040	0.1212	0.1394	0.1586	0.1900	0.2284	0.2926	0.4102	2.3945	NA
	50	0.1108	0.1368	0.1663	0.1999	0.2599	0.3383	0.4592	0.6589	4.0672	NA
	100	0.1128	0.1426	0.1773	0.2179	0.2934	0.3961	0.5576	0.8169	5.1080	NA
	200	0.1160	0.1491	0.1891	0.2372	0.3301	0.4629	0.6789	1.0148	6.4104	NA
	600	0.1231	0.1611	0.2091	0.2695	0.3935	0.5862	0.9237	1.4355	9.2498	NA
	1000	0.1276	0.1676	0.2191	0.2852	0.4248	0.6502	1.0634	1.6902	10.9428	NA
	Rt2/P	Epsilon (rad)									
		0.000	0.175	0.349	0.524	0.785	1.047	1.309	1.484	1.570	1.571
KI	0	-0.1592	-0.1592	-0.1592	-0.1592	-0.1592	-0.1592	-0.1592	-0.1592	-0.1591	--
	10	-0.2772	-0.2761	-0.2734	-0.2695	-0.2639	-0.2662	-0.3025	-0.4111	-2.3949	NA
	50	-0.4214	-0.4211	-0.4204	-0.4200	-0.4224	-0.4361	-0.4911	-0.6624	-4.0671	NA
	100	-0.5059	-0.5062	-0.5072	-0.5097	-0.5187	-0.5414	-0.6096	-0.8231	-5.1070	NA
	200	-0.6078	-0.6087	-0.6122	-0.6190	-0.6382	-0.6751	-0.7630	-1.0255	-6.4128	NA
	600	-0.8128	-0.8152	-0.8247	-0.8412	-0.8847	-0.9601	-1.0995	-1.4618	-9.2490	NA
	1000	-0.9299	-0.9336	-0.9461	-0.9696	-1.0291	-1.1298	-1.3062	-1.7280	-10.9464	NA
	M0/PR	Epsilon (rad)									
		0.000	0.175	0.349	0.524	0.785	1.047	1.309	1.484	1.570	1.571
KI	0	0.2387	0.2387	0.2387	0.2387	0.2387	0.2387	0.2387	0.2387	0.2386	-
	10	0.1763	0.1765	0.1773	0.1786	0.1809	0.1819	0.1747	0.1497	0.0590	0.0
	50	0.1258	0.1261	0.1269	0.1283	0.1312	0.1337	0.1306	0.1143	0.0452	0.0
	100	0.1074	0.1077	0.1085	0.1099	0.1128	0.1159	0.1150	0.1016	0.0402	0.0
	200	0.0913	0.0916	0.0923	0.0937	0.0966	0.1001	0.1009	0.0903	0.0358	0.0
	600	0.0702	0.0704	0.0711	0.0722	0.0749	0.0787	0.0815	0.0747	0.0298	0.0
	1000	0.0620	0.0622	0.0628	0.0639	0.0664	0.0702	0.0735	0.0683	0.0274	0.0

APPENDIX D THEORETICAL CALCULATIONS

D.1 An example of Pippard’s Calculations

Table D.1-3. Tangential load scenario calculated using and compared to Pippard and White (1932 p223 & 229)

	Rt1/P	Epsilon (rad)									
		0.087	0.175	0.349	0.524	0.785	1.047	1.309	1.484	1.569	1.570
KI	0	1.0722	0.6174	0.3918	0.3183	0.2717	0.2510	0.2415	0.2390	0.2388	0.2389
	10	1.0906	0.6406	0.4242	0.3595	0.3258	0.3200	0.3386	0.3938	0.7181	0.9507
	50	1.1155	0.6688	0.4593	0.4021	0.3812	0.3906	0.4269	0.5002	0.9319	1.2379
	100	1.1254	0.6802	0.4740	0.4206	0.4063	0.4244	0.4714	0.5570	1.0437	1.3877
	200	1.1347	0.6910	0.4882	0.4387	0.4319	0.4602	0.5213	0.6211	1.1695	1.5561
	600	1.1479	0.7065	0.5091	0.4661	0.4722	0.5199	0.6106	0.7395	1.4015	1.8666
	1000	1.1534	0.7130	0.5180	0.4781	0.4905	0.5484	0.6564	0.8025	1.5249	2.0316
	M	Epsilon (rad)									
		0.087	0.175	0.349	0.524	0.785	1.047	1.309	1.484	1.569	1.570
KI	0	-0.6354	-0.6354	-0.6354	-0.6354	-0.6354	-0.6354	-0.6354	-0.6354	Pippard and White (1932) did not have calculations at this value of ε.	-0.6350
	10	-0.0375	-0.0376	-0.0379	-0.0384	-0.0392	-0.0396	-0.0365	-0.0262		0.0000
	50	-0.0197	-0.0198	-0.0200	-0.0204	-0.0212	-0.0219	-0.0208	-0.0159		-0.0004
	100	-0.0145	-0.0146	-0.0148	-0.0151	-0.0159	-0.0166	-0.0162	-0.0126		-0.0003
	200	-0.0106	-0.0106	-0.0108	-0.0110	-0.0117	-0.0124	-0.0125	-0.0100		-0.0004
	600	-0.0063	-0.0063	-0.0064	-0.0066	-0.0071	-0.0077	-0.0082	-0.0069		-0.0003
	1000	-0.0049	-0.0050	-0.0050	-0.0052	-0.0056	-0.0062	-0.0067	-0.0058		-0.0003

Table D.1-4. Side load scenario calculated using and compared to Pippard and Francis (1932 p444)

Rtsin(phi)/P		Epsilon (rad)									
		0.000	0.175	0.349	0.524	0.785	1.047	1.309	1.484	1.570	1.571
KI	0	0.1592	0.1592	0.1592	0.1593	0.1594	0.1595	0.1596	0.1600	0.1710	461.6004
	10	0.3495	0.3491	0.3459	0.3408	0.3366	0.3572	0.3408	0.5961	2.9839	INF
	50	0.4994	0.4982	0.4939	0.4868	0.4744	0.4946	0.9473	0.9663	5.3833	INF
	100	0.5847	0.5830	0.5777	0.5689	0.5512	0.5611	0.8513	1.1238	6.9933	INF
	200	0.6870	0.6848	0.6782	0.6672	0.6434	0.6370	0.7184	1.3643	8.3304	INF
	600	0.8922	0.8892	0.8800	0.8645	0.8292	0.7920	1.2996	1.8525	10.5704	INF
	1000	1.0094	1.0059	0.9952	0.9772	0.9356	0.8839	1.1726	2.1316	13.0406	INF

**APPENDIX E. OPTIMISED GEOMETRY
RESULTS**

APPENDIX E OPTIMISED GEOMETRY RESULTS

E.1 Optimised Wheel Geometry for Rear Wheels with a 55 mm hub

E.1 Optimised Wheel Geometry for Rear Wheels with a 55 mm hub

Table E.1-1. Optimised geometry table for 20 and 24 spoke rear wheels with 55 mm hub. Opt. – Optimal; Stiff. – stiffness; Max – maximum.

Optimisation Summary	20 Spoke					24 spoke				
Property	Max TS	Max LS	Opt (TS)	Opt (LS)	Opt	Max TS	Max LS	Opt (TS)	Opt (LS)	Opt
Number of Spokes LHS	4	16	8	8	Optimal by LS	4	20	8	10	Optimal by LS
Number of Spokes RHS	16	4	12	12		20	4	16	14	
Spoke angle LHS	83	0	47	72		83	0	53	76	
Spoke angle RHS	83	0	81	78		83	0	82	64	
Spoke length LHS	299.7	276.9	285.3	295.0		299.7	276.9	287.4	296.7	
Spoke length RHS	298.5	275.5	297.6	296.3		298.5	275.5	298.0	290.4	
LHS stiffness	0.7	9.2	6.6	7.3		-0.4	11.3	5.8	9.7	
RHS stiffness	9.1	9.0	5.9	4.5		11.9	11.0	8.1	4.8	
	Max. Stiff.	Opt (TS)	Opt (%)	Opt (LS)	Opt%	Max. Stiff.	Opt (TS)	Opt (%)	Opt (LS)	Opt %
Torsional Stiffness	12733	10823	85%	12459	98%	15286	13910	91%	14164	93%
Lateral Stiffness	9.0	6.2	69%	5.9	66%	11.1	6.9	62%	7.2	65%
Average:			76.9%		81.7%			76.6%		78.8%

Table E.1-2. Optimised geometry table for 28 and 32 spoke rear wheels with 55 mm hub.

Optimisation Summary	28 spoke					32 spoke				
Property	Max TS	Max LS	Opt (TS)	Opt (LS)	Opt	Max TS	Max LS	Opt (TS)	Opt (LS)	Opt
Number of Spokes LHS	4	24	10	10	Optimal by TS	4	28	12	12	Optimal by LS
Number of Spokes RHS	24	4	18	18		28	4	20	20	
Spoke angle LHS	83	0	78	69		83	0	60	70	
Spoke angle RHS	83	0	78	68		83	0	71	69	
Spoke length LHS	299.7	276.9	297.5	293.7		299.7	276.9	290.1	294.1	
Spoke length RHS	298.5	275.5	296.3	292.1		298.5	275.5	293.3	292.5	
LHS stiffness	-1.5	13.3	8.2	8.5		-2.7	15.4	10.3	10.6	
RHS stiffness	14.6	13.0	7.7	7.9		17.4	15.0	8.9	8.3	
	Max. Stiff.	Opt (TS)	Opt (%)	Opt (LS)	Opt%	Max. Stiff.	Opt (TS)	Opt (%)	Opt (LS)	Opt %
Torsional Stiffness	17838	17660	99%	16625	93%	20391	18557	91%	19175	94%
Lateral Stiffness	13.1	7.9	60%	8.1	62%	15.1	9.5	63%	9.4	62%
Average:			79.7%		77.5%			77.0%		78.1%

APPENDIX E OPTIMISED GEOMETRY RESULTS

E.1 Optimised Wheel Geometry for Rear Wheels with a 55 mm hub

Table E.1-3. Optimised geometry table for 36 and 48 spoke rear wheels with 55 mm hub.

Optimisation Summary	36 spoke					48 spoke				
Property	Max TS	Max LS	Opt (TS)	Opt (LS)	Opt	Max TS	Max LS	Opt (TS)	Opt (LS)	Opt
Number of Spokes LHS	4	32	12	12	Optimal by LS	4	44	20	18	Optimal by LS
Number of Spokes RHS	32	4	24	24		44	4	28	30	
Spoke angle LHS	83	0	45	76		83	0	46	80	
Spoke angle RHS	83	0	75	80		83	0	67	60	
Spoke length LHS	299.7	276.9	284.7	296.7		299.7	276.9	285.0	298.4	
Spoke length RHS	298.5	275.5	295.0	297.2		298.5	275.5	291.6	288.8	
LHS stiffness	-3.8	17.5	8.0	9.2		-7.2	23.7	17.1	16.3	
RHS stiffness	20.2	17.0	13.4	10.8		28.5	23.0	13.6	11.8	
	Max. Stiff.	Opt (TS)	Opt (%)	Opt (LS)	Opt %	Max. Stiff.	Opt (TS)	Opt (%)	Opt (LS)	Opt %
Torsional Stiffness	22944	19503	85%	22731	99%	30602	24176	79%	27405	90%
Lateral Stiffness	17.2	10.6	62%	9.9	58%	23.2	15.3	66%	13.9	60%
Average:			73.3%		78.3%			72.5%		74.7%

**APPENDIX F. REVISED MATLAB® SCRIPT
AND RESULTS**

F.1 Optimised_wheel_stiffness_Ver_2.m

```

%% Goldberg Optimisation Calculations for Torsional and Lateral
Stiffness
%
% This code will output the optimised geometry for wire spoked wheels
% based on the calculated Torsional and Lateral Stiffness using the
% equations formulated by Goldberg (1984).
%
% For my project it will be used to find the optimised geometry of
% 20, 24, 28, 32, 36 and 48 spoke wheels
%
clc; clear all;
close all;
% Display start time
disp('Geometry Optimisation for Wire Spoked Wheels')
disp('_____')
Start_time=datestr(now,0);
disp('Analysis Start:')
fprintf(Start_time)
disp(' ')
disp('-----')
disp('----')
%% Nomenclature
%      Rw      - Radius rim (mm)
%      Rh      - Radius hub (mm)
%      mu      - Spoke angle (radians)
%      gS      - Calculated spoke length (mm)
%      E      - Effective Elasticity (hub/rim/spoke combination) -
kg/mm^2
%      Spd     - Spoke diameter
%      gA      - Cross-sectional area of spoke - (mm^2)
%      muf     - Torque induced wind-up angle (between 0 and 1
degree)
%      N      - Total number of spokes (NL - spokes LHS; NR - spokes
RHS)
%      gLS     - L and R for load coming from the LHS or RHS of the
rim
%              respectively
%      D      - amount of dish in mm
%      df/Df  - change in dish cause by applied force (mm)
%      Defrat  - change in dish of rim due to load (mm)
%      LS     - lateral stiffness (kg/mm)
%      gTS    - torsional stiffness (kg.mm/deg)
%      T      - spoke tension (kg)
%      Trm    - tension ratio (RHS tension:LHS tension)
%
%% Set Known Values - all of these are used in Torsional and Lateral
stiffness
E=6895;
% value 1e7 psi used by Goldberg converted
disp('Please enter the total number of spokes to be used in the
wheel')
N=input...
('Total spoke number (minimum 8 spokes): ');
while N<8;
disp('*****Total spoke count must be greater than or equal to
8!*****')
N=input...
('Total spoke number (minimum 8 spokes): ');

```

APPENDIX F REVISED MATLAB® SCRIPT AND RESULTS
 F.1 Optimised_wheel_stiffness_Ver_2.m

```

end
% Set spokes for LHS of wheel - NL (minimum 4 spokes on each side
NL=4:2:N-4;
% Calculate respective spokes on RHS (Total spokes - LHS spokes)
% Set up matrix to improve calculation time
NR=N-NL;
% Wheel radii - rim and hub
Rw=300;
Rh=25;%input('Enter hub flange radius (both sides) (mm): ');
% Syntax [dish LHS;dish RHS] 10sp freehub length - 45mm RHS, distance
between
% dropouts 130mm - allow 10mm clearance LHS measured centre of flange
to
% centre of rim
D=[32;17];
% Spoke angle
muD=0:1:90;
mu=muD.*pi/180;
% Spoke diameter
Spd=1.8;%input('Enter the spoke diameter (mm): ');
% Spoke cross-sectional area
gA=1/4*pi*Spd.^2;
% LHS Spoke tension
T=45.36;
% 100 lb (Goldberg) converted;
% RHS Multiplication factor
Trm=1.4;% 1.4;
T(2)=Trm*T(1);
% Load from right to left (limiting deflection 2mm)- Defrat -
deflection ratio (small % of dish)
df=input('Enter allowable deflection (mm): ');
Defrat=D(2)/df;
DfR=D(2)/Defrat;
DfL=-DfR;
% Load from left to right - proportional deflected equivalent to DfR
xl=Defrat*D(1)/D(2);
DfLl=D(1)/xl;
DfRl=-DfLl;
% Wind up angle (default value: typically less than 1%)
mufL=0.8*pi/180;
mufR=0.8*pi/180;
%
%% Lateral and Torsional Stiffness
% Calculate spoke length for different hub radius, dish and spoke
angle mu;
% syntax [mu value, dish value, Rh value]
gS=zeros(length(mu),2,length(Rh)); % Preallocation to improve speed
for n=1:length(Rh)
    for i=1:length(mu);
        gS(i,1,n)=sqrt(Rw.^2+Rh(n).^2+D(1).^2-
2.*Rw.*Rh(n).*cos(mu(i)));
        gS(i,2,n)=sqrt(Rw.^2+Rh(n).^2+D(2).^2-
2.*Rw.*Rh(n).*cos(mu(i)));
    end
end
end
%
% Calculate Torsional stiffness depending on N, A, mu, D, Rh and NL/NR
disp('-----')
disp('Identifying the maximum torsional and lateral stiffness
possible')
disp('Please be patient - analysis may take up to 4 hours...')

```

APPENDIX F REVISED MATLAB® SCRIPT AND RESULTS

F.1 Optimised_wheel_stiffness_Ver_2.m

```

% Preallocate matrix to reduce computation time
gTS=zeros(length(mu),length(NL),length(mu),length(Rh)...
    ,length(Rh),length(gA),length(gA));
gLSR=gTS;
gLSL=gTS;
LSave=gTS;
% Create loop - LSave is calculated only when gLSR and gLSL are
positive
for j=1:length(NL);
% Changes spokes LHS - NL
    for k=1:length(mu);
% Changes spoke angle LHS - mu
        for l=1:length(mu);
% Changes spoke angle RHS - mu
            for m=1:length(Rh);
% Changes hub radius LHS - Rh
                for n=1:length(Rh);
% Changes hub radius RHS - Rh
                    for o=1:length(gA);
% Changes spoke cross-sectional area LHS - gA
                        for p=1:length(gA);
% Changes spoke cross-sectional area RHS - gA
                            % Goldberg's equation for Torsional
                            % Stiffness

gTS(k,j,l,m,n,o,p)=(pi.*E.*Rw.^2)./180)...
    .* (NL(j).*gA(o).*Rh(m).^2.*...
    sin(mu(k)).^2./(gS(k,1,m).^3)...
    +NR(j).*gA(p).*Rh(n).^2.*...
    sin(mu(l)).^2./(gS(1,2,n).^3));
                            % Lateral stiffness for any wheel

gLSR(k,j,l,m,n,o,p)=(NL(j).*(T(1)./gS(k,1,m)...
    +((T(1)+E.*gA(o)).*D(1).^2)...
    ./ (gS(k,1,m).^3)-((T(1)+E.*gA(o))...
    .*D(1).*Rw.*Rh(m))...
    ./ (gS(k,1,m).^3.*DfL)...
    .* (cos(mu(k)+mufL)-cos(mu(k))))...
    + (NR(j).*(T(2)./gS(1,2,n)...
    +((T(2)+E.*gA(p)).*D(2).^2)...
    ./ (gS(1,2,n).^3)-...
    ((T(2)+E.*gA(p)).*D(2)...
    .*Rw.*Rh(n))./(gS(1,2,n).^3.*DfR)...
    .* (cos(mu(l)+mufR)-cos(mu(l))))))/2;

gLSL(k,j,l,m,n,o,p)=(NL(j).*(T(1)./gS(k,1,m)...
    +((T(1)+E.*gA(o)).*D(1).^2)...
    ./ (gS(k,1,m).^3)-((T(1)+E.*gA(o))...
    .*D(1).*Rw.*Rh(m))...
    ./ (gS(k,1,m).^3.*DfL1)...
    .* (cos(mu(k)+mufL)-cos(mu(k))))...
    + (NR(j).*(T(2)./gS(1,2,n)...
    +((T(2)+E.*gA(p)).*D(2).^2)...
    ./ (gS(1,2,n).^3)-...
    ((T(2)+E.*gA(p)).*D(2)...
    .*Rw.*Rh(n))./(gS(1,2,n).^3.*DfR1)...
    .* (cos(mu(l)+mufR)-cos(mu(l))))))/2;
                            % Calculate the average LS

LSave(k,j,l,m,n,o,p)=(gLSL(k,j,l,m,n,o,p)...
    +gLSR(k,j,l,m,n,o,p))./2;
    end
end

```

APPENDIX F REVISED MATLAB® SCRIPT AND RESULTS
 F.1 Optimised_wheel_stiffness_Ver_2.m

```

                                end
                            end
                        end
                    end
                end
            end
        end
    end
end
%% Find maximum combined lateral stiffness
% Locate maximum combined lateral stiffness in LSave
LSav=LSave;
% Turn all values to zero in LSave where gLSL or gLSR are <1
LSave(gLSL<1)=0;
LSave(gLSR<1)=0;
[max_LS,lposition]=max((LSave(:)));
[h,i,j,k,l,m,n]=ind2sub(size(LSave),lposition);
% Create Geometry matrix for maximum lateral stiffness
% syntax [NL,NR,mu-LHS,mu-RHS,Rh-LHS,Rh-RHS,Spd-LHS,Spd-RHS]
gLSgeo=[NL(i),NR(i),muD(h),muD(j),Rh(k),Rh(l),Spd(m),Spd(n)];
% Maximum Lateral stiffness
LSm=max_LS;
% Convert to imperial units - compare with recorded results
LSmimp=LSm*25.4*2.2;
% Print to command window
fprintf('\nThe geometry of maximum lateral stiffness - %2.0f spoked
wheel:\n\n',N)
fprintf('Number of spokes LHS:           %2.0f spokes.\n',gLSgeo(1))
fprintf('Number of spokes RHS:           %2.0f spokes.\n',gLSgeo(2))
fprintf('Spoke angle LHS:                   %2.0f degrees.\n',gLSgeo(3))
fprintf('Spoke angle RHS:                   %2.0f degrees.\n',gLSgeo(4))
fprintf('Hub Radius LHS:                     %2.1f mm.\n',gLSgeo(5))
fprintf('Hub Radius RHS:                     %2.1f mm.\n',gLSgeo(6))
fprintf('Spoke Diameter LHS:                  %1.1f mm.\n',gLSgeo(7))
fprintf('Spoke Diameter RHS:                  %1.1f mm.\n\n',gLSgeo(8))
fprintf('The maximum lateral stiffness - %2.0f spoked wheel:      %4.1f
kg/mm.\n',N,LSm)
fprintf('Lateral Stiffness (imperial):                %4.1f
lb/in.\n\n',LSmimp)
%% Find maximum torsional stiffness
% Locate maximum torsional stiffness in gTS
[max_TS,tposition]=max((gTS(:)));
[a,b,c,d,e,f,g]=ind2sub(size(gTS),tposition);
% Create Geometry matrix for maximum torsional stiffness
% syntax [NL,NR,mu-LHS,mu-RHS,Rh-LHS,Rh-RHS,Spd-LHS,Spd-RHS]
gTSgeo=[NL(b),NR(b),muD(a),muD(c),Rh(d),Rh(e),Spd(f),Spd(g)];
% Maximum torsional stiffness
TSm=max_TS;
% Convert to imperial units - compare with reported values
TSmimp=TSm*2.2/25.4;
% Print to command window
fprintf('The geometry of maximum torsional stiffness - %2.0f spoked
wheel:\n\n',N)
fprintf('Number of spokes LHS:           %2.0f spokes.\n',gTSgeo(1))
fprintf('Number of spokes RHS:           %2.0f spokes.\n',gTSgeo(2))
fprintf('Spoke angle LHS:                   %2.0f degrees.\n',gTSgeo(3))
fprintf('Spoke angle RHS:                   %2.0f degrees.\n',gTSgeo(4))
fprintf('Hub Radius LHS:                     %2.1f mm.\n',gTSgeo(5))
fprintf('Hub Radius RHS:                     %2.1f mm.\n',gTSgeo(6))
fprintf('Spoke Diameter LHS:                  %1.1f mm.\n',gTSgeo(7))
fprintf('Spoke Diameter RHS:                  %1.1f mm.\n\n',gTSgeo(8))
%
fprintf('The maximum torsional stiffness - %2.0f spoked wheel:
%4.1f kg.mm/deg.\n',N,TSm)

```

APPENDIX F REVISED MATLAB® SCRIPT AND RESULTS
 F.1 Optimised_wheel_stiffness_Ver_2.m

```

fprintf('Maximum torsional stiffness (imperial):                %4.1f
lb.in/deg.\n\n',TSmimp)
disp('Please review data before continuing...')
%
% End time - Stops time after longest part of the program
Int_time=datestr(now,0);
disp('First Analysis Completed:')
fprintf(Int_time)
fprintf('\n')
% Repeat Optimisation loop until results are accepted
while true
    Q1=...
        input('\nDo you wish to continue optimisation?\nEnter ''1''
for yes or ''2'' to quit: ');
    while Q1<1 || Q1>2 || Q1>1 && Q1<2
        disp('Error: Please select either 1 or 2')
        Q1=...
            input('\nDo you wish to continue optimisation?\nEnter
''1'' for yes or ''2'' to end: ');
    end
    if Q1==1;
        %% Optimisation loop
        disp('-----')
        disp('Find optimal combination depending on requirements:')
        disp('-----')
        %
        LSper=input('\nEnter the minimum percentage of lateral
stiffness required as a decimal: ');
        while LSper<0 || LSper>1
            disp('****Error: Please enter a value between 0 and
1!****')
            LSper...
                =input('\nEnter the minimum percentage of lateral
stiffness required as a decimal: ');
        end
        %% Locate and post optimal values
        LSave(LSav<LSm.*LSper)=0;
        gTS(LSave==0)=0;
        LSp=LSave./LSm*100;
        TSp=gTS./TSm*100;
        Avp=(LSp+TSp)./2;
        [opt_Avp,pos]=max((Avp(:)));
        [aa,bb,cc,dd,ee,ff,gg]=ind2sub(size(Avp),pos);

Optgeo={ [NL(bb),NR(bb),muD(aa),muD(cc),Rh(dd),Rh(ee),Spd(ff),Spd(gg)] }
;

    Optg=cell2mat(Optgeo);
    LSop=LSave(pos);
    LSpe=LSop/LSm*100;
    TSop=gTS(pos);
    TSpe=TSop/TSm*100;
    % Display results for optimal geometry
    disp('-----')
    disp(' ')
    fprintf('The optimal geometry of a %2.0f spoked wheel
is:\n\n',N)
    fprintf('Number of spokes LHS:                %2.0f
spokes.\n',Optg(1))

```

APPENDIX F REVISED MATLAB® SCRIPT AND RESULTS
F.1 Optimised_wheel_stiffness_Ver_2.m

```
        fprintf('Number of spokes RHS:           %2.0f\n',Optg(2))
    spokes.\n',Optg(2))
        fprintf('Spoke angle LHS:               %2.0f\n',Optg(3))
    degrees.\n',Optg(3))
        fprintf('Spoke angle RHS:               %2.0f\n',Optg(4))
    degrees.\n',Optg(4))
        fprintf('Hub Radius LHS:                   %2.1f mm.\n',Optg(5))
        fprintf('Hub Radius RHS:                   %2.1f mm.\n',Optg(6))
        fprintf('Spoke Diameter LHS:              %1.1f mm.\n',Optg(7))
        fprintf('Spoke Diameter RHS:              %1.1f\n',Optg(8))
    mm.\n\n',Optg(8))
        fprintf('Stiffness Properties for the above geometry:\n')
        fprintf('The optimal torsional stiffness - %2.0f spoked wheel:\n',N,TSop,TSpe)
    %4.1f kg.mm/deg (%2.0f%% of max).\n',N,TSop,TSpe)
        fprintf('Torsional Stiffness (imperial):\n',TSop*2.2/25.4)
    %4.1f lb.in/deg.\n',TSop*2.2/25.4)
        fprintf('The optimal lateral stiffness - %2.0f spoked wheel:\n',N,LSop,LSpe)
    %4.1f kg/mm (%2.0f%% of max).\n',N,LSop,LSpe)
        fprintf('Lateral Stiffness (imperial):\n',LSop*2.2*25.4)
    %3.1f lb/in.\n',LSop*2.2*25.4)
        %% Complete Q1 loop - Re: Continue to Optimisation
    end
    if Q1==2;
        break
    end
end
%% Display Run time
% End timer
disp('-----')
disp('-----')
% Display end time
disp('Analysis Completed:')
end_time=datestr(now,0);
fprintf(end_time)
fprintf('\n\n')
disp('Code written by Jason Keller as part of ENG4111 and ENG4112\nResearch Project')
disp('Student ID: 0050093222 University of Southern Queensland -\nBENG(Mechanical)')
disp('_____')
disp('_____')
```

LIST OF REFERENCES

Brandt, J 1988, *The bicycle wheel*, Avocet Inc., Menlo Park.

Burgoyne, C & Dilmaghanian, R 1993, 'Bicycle wheel as prestressed structure', *Journal of Engineering Mechanics*, vol. 119, no. 3, pp. 439-55, <<http://ascelibrary.org/doi/abs/10.1061/%28ASCE%290733-9399%281993%29119%3A3%28439%29>>.

Burrows, M 2008, *Bicycle design*, Snowbooks Ltd, London.

Gavin, HP 1996, 'Bicycle wheel spoke patterns and spoke fatigue', *ASCE Journal of Engineering Mechanics*, vol. 122, no. 8, pp. 736-42, <<http://people.duke.edu/~hpgavin/papers/HPGavin-Wheel-Paper.pdf>>.

Goldberg, L 1980, 'Spoking geometry and wheel strength', *Bicycling*, vol. 10, no. 8, pp. 58-63.

Goldberg, L 1984, *The spoking word*, Cascade Bicycle Products, Bellingham

Hartz, AD 2002, *Finite element analysis of the classic bicycle wheel*, Raytheon Engineering and Production Support, Indianapolis, <<http://www.rose-hulman.edu/~fine/FE2002/Projects/Hartz.pdf>>.

Hetenyi, M 1979, *Beams on elastic foundations: Theory with applications in the fields of civil and mechanical engineering*, The University of Michigan Press, Rexdale.

Mariappan, DD, Vijay, S & Ramamurti, V 2003, 'An efficient algorithm for solving spoked wheels', *Advances in Engineering Software*, vol. 34, no. 1, pp. 25-30, <<http://www.sciencedirect.com/science/article/pii/S0965997802000935>>.

Old wooden wheel, viewed 28 February, <http://textures.funpic.de/tex/0000012/0000012_iso_holzrad_bereinigt_512.png>.

LIST OF REFERENCES

- Papadopoulos, JM 1995, 'Bicycle wheel as prestressed structure', *Journal of Engineering Mechanics*, vol. 121, no. 7, p. 847,a9h, EBSCOhost, <<http://ezproxy.usq.edu.au/login?url=http://search.ebscohost.com/login.aspx?direct=true&db=a9h&AN=6784661&site=ehost-live>>.
- Pippard, AJS 1952, *Studies in elastic structures*, Edward Arnold Co., London.
- Pippard, AJS & Baker, JF 1926, 'Cxviii. On the stresses in a spoked wheel under loads applied to the rim', *Philosophical Magazine Series 7*, vol. 2, no. 12, pp. 1234-53.viewed 2013/03/26, <<http://www.tandfonline.com/doi/abs/10.1080/14786442608564158>>.
- Pippard, AJS & Francis, WE 1931, 'Xx. On a theoretical and experimental investigation of the stresses in a radially spoked wire wheel under loads applied to the rim', *Philosophical Magazine Series 7*, vol. 11, no. 69, pp. 233-85.viewed 2013/03/26, <<http://www.tandfonline.com/doi/abs/10.1080/14786443109461681>>.
- Pippard, AJS & Francis, WE 1932, 'Xlix. The stresses in a wire wheel under side loads on the rim', *Philosophical Magazine Series 7*, vol. 14, no. 91, pp. 436-45.viewed 2013/03/26, <<http://www.tandfonline.com/doi/abs/10.1080/14786443209462081>>.
- Pippard, AJS & White, MJ 1932, 'Xxii. The stresses in a wire wheel with non-radial spokes under loads applied to the rim', *Philosophical Magazine Series 7*, vol. 14, no. 90, pp. 209-33.viewed 2013/03/26, <<http://www.tandfonline.com/doi/abs/10.1080/14786443209462053>>.
- Price, D & Akers, A 1985, 'Stiffness characteristics of bicycle wheels', *Bike Tech*, vol. 4, no. 3, pp. 1-7.
- Great wheel test - part 3 - stiffness: Stiffness tests, 2008, Roues Artisanales.com, viewed 30 August 2013, <<http://www.rouesartisanales.com/article-23159755.html>>.
- Salamon, NJ & Oldham, RA 1991, 'Analysis for design of spoked bicycle wheels', *Finite Elements in Analysis and Design*, vol. 10, no. 4, pp. 319-33.

LIST OF REFERENCES

Wilson, DG & Papadopoulos, J 2004, *Bicycling science*, Third edn, The MIT Press, Cambridge.